AD_____

Award Number: DAMD17-98-1-8607

TITLE: Molecular Mechanisms of Schwann Cell Proliferation in NF1

PRINCIPAL INVESTIGATOR: George H. DeVries, Ph.D.

CONTRACTING ORGANIZATION: Chicago Association for Research and Education in Science
Hines, Illinois 60141

REPORT DATE: September 2001

TYPE OF REPORT: Annual

PREPARED FOR: U.S. Army Medical Research and Materiel Command
Fort Detrick, Maryland 21702-5012

DISTRIBUTION STATEMENT: Approved for Public Release;
Distribution Unlimited

REPORT DOCUMENTATION PAGE

Form Approved
OMB No. 074-0188

1. AGENCY USE ONLY (Leave blank)	2. REPORT DATE	3. REPORT TYPE AND DATES COVERED
	September 2001	Annual (1 Aug 00 - 1 Aug 01)

4. TITLE AND SUBTITLE
Molecular Mechanisms of Schwann Cell Proliferation in NF1

5. FUNDING NUMBERS
DAMD17-98-1-8607

6. AUTHOR(S)
George H. DeVries, Ph.D.

7. PERFORMING ORGANIZATION NAME(S) AND ADDRESS(ES)
Chicago Association for Research and Education in Science
Hines, Illinois 60141

E-Mail: gdevrie@lumc.edu

8. PERFORMING ORGANIZATION REPORT NUMBER

9. SPONSORING / MONITORING AGENCY NAME(S) AND ADDRESS(ES)
U.S. Army Medical Research and Materiel Command
Fort Detrick, Maryland 21702-5012

10. SPONSORING / MONITORING AGENCY REPORT NUMBER

11. SUPPLEMENTARY NOTES
Report contains color.

12a. DISTRIBUTION / AVAILABILITY STATEMENT
Approved for Public Release; Distribution Unlimited

12b. DISTRIBUTION CODE

13. ABSTRACT *(Maximum 200 Words)*

Neurofibromatosis type 1 (NF1) is a genetic disorder characterized by Schwann cell tumors called neurofibromas, which can potentially become malignant to form neurofibrosarcomas. Previously, our laboratory has reported that Schwann cells derived from neurofibromas abnormally express high levels of the receptor tyrosine kinase c-Kit, which contributes weakly to Schwann cell proliferation (Badache et al, 1998a). It is possible that c-Kit plays an important role during development and that its aberrant re-expression by adult NF1 cells contributes to the development of Schwann cell tumors. We now report that neurofibromin expression and c-Kit expression are inversely regulated in rat sciatic nerves during development. Normal adult Schwann cells contain neurofibromin and do not express c-Kit, while human Schwann cell lines from NF1 tumors express c-Kit but do not express neurofibromin. In neonates, c-Kit is expressed by cultured Schwann cells. Its activation by SCs prevents programmed cell death via the activation of Akt but does not induce Schwann cell proliferation or differentiation.

14. SUBJECT TERMS	15. NUMBER OF PAGES
NF1, cAMP, Cancer, Neurofibromin	136
	16. PRICE CODE

17. SECURITY CLASSIFICATION OF REPORT	18. SECURITY CLASSIFICATION OF THIS PAGE	19. SECURITY CLASSIFICATION OF ABSTRACT	20. LIMITATION OF ABSTRACT
Unclassified	Unclassified	Unclassified	Unlimited

Table of Contents

A. Introduction

The subject of this investigation is Type 1 neurofibromatosis (NF-1), which is an inherited disease that occurs at a frequency of approximately 1 in 3,000. Two types of tumors are evident in this disease: relatively benign neurofibromas, which occur as subcutaneous tumors, and neurofibrosarcomas (NFS), the more invasive and aggressive type tumors that can potentially be life-threatening. The major cell type that proliferates and forms either of these tumors is the Schwann cell. Our laboratory has obtained and developed a number of different Schwann cell lines derived from neurofibrosarcomas and/or neurofibromas, which we are currently using to study this disease. In addition, we have obtained benign Schwann cell tumors (Schwannomas) from patients who are not affected by NF-1 to serve as controls for the neurofibromatosis-derived Schwann cells. The purpose of this investigation is to understand the molecular mechanisms that are responsible for the abnormal proliferation of Schwann cells, which characterizes NF-1. In particular, we would like to understand how the absence of neurofibromin leads to changes in intercellular signaling, which ultimately leads to a sustained proliferation of Schwann cells.

Our approach to understanding the abnormal proliferation of Schwann cells is to evaluate growth receptor expression in NF-derived and non-NF-derived Schwann cells. The presence of additional growth factor receptors is closely related to increased proliferative potential of Schwann cells. In the presence of the appropriate ligand to activate the receptor, these additional receptors could be responsible for the abnormal proliferation, which is observed in NF-derived Schwann cells. As outlined in the original proposal, we proposed to manipulate receptor expression in order to create Schwann cells that mimic cells obtained from NF-1 patients. We also extended our investigation to ask whether or not other growth factor receptors were overexpressed in these cells and what intercellular metabolic pathways could be responsible for increased growth factor expression.

We are also documenting signal transduction pathways activated by growth factor receptor stimulation as well as the functional consequences of such activation. In addition, we are characterizing for the first time the types of synthetic enzymes, adenylyl cyclases and prostaglandin receptors, which may play key roles in maintaining the abnormal growth factor receptor expression and is characteristic of Schwann cells derived from neurofibromas and neurofibrosarcomas.

B. Body

This section of the progress report will include experimental methods, results, and discussion in relation to the statement of work outlined in the award proposal. Progress in achieving the specific aims and associated tasks will be reported. In addition, we will document further research that has amplified and extended the original tasks. This additional research is entirely supportive of the original specific aims. The statement of work and specific tasks from the previously funded proposal are indicated below:

STATEMENT OF WORK

Specific Aim 1:
Effect of decreased neurofibromin expression on human Schwann cell proliferation

Task 1: Culture and expansion of human Schwann cells; determination of basal proliferation levels.

Task 2: Transfection of human Schwann cells with oligonucleotide antisense to neurofibromin; determination of the optimal conditions for viability and efficiency of transfection; Northern blot analysis; proliferation assay.

Specific Aim 2:
Role of Kit expression in NF-1 derived Schwann cell proliferation

Task 3: Establishment of cultures from frozen stocks. Verify basal doubling time.

Task 4: Determination of optimal conditions for transfection for each NF1-cell line; generation of clonal transfected cell lines.

Task 5: Collection of RNA for determination of DN-Kit transcript level of expression; proliferation assay.

Task 6: Northern blot; quantitation of DN-Kit expression; correlative analyses DN-Kit expression/level of proliferation.

Specific Aim 3:
Effect of simultaneous Kit expression and neurofibromin alteration on human Schwann cell proliferation.

Task 7: Determination of optimal conditions for transfection of Kit constructs into human Schwann cells.

Task 8: Establishment of clonal cell lines; determination of levels of Kit expression in various clones; proliferation assay.

Task 9: Transfection with antisense oligonucleotide against neurofibromin of Kit expressing human Schwann cells selected in Task 8, using optimal conditions determined in Task 2. Proliferation assay; collection of RNA for Northern Blot.

Task 10: Northern blot on double transfected Schwann cells. Correlative analysis level of Kit/neurofibromin expression and proliferation.

In this year of continuation without additional funding, we have taken some new approaches to understanding the role of growth factor receptors in the proliferation of Schwann cells (SCs). In order to understand the role of aberrant expression of c-Kit in the NF1-derived Schwann cells. We decided to investigate the role of this receptor in development. The results of this study are

documented in the appended manuscript "The Role and Developmental Regulation of c-Kit Receptor in Normal Human Schwann Cells and NF1-derived Schwann Cells." We found that this receptor was expressed in a manner that was inversely related to the expression of neurofibromin. Early in development, c-Kit was evident. As development ensued, c-Kit expression was dramatically downregulated while neurofibromin expression was upregulated. We had already reported that in the absence of neurofibromin in the adult cells, c-Kit was once again expressed. Activation of the c-Kit receptor by stem cell factor prevented programmed cell death by the activation of the Akt pathway. Activation of the c-Kit by stem cell factor had no appreciable effect on Schwann cell proliferation or differentiation. These results lead us to conclude that other growth factors, which may be coupled in an unusual manner to intracellular pathways, may also be involved in the abnormal proliferation characteristic of NF1-derived SC. Therefore, we investigated the role of PDGF signaling pathways in SC as detailed in the attached manuscript "Stimulation of Intracellular Signaling Pathways in Response to PDGF-BB in NF-1 Schwann Cells." We found that PDGF activates the ERK and PI3K pathways in both NF1-derived SC and normal human SC. Inhibition of the PI3K pathway decreased the proliferation of the NF1-derived SCs. A most interesting finding is that the addition of PDGF-BB to the NF1-derived SC lead to an increase in intracellular calcium, which was not observed when this comparable experiment was carried out on normal human SC.

Phosphorylation of Calmodulin Kinase (CAMII) was also induced by PDGF-BB in the NF1-derived SC. Inhibition of CAMII led to a decreased proliferation of the NF1-derived SC. These results were interesting because they showed, for the first time, that there was aberrant calcium signaling pathways operative in the NF1-derived SCs, and that these signaling pathways may contribute to the overall proliferative potential of these cells.

Since cAMP elevation is associated with increased proliferation and activation of prostaglandin receptors by prostaglandins or from thromboxane receptors by thromboxanes, leads to elevation of cAMP, it was of interest to examine prostaglandin metabolism as it relates to cAMP in normal SC and NF1-derived SC. In our first study, "Identification and Functional Characterization of Thromboxane A2 receptors in SC" we reported that both primary rat SCs and NF1-derived SCs have functional thromboxane A2 receptors. Moreover, activation of the thromboxane receptor led to a sustained calcium mobilization in the NF1-derived SC but not in primary rat SC. Furthermore, the phosphorylation of this transcription factor, CREB, was stimulated by the activation of the thromboxane receptors. These results demonstrate that thromboxane A2 activation leads to CREB phosphorylation in a manner that changes the intracellular levels of calcium. In contrast, stimulation of these same receptors in primary SCs lead to increased intracellular cAMP and CREB phosphorylation but no changes in intracellular calcium. These results are important since they demonstrate, once again, another altered signaling pathway (that of thromboxane A2 receptor) specifically in NF1-derived SC. Next we further characterized the prostaglandin metabolism in SCs in our next manuscript, which has been submitted to the *Journal of Biological Chemistry*, "Activation of the cAMP-dependent Signaling Cascade in Primary Schwann Cells by Prostaglandins." First we investigated the type of prostaglandin receptors that were present in the SCs and found that the EP2, EP4, and IP prostaglandin receptors were all expressed at the level of the mRNA. Furthermore, stimulation of these prostaglandin receptors with the appropriate ligands resulted in a dose-dependent elevation of cAMP in primary SCs. Downstream of the activation of prostaglandin receptor, we noted the phosphorylation of CREB within five minutes of exposure to the cultured primary SC to prostaglandins. This study is important because it showed us that the SCs contain all the necessary transduction machinery to stimulate an increase in cAMP, which could be related to SC proliferation.

The next question was whether or not prostaglandins could influence cAMP levels in NF1-derived SC. If this was the case, and the cells were constituitively-producing prostaglandins, it would result in a constitutive elevation of cAMP. This study is documented in a manuscript "NF-1 Schwann Cells have Elevated cAMP levels and increased secretion of Prostaglandin PGE1," which has been submitted for publication.

Finally, we wished to understand the relationship between increased cAMP levels and prostaglandins, which are known to elicit increases in intracellular cAMP. The results of this study are in the manuscript "NF1 Schwann Cells have Elevated cAMP Levels and Increased Secretion of Prostaglandin PGE1." First, we wished to understand the types of enzymes that synthesize cAMP (adenylyl cyclase). We carried out PCR analysis using mRNA isolated from normal adult human SCs and found types III, IV, and IX of adenylyl cyclase. It was of considerable interest to note that the NF1-derived SC expressed all these isotypes in addition to types II, V, VII and VIII. Therefore, the increased synthetic potential of these cells may be related in some way to the elevated cAMP levels, which are characteristic of these cells.

In order to investigate the role of prostaglandins, we first evaluated the level of the enzyme that releases the enzyme cytoplasmic phospholypase A_2 ($cPLA_2$) in the normal human SCs and NF1-derived SCs. We found higher levels of $cPLA_2$ in the neurofibromatosis-derived cells. In addition, the key synthetic enzyme of prostaglandin metabolism, cyclooxygenase (COX2) was also elevated in the NF1-derived SCs. The NF1-derived SCs also expressed the additional prostaglandin receptors EP2 and EP4, while the normal human SC expressed only the EP2 receptor. We found that the addition of prostaglandins to NF1 SCs gave a further increase in cAMP levels and increased their proliferation. This proliferation could be blocked by blocking COX2 and cAMP metabolism. These results support the view that abnormal prostaglandin metabolism leads to abnormal cAMP elevation, and in turn, is a key contributory factor to the increased proliferation noted in these cells.

C. Key Research Accomplishments:

- c-Kit is expressed at high levels during SC development when proliferation takes place.

- Expression of c-Kit and neurofibromin during development are inversely related; c-Kit is highly expressed in early development whereas neurofibromin is expressed at high levels only in later stages of development.

- MAP Kinase and PI3 Kinase pathways are activated in response to PDGF-BB in both normal adult human SC and NF1-derived SCs. There is no increase in intracellular calcium in normal human SCs stimulated with PDGF-BB, whereas similar stimulation of NF1-derived SCs results leads to a pronounced increase in intracellular calcium. PDGF-BB also activates CAMII.

- Inhibition of CAMII decreases the proliferation of SCs. Primary SCs express the mRNA transcripts in coding EP2, EP4, and IP prostaglandin receptors. Stimulation of these receptors with PGE1, PGE2 or PGI2 produces a dose-dependent elevation of cAMP. Prostaglandin stimulation of SCs also produces an increase in the active form of the cAMP response element binding protein, CREB.
- Thomboxane A_2 receptors are present in both rat SCs and an NF1-derived SC line. Activation of the thromboxane A_2 receptors in the NF1-derived SCs produced a calcium response that was not observed under similar conditions in normal human SCs. The phosphorylation of CREB was also stimulated by the activation of the thromboxane A_2 receptors.

- Pronounced elevation of cAMP was detected in both primary rat SCs (20 fold) and NF1-derived SCs (15 fold) when the cells were treated with an agonist that activated the thromboxane A_2 receptor.

- Normal adult human SCs contain three isoforms of adenylyl cyclase.

- NF1-derived SCs contain the same three isoforms of adenylyl cyclase as normal human SCs plus an additional three isoforms of adenylyl cyclase.

- NF1-derived SCs express higher levels of cytoplasmic phospholypase A_2 and COX2 than normal human SCs. NF1-derived SCs expressed the mRNA for both the EP2 and EP4 prostaglandin receptor, while normal human SCs express only the EP2 receptor.

- Additional of exogenous prostaglandins to NF1-derived SC induces further increases in intracellular cAMP. Addition of exogenous prostaglandins to NF1-derived SC induces a proliferation of NF-1 SCs .

- The proliferation of NF1-derived SCs, in response to PDGF-BB can be decreased by inhibition of COX2 and Protein Kinase A.

D. Reportable Outcomes:

Papers Published:

Muja, N., Blackman, SC, LeBreton, GC. and DeVries, GH (2001). Identification and functional characterization of thromboxane A2 receptors in Schwann Cells. *J. of Neurochem,* August; 78(3);446-56.

Papers in Preparation:

Klein, KA and DeVries, GH. (2002), "Phenotypic characterization of normal human Schwann cell lines derived from malignant nerve sheath tumors," in preparation.

Dang, I., and DeVries, GH (2002), "Stimulation of intracellular signaling pathways in response to PDGF BB in NF1 Schwann Cells," in preparation.

Dang, I., and DeVries, GH (2002), "NF1-derived SC have elevated cAMP levels and increased secretion of prostaglandin PGE_2," in preparation.

Papers Submitted:

Badache, A., and DeVries, G.H. (2001), Platelet-Derived Growth Factor BB stimulate Neurofibrosarcoma-derived Schwann Cell Directed Migration, *J. of Cancer Research*, submitted.

Muja, N., and DeVries, GH., (2001), Activation of the cAMP-dependent Signaling Cascade in Primary Schwann Cells by Prostaglandins E_1, E_2, and Prostacyclin, *J. Neuroscience*, submitted.

Abstracts:

Lertsburapa T, McNulty JA, Nahas SL, and DeVries GH, (2001) "Axonal control of angiogenesis in Normal and neurofibromatosis Type-1 Derived Schwann Cells," *J of Neurochem,* Vol. 78, suppl. 1.

Muja N, and DeVries GH, (2001), "Elevated Prostaglandin Release from Degenerating Sciatic Nerve Explants: contribution of Cyclooxygenase 2," *J of Neurochem*, Vol. 78, suppl. 1.

Gollapudi L, Reinhard S, Vela E, Varga J, Raabe TD and DeVries GH (2001) "Developmental regulation of neuregulin and ErbB receptor expression in rat DRG neurons" *J of Neurochem*, Vol. 78, suppl. 1.

Muja N, and DeVries GH, (2001) "The Role of Prostaglandins in Schwann Cell Proliferation during Wallerian Degeneration" *J of Periph Nervous System,* Vol 6, No. 3, p162.

- **Degrees obtained that have been supported by this award**:

Naser Muja, PhD – Neuroscience Program, Loyola University of Chicago
Currently working in the Laboratory of Dr. Nancy Ratner at the National Institutes of Health in Bethesda, Maryland

Ian Dang, PhD – Cell Biology, Neurobiology and Anatomy Program, Loyola University of Chicago. Currently working at The Scripps Research Institute in the Laboratory of Peter Hoyt, SanDiego, California.

- **Development of cell lines, tissue or serum repositories**:
  1. T265 Cell Line. This cell line was developed in our laboratory from a neurofibrosarcoma and has been used by several laboratories in their studies.
  2. Cell Lines and Development: We have obtained neurofibromas from three different NF patients, and are currently developing cell lines derived from these primary tumors, which will be labeled 36R, 313, and 315.

- **Funding applied for based on work supported by this award:** Grant proposal submitted to US Army and Materiel Command, "Regulation of Intracellular cAMP by Neurofibromin," submitted in August of 2001.

E. Conclusions:

We began our studies of Neurofibromatosis with the finding of abnormal expression of a tyrosine Kinase growth factor receptor, c-Kit, which we believe could be related to the abnormal proliferation of these cells. Work completed during this phase of the grant has shown that, indeed, c-Kit in normal SCs developmentally, the expression of c-Kit appears to parallel the time in which the cells are actively dividing. However, activation of this receptor led to a very weak proliferative response and seemed to be more involved in protecting these cells from apoptosis and not stimulating proliferation. Therefore, we investigated how other growth factor receptors may be involved in the abnormal proliferative response. We found that abnormal calcium metabolism was shown by the NF1-derived SCs in two cases: stimulation of the thromboxane A_2 receptor and stimulation of the

PDGF-BB receptor. The increased calcium appeared to be very closely related to the proliferative response, since using specific drugs to block metabolic pathways upstream or downstream of the elevated calcium response led to a marked decrease in proliferation. Since cAMP is known to be a key player in SC metabolism, we investigated the role that it may play. We next turned to the investigation of cAMP, a key intermediate in SC metabolism, to investigate whether or not it could play a role. First, we definitively showed that the NF1-derived SC had a marked elevation in cAMP. Second, we believe this elevation of cAMP comes from a number of different factors. First, there is an increased synthetic potential in these cells as exhibited by increased expression of adenylyl cyclase. Secondly, these cells have elevated levels of the cytosolic form of phospholypase A_2, which provides the starting arachidonic acid substrate for prostaglandin synthesis. In turn, prostaglandins are secreted at high levels, interact with specific receptors that are expressed at higher levels on the NF1-derived SCs. In turn, this leads to elevated cAMP and elevated proliferation. We have shown by intervention in these pathways that the constitutive expression of these pathways is critical for the sustained proliferation of these cells.

So What?

As a whole, our studies have given new insights into the mechanisms of proliferation in NF1-derived SCs. Abnormal prostaglandin metabolism, cAMP metabolism, and calcium metabolism are all integrally related to the sustained proliferation of these cells. In turn, therapeutic intervention in these pathways may be effective in helping to block the proliferation that is characteristic of these cells.

F. References:

1. Araujo, H., Menezes, M., and Mandez-Otero, R. 1997, Blockade of 9-*O*-acetyl gangliosides indices microtubule depolymerization in growth cones and neurites. *Euro. J. Cell. Bio.* **72:** 202-213.

2. Ariga, T., Blaine, G. M., Yoshino, H., Dawson, G., Kanda, T., Zeng, G. C., Kasama, T., Kushi, Y., and Yu, R. K. 1995. Glycosphingolipid composition of murine neuroblastoma cells: *O*-acetylesterase gene downregulates the expression of *O*-acetylated GD3. *Biochem.* **34:** 11500-11507.

3. Badache, A., and De Vries, G. H. 1998. Neurofibrosarcoma-derived Schwann cells overexpress platelet-derived growth factor (PDGF) receptors and are induced to proliferate by PDGF BB. *J. Cell Physiol.* 177:334-342.

4. Badache, A., Muja, N., and De Vries, G. H. 1998. Expression of Kit in neurofibromin-deficient human Schwann cells: role in Schwann cell hyperplasia associated with type 1 neurofibromatosis. *Oncogene.* **17:** 795-800.

5. Barker, E., Mueller, B. M., Handgretinger, R., Herter, M., Yu, A. L., Reisfeld, R. A. 1991. Effect of a chimeric anti-ganglioside GD2 antibody on cell-mediated lysis of human neuroblastoma cells. *Cancer Res.* **51(1):** 144-149.

6. Birkle, S., Ren, S., Slominski, A., Zeng, G., Gao, L., and Yu, R. K. 1999. Down-regulation of the expression of *O*-acetyl-GD3 by the *O*-acetylesterase cDNA in hamster melanoma cells: effects on cellular proliferation, differentiation, and melanogenesis. *J. Neurochem.* **72:** 954-961.

7. DeVries, G.H. (1993) Schwann cell proliferation. In: *Peripheral Neuropathy*. P. Dyck and P. Thomas, Eds. 3rd edition, 290-298.

8. Farrer, R. G., and Quarles, R. H. 1999. GT3 and its *O*-acetylated derivative are the principal A2B5-reactive gangliosides in cultured O2A lineage cells and are down regulated along with *O*-acetyl GD3 during differentiation to oligodendrocytes. *J. Neurosci. Res.* **57:** 371-380.

9. Golubic, M., Harwalkar, J. A., Bryant, S. S., Sundaram, V., Jove, R., and Lee, J. H. 1998. Differential regulation of neurofibromin and p120 GTPase-activating protein by nutritionally relevant fatty acids. *Nutrition and Cancer.* **30(2):** 97-107.

10. Kasid, U., Suy, S., Dent, P., Ray, S., Whiteside, T. L., and Sturgill, T. W. 1996. Activation of Raf by ionizing radiation. *Nature.* **382(6594):** 813-816.

11. Kim, H.A., Ling, B., and Ratner, N. 1997. *Nf1*-deficient mouse schwann cells are angiogenic and invasive and can be induced to hyperproliferate: reversion of some phenotypes by an inhibitor of farnesyl protein transferase. *Mol. and Cell Bio.* **17(2):** 862-872.

12. Lee, M. M., Badache, A., and De Vries, G. H. 1999. Phosphorylation of CREB in axon-induce Schwann cell proliferation. *J. Neurosci. Res.* **55:** 702-712.

13. Mendez-Otero, R., and Friedman, J. E. 1996. Role of acetylated gangliosides on neurite extension. *Euro. J. Cell. Bio.* **71:** 192-198.

14. Mendez-Otero, R., Schlosshauer, B., Barnstable, C. J., and Constantine-Paton, M. 1988. A developmentally regulated antigen associated with neural cell and process migration. *J. Neurosci.* **8(2):** 564-579.

15. Morioka, N., Tsuchida, T., Etoh, T., Ishibashi, Y., and Otsuka, F. 1990. A case of neurofibrosarcoma associated with neurofibromatosis: light microscopic, ultrastructural, immunohistochemical and biochemical investigations. *J. Deramtol.* **17(5):** 312-316.

16. Morioka, N., Tsuchida, T., Ishibashi, Y., and Otsuka, F. 1991. A case of neurofibrosarcoma associated with neurofibromatosis--ganglioside analysis. *Clin. Exp. Dermatol.* **16(6):** 467-470.

17. Pyne, N. J., Tolan, D., and Pyne, S. 1997. Bradykinin stimulates cAMP synthesis via mitogen-activated protein kinase-dependent regulation of cytosolic phospholipase A_2 and prostaglandin E_2 release in airway smooth muscle. *Biochem. J.* **328:** 689-694.

18. Qiu, Z., Gijon, M. A., Carvalho, M. S., Spencer, D. N., and Leslie, C. C. 1998. The role of calcium and phosphorylation of cytosolic phospholipase A_2 in regulating arachidonic acid release in macrophages. *J. Bio. Chem.* **273(14):** 8203-8211.

19. Prendergast, G. C., Davide, J. P., deSolms, S. J., Giulani, E. A., Graham, S. L., Gibbs, J. B., Oliff, A., and Kohl, N. E. 1994. Farnesyltransferase inhibition causes morphological reversion of *ras*-transformed cells by a complex mechanism that involves regulation of the actin cytoskeleton. *Mol. Cell. Biol.* **14:** 4193-4202.

20. Rosenbaum C., Karyala S., Marchionni MA, Kim HA, Krasnoselsky AL, Happel B, Isaacs, I., Brackenbury, R., and Ratner, N. 1997. Schwann cells express NDF and SMDF/n-ARIA mRNAs, secrete neuregulin, and show constitutive activation of erbB3 receptors; evidence for a neuregulin autocrine loop. *Exp Neurol.* 148(2):604-15.

21. Ritter, G., Ritter-Boosfeld, E., Adluri, R., Calves, M., Ren, S., Yu, R. K., Oettgen, H. F., Old, L. J., and Livingston, P. O. 1995. Analysis of the antibody response to immunization with purified *O*-acetyl GD3 gangliosides in patients malignant melanoma. *Int. J. Cancer.* **62(6):** 668-672.

22. Rosenbaum, T., Patrie, K. M., and Ratner, N. 1997. Neurofibromatosis type 1: genetic and cellular mechanisms of peripheral nerve tumor formation. *Neuroscientist.* **3:** 412-420.

23. Sjoberg, E. R., Manzi. A. E., Khoo, K., Dell, A., and Varki, A. 1992. Structural and immunological characterization of *O*-Acetylated G_{D2}. *J. Biol. Chem.* **267:** 16200-16211.

24. Sjoberg, E. R., Powell, L. D., Klein, A., and Varki, A. 1994. Natural ligands of the B cell adhesion molecule CD22B can be masked by 9-*O*-acetylation of sialic acids. *J. Cell. Bio.* **126(2):** 549-562.

25. Suy, S., Anderson, W. B., Dent, P., Chang, E., and Kasid, U. 1997. Association of Grb2 with Sos and Ras with Raf-1 upon gamma irradiation of breast cancer cells. *Oncogene.* **15(1):** 53-61.

26. Suy, S., Mitchell, J. B., Ehleiter, D., Haimovitz-Friedman, A., and Kasid, U. 1998. Nitroxides tempol and tempo induce divergent signal transduction pathways in MDA-MB 231 breast cancer cells. *J. Biol. Chem.* **273(28):** 17871-17878

27. Tsuchida, T., Otsuka, H., Niimura, M., Inoue, Y., Kukita, A., Hashimoto, Y., Seyama, Y., and Yamakawa, T. 1984. Biochemical study on gangliosides in neurofibromas and neurofibrosarcomas of Recklinghausen's disease. *J. Dermatol.* **11(2):** 129-138.

28. Weinmaster G., Lemke G., 1990. Cell-specific cyclic AMP-mediated induction of the PDGF receptor. *EMBO J.* 9:915-920.

29. Yoshino, J. E., Dinneen, M.P., Lewis, B.L., Meador-Woodruff, J. H., and De Vries, G. H. 1984. Differential proliferative response of cultured Schwann cells to axolemma- and myelin-enriched fractions. I. Biochemical studies. *J. Cell. Bio.* **99**: 2309-2313.

G. APPENDICES

Muja, N., Blackman, SC, LeBreton, GC and DeVries, GH (2001). Identification and functional characterization of thromboxane A2 receptors in Schwann Cells. *J. of Neurochem,* August; 78(3);446-56.

Muja, N. and DeVries, GH. Activation of cAMP-dependent signaling cascade in primary Schwann cells by Prostaglandins. *Journal of Biological Chemistry*, submitted (23 pages).

Dang, I. and DeVries GH. c-Kit receptor expression in normal Schwann cells and Schwann cell lines derived from NF1 tumors. *Journal of Neuroscience Research*, in preparation (25 pages).

Dang, I. and DeVries GH. Stimulation of intracellular signaling pathways in response to PDGF BB in NF1 Schwann Cells. *Journal of Neuroscience Research*, in preparation (29 pages).

Dang, I. And DeVries GH. NF1 derived SC have elevated cAMP levels and increased secretion of prostaglandin PGE_2. *Journal of Neuroscience Research*, in preparation (35 pages).

Journal of Neurochemistry, 2001, **78**, 446–456

Identification and functional characterization of thromboxane A_2 receptors in Schwann cells

Naser Muja,*[,1] Samuel C. Blackman,†[,1] Guy C. Le Breton† and George H. DeVries‡[,§]

**Neuroscience Graduate Program, and ‡Department of Cell Biology, Neurobiology and Anatomy, Loyola University of Chicago, Maywood, Illinois, USA*

§Research Service, Edward Hines Jr. VA Hospital, Hines, Illinois, USA

†Department of Pharmacology, University of Illinois at Chicago, Chicago, Illinois, USA

Abstract

Previous reports have demonstrated the presence of functional thromboxane A_2 (TP) receptors in astrocytes and oligodendrocytes. In these experiments, the presence and function of TP receptors in primary rat Schwann cells (rSC) and a neurofibrosarcoma-derived human Schwann cell line (T265) was investigated. Immunocytochemical and immunoblot analyses using polyclonal anti-TP receptor antibodies demonstrate that both cell types express TP receptors. Treatment with the stable thromboxane A_2 mimetic U46619 (10 μM) did not stimulate intracellular calcium mobilization in rSC, whereas T265 cells demonstrated a calcium response that was inhibited by prior treatment with TP receptor antagonists. U46619 also stimulated CREB phosphorylation on Ser133 in T265 cells and, to a lesser extent, in rSC. To identify potential mechanisms of CREB phosphorylation in rSC, we monitored intracellular cAMP levels following U46619 stimulation. Elevated levels of cAMP were detected in both rSC (20-fold) and T265 (15-fold) cells. These results demonstrate that TP receptor activation specifically stimulates CREB phosphorylation in T265 cells, possibly by a calcium- and/or cAMP-dependent mechanism. In contrast, TP receptor activation in rSC stimulates increases in cAMP and CREB phosphorylation but does not elicit changes in intracellular calcium.

Keywords: cAMP, neurofibromatosis type 1, peripheral nerve, Schwann cell, thromboxane A_2, Wallerian degeneration.

J. Neurochem. (2001) **78**, 446–456.

Thromboxane A_2 (TXA_2) is a labile lipid mediator which is synthesized by the sequential metabolism of arachidonic acid by cyclooxygenase and thromboxane synthase (Smith 1992; Halushka *et al.* 1995). Thromboxane A_2 is produced following the activation of a variety of cell types. The subsequent release of TXA_2 into the extracellular environment potently stimulates platelet aggregation, smooth muscle constriction and hypertrophy, and cellular proliferation (Vane *et al.* 1998). The abnormal production and release of TXA_2 has been implicated in a wide variety of thrombotic and vasospastic disorders (FitzGerald 1991).

The receptor for TXA_2 has been purified, cloned and sequenced (Hirata *et al.* 1991; Kim *et al.* 1992; Nusing *et al.* 1993). The sequence of the gene indicates that the receptor is a member of the heptahelical superfamily of G protein-coupled receptors. Human TXA_2 receptor (TP) is encoded by a single gene on chromosome 19p13.3, which can be alternatively spliced to produce two variants of exon 3 encoding the C-terminal tail, TPα and TPβ (Raychowdhury *et al.* 1994; Miggin and Kinsella 1998). The different C-terminal regions have been shown to influence the mechanism and kinetics of receptor desensitization (Yukawa *et al.* 1997; Walsh *et al.* 2000) and internalization (Parent *et al.* 1999). Thromboxane receptors have been shown to couple to multiple heterotrimeric G-proteins including G_q

Received January 8, 2001; revised manuscript received March 28, 2001; accepted March 29, 2001.

Address correspondence and reprint requests to George H. DeVries, Hines VA Hospital, Research 151, Bldg 1, Room C423, 5th Avenue & Roosevelt Rd, Hines, IL 60141, USA. E-mail: gdevrie@orion.it.luc.edu

[1]N. Muja and S. C. Blackman contributed equally to this work.

Abbreviations used: CREB, cyclic AMP response-element binding protein; DMEM, Dulbecco's modified Eagle's medium; D-PBS, Dulbecco's modified phosphate-buffered saline; Fura-2AM, fura-2 acetoxymethyl ester; G protein, GTP-binding protein; HEL, human erythroleukemia cell line; HBSS, Hank's balanced salt solution; NaF, sodium fluoride; NDF, Neu-differentiation factor; rSC, primary rat Schwann cells; SMP, solubilized platelet membranes; TP, thromboxane; TXA_2, thromboxane A_2; TXB_2, thromboxane B_2; U46619, 9,11-dideoxy-9α,11α-epoxymethanoprostaglandin $F_{2\alpha}$

(Knezevic *et al.* 1993; Allan *et al.* 1996), $G_{12/13}$ (Offermanns *et al.* 1994; Allan *et al.* 1996; Djellas *et al.* 1999) and G_i (Gao *et al.* 2001; Ushikubi *et al.* 1994). Also, TPα couples to a novel high molecular mass G protein, G_h (Vezza *et al.* 1999). Activation of TP receptors has been shown to modulate intracellular cAMP levels ($[cAMP]_i$) in platelets and transfected Chinese hamster ovary and HEK293 cells (Hirata *et al.* 1996; Walsh *et al.* 1998; Cracowski *et al.* 2000). To date, however, there has been no demonstration of the TP receptor directly coupling to G_s.

In addition to their classical identification in platelets and smooth muscle cells, TP receptors have also been described in astrocytes (Nakahata *et al.* 1992), myelinated fiber tracts (Borg *et al.* 1994) and oligodendrocytes (Blackman *et al.* 1998). The presence of TP receptors in these cells suggests that these receptors may be involved in normal or abnormal CNS physiology. Microglia (Minghetti and Levi 1995) and astrocytes (Pearce *et al.* 1989; Bruner and Murphy 1993) have been shown to release TXA_2 following activation by bacterial lipopolysaccharide and ATP, respectively. Thus, the elevation in extracellular pyrimidine nucleotides (Langley and Pearcé 1998) and microglial activation seen following CNS tissue damage may lead to the release of TXA_2 and the subsequent autocrine or juxtacrine activation of TP receptors in the CNS.

In comparison, the presence and function of TP receptors in peripheral nerve physiology have not been investigated. Evidence supporting the potential existence of TP receptors stems from the finding that macrophages, which are recruited to the sites of peripheral nerve injury to remove debris and form an environment that is conducive to nerve regeneration (Beuche and Friede 1986; Goodrum *et al.* 1994; Brück 1997), release inflammatory cytokines and lipid mediators such as prostaglandins and TXA_2 (Rothwell and Hopkins 1995; Brock *et al.* 1999). Evidence also exists for the endogenous production of thromboxane by Schwann cells (Constable *et al.* 1994). Given that functional TP receptors have been identified in CNS glia and that sources for thromboxane exist in the PNS, we hypothesized that functional TP receptors were also present in Schwann cells, which are the myelin-forming cells of the PNS. Thus, in these experiments, we used primary Schwann cells isolated from neonatal rat sciatic nerve (rSC) and a human Schwann cell line (T265) to determine whether Schwann cells expressed functional TP receptors.

Materials and methods

Isolation and culture of primary rat Schwann cells

Primary rSC were cultured from neonatal rat sciatic nerves as described by Brockes *et al.* (1979). Sciatic nerves from 2-day-old Sprague–Dawley rat pups were extracted and digested enzymatically with 0.3% collagenase (Serva) in serum-free Dulbecco's modified Eagle's medium (DMEM) with low glucose and 10 mM HEPES for 3 h at 37°C. Following digestion, the cells were centrifuged at 100 *g* for 5 min, resuspended in 4–5 mL of low-glucose DMEM (1.0 g/L glucose) supplemented with 3.7 g/L $NaHCO_3$, 10 μg/mL gentamicin and 5% fetal calf serum. Cells were dispersed (1 mL/dish) into 100-mm culture dishes containing an additional 9 mL of the same medium. Cells were maintained in a humidified incubator at 37°C in the presence of 5% CO_2 and 95% air.

The following day, adherent cells were rinsed with calcium- and magnesium-free Dulbecco's modified phosphate-buffered saline (D-PBS) to dilute divalent cations in preparation for differential adhesion. The rinse media was aspirated and fresh D-PBS (4 mL) supplemented with 0.2% EDTA was added to the cells. After 1 min, the culture dishes were transferred to the stage of an inverted microscope. Under visual inspection, the side of the culture dish was tapped gently until the majority of the primary rSC was dislodged. Excess incubation in collecting media, as well as excess tapping, increased the release of fibroblasts from cultureware. Furthermore, rSC directly associated with fibroblasts were difficult to dislodge using this technique and were omitted to minimize fibroblast contamination. Medium containing detached primary rSC was collected and the cells were concentrated by centrifugation (100 *g*, 5 min) in 15 mL centrifuge tubes containing 4–5 mL of low-glucose DMEM to improve pellet formation. The supernatant was discarded and the cell pellet was resuspended in low-glucose DMEM for cell distribution to cultureware. Cultures obtained using this method were estimated to consist of 97–99% primary rSC according to their phase bright, narrow, bipolar morphology under microscopic view. In some cases, primary Schwann cells cultures were treated with 10 μM cytosine β-D-arabinofuranoside (Sigma, St Louis, MO, USA) for 24–48 h to eliminate any remaining fibroblasts.

Culture of T265 cells

A human Schwann cell line (T265) established from a neurofibrosarcoma isolated from an individual with neurofibromatosis type 1 was maintained by continuous culture in high-glucose DMEM (4.5 g/L glucose) supplemented with 5% fetal calf serum, 3.7 g/L $NaHCO_3$ and 10 μg/mL gentamicin (Badache *et al.* 1998). T265 cells were split (1 : 5 dilution) weekly using D-PBS supplemented with 0.2% EDTA and 0.0025% acetylated bovine trypsin. Cells used in this study were between passages 18 and 22.

Immunoblot analysis

Immunoblot analysis of phosphorylated CREB (Ser133) was performed according to the procedure of Tabernero *et al.* (1998) with some modifications. Cells were seeded onto six-well culture clusters at a density of 1×10^6 cells/well and serum deprived overnight. Cells were treated with low-glucose DMEM (primary rSC) or high-glucose DMEM (T265) containing 10 μM of the stable TP receptor agonist U46619, 200 μM 3-isobutyl-1-methylxanthine, and 1 mM sodium fluoride (NaF) for 0, 5, 10, 15, 30 or 60 min. Immediately following incubation with agonist, 200 μL of lysis buffer [5 mM Tris–HCl, 10% glycerol, 1% sodium dodecyl sufate (SDS), 2 mM EDTA, 2 mM EGTA, 1 mM NaF and 10 μg/mL leupeptin] was added and the cell lysates were collected from the culture plates using a cell scraper and placed on ice. Lysates were boiled for 10 min and centrifuged for 1 min at 500 *g*. Twenty micrograms of protein was loaded in each lane of a 4–20% SDS-polyacrylamide gel (Novex, Carlsbad, CA, USA). Proteins

were resolved electrophoretically and then transferred to a poly(vinylidene) difluoride (PVDF) membrane. Membranes were incubated in PBS containing 4% milk (PBS-MLK) for 30 min and transferred to a solution of PBS-MLK containing rabbit anti-phosphorylated CREB Ser133 (1 : 1000 dilution, Upstate Biotechnology, Lake Placid, NY, USA) for 16 h at 4°C. Poly(vinylidene) difluoride membranes (DuPont, NEN, Boston, MA, USA) were rinsed in PBS (3 × 5 min) and incubated in PBS-MLK containing horseradish peroxidase-conjugated goat anti-rabbit immunoglobulins (1 : 5000 dilution, Transduction Laboratories, Lexington, KY, USA) for 1 h at room temperature (22°C). Membranes were rinsed as above and developed using Kodak BioMax II film and Super Signal chemiluminescent reagent (Pierce, Rockford, IL, USA).

Immunoblot analysis of TP receptor expression in rSC and T265 cells was performed as described in detail previously (Blackman *et al.* 1999) using a polyclonal antibody raised against a decapeptide sequence (HAALFEWHAV; residues 89–98) from the first extracellular loop of the receptor protein (Borg *et al.* 1993, 1994). Twenty micrograms of cell lysates was prepared and resolved as described above for phosphorylated CREB. Primary (1 : 1000) and secondary (1 : 5000) antibodies were diluted in blocking buffer containing 0.05% Tween-20. Primary and secondary antibody solutions were incubated with PVDF membrane for 1 h on a platform shaker at room temperature. Protein extracts of solubilized human platelet membranes (SMP, 10 μg) and a human erythroleukemia cell line (HEL, 20 μg) were used a positive controls for TP receptor protein expression (Mayeux *et al.* 1989; Borg *et al.* 1994; Allan *et al.* 1996).

Immunocytochemistry

Immunocytochemical analyses of TP receptor expression in primary rSC and the T265 cell line were performed as described previously (Blackman *et al.* 1999) with some modifications. Cells were grown on 12-mm cover glasses and fixed with cold methanol at −10°C for 5 min. Non-specific immune binding sites were blocked by incubation with 10% normal goat serum diluted in PBS (PBS/NGS) for 1 h. Cells were then incubated with primary antibody raised against a peptide sequence from the first extracellular loop of the TP receptor (P2Ab; 1 : 50 in PBS/NGS) for 1 h. In some cases, immunocytochemistry was performed using a primary antibody raised against the purified TP receptor protein (TxAb; diluted 1 : 50 in PBS/NGS). Following a PBS wash (3 × 5 min), cells were incubated with fluorescein isothiocyanate-conjugated goat anti-rabbit antibody (Santa Cruz Biotechnology, Santa Cruz, CA, USA) diluted (1 : 100) in PBS/NGS for 45 min. Cells were then washed using PBS and mounted using FluoroGuard (Vector Laboratories, Burlingame, CA, USA). Fluorescence was visualized using a Jenaval microscope equipped for epi-fluorescence. Immunocytochemical detection of phosphorylated CREB (Ser133) in the T265 cell line was performed as described previously (Tabernero *et al.* 1998) except for the use of VIP (Vector Laboratories, Burlingame, CA, USA) as an horseradish peroxidase substrate.

Radioligand binding assay

Binding of [^{3}H]SQ29,548 to intact primary rSC and T265 cells was evaluated in confluent monolayers of cells cultured in six-well plates. Briefly, cells were washed gently (2 × 1 mL) with warm phenol red-free Hank's balanced salt solution (HBSS). The binding reaction took place in a final volume of 1 mL of HBSS. Following 5 min incubation at room temperature with either vehicle (total binding) or 20 μM unlabeled SQ29,548 (non-specific binding), the cells were incubated for 30 min at room temperature on an orbital shaker with various concentrations of [^{3}H]SQ29,548 (0.625–20 nM). At the end of the incubation period, the cells were washed quickly (2 × 2 mL) with ice-cold HBSS (wash time < 10 s). The monolayers were solubilized by adding 1 mL of 0.5 N NaOH/0.5% SDS and incubating on an orbital shaker for 5 min. The cell lysate was neutralized by adding 3 N HCl and a sample was retained for protein concentration analysis using the BCA assay (Pierce, Rockford, IL, USA). The receptor-bound radioligand was measured by liquid scintillation spectrometry. Radioactivity counts were normalized to the measured protein concentration. Specific binding was calculated as the difference between binding measured in the absence and in the presence of 20 μM unlabeled SQ29,548. Analysis of radioligand binding data was performed using GRAPHPAD PRISM 3.0 (GraphPad Software). Saturation curves were subjected to non-linear regression analysis. Curves were fit to both one-site and two-site bindings and were compared with an F-test. K_D and B_{max} were determined from the best fit equation.

Digital fluorescence ratio imaging of intracellular calcium using fura-2 acetoxymethyl ester

Cells were seeded onto 25-mm glass coverslips in low-glucose DMEM (primary rSC) or high-glucose DMEM (T265 cells) at 37°C in the presence of 5% CO_2 for 6 h and then serum deprived overnight. To avoid the apoptotic death reported in serum-deprived Schwann cells (Delaney *et al.* 1999) cultures were switched to serum-free medium without an intermediate rinse step. This method allows for the maintenance of primary Schwann cell cultures for up to 18 h. Cells were loaded with 3 μM fura-2 acetoxymethyl ester (Fura-2AM; Molecular Probes, Eugene, OR, USA) for 20 min at 37°C in HBSS [in mM: 137.0 NaCl, 5.0 KCl, 2.0 $CaCl_2$, 1.0 $MgSO_4$, 0.44 KH_2PO_4, 0.34 $Na_2HPO_4(7H_2O)$, 20.0 Na^+ HEPES, 1.0 $NaHCO_3$ and 5.0 glucose, pH 7.4], rinsed twice and imaged in the same medium at room temperature using the Zeiss AttoFluor RatioVision system (Rockville, MD, USA). Coverslips were mounted in an AttoFluor chamber with a maximum holding volume of 1 mL. The chamber was filled with 1 mL of warm HBSS and mounted onto the microscope stage of a Zeiss Axiovert 135 inverted microscope equipped for digital fluorescence microscopy. A computer image of the cells was captured using an ICCD camera and 25–30 cellular regions of interest were selected to be digitally monitored. Baseline ratios of Fura-2 fluorescence emission at 520 nm were measured during high-frequency alterations of 334 nm (Ca^{2+} bound) and 380 nm (Ca^{2+} free) excitation filters. Following 90 s of baseline measurements, 10 μL of 1 mM U46619 (Biomol, Plymouth Meeting, PA, USA), a stable TXA_2 mimetic, was diluted into the 1 mL holding volume (≈10 μM final concentration) and assayed for a change in Fura-2 ratio for 90 s. In some experiments, TP receptor antagonists were added after baseline measurements were obtained. Thromboxane receptor antagonists BMS180,291, BM13,505 were generous gifts of Dr K. Stegmeier (Boehringer Mannheim GmbH, Germany). The TP receptor antagonist SQ29,548 was obtained from Biomol. Following 90 s of antagonist treatment, U46619 was added and the cells were further monitored for a calcium response. In the absence of a calcium transient, 10 μM ATP (RBI) was added to elicit a

physiologic response prior to termination of the experiment. All experiments were performed in triplicate. Representative experiments are reported for each experiment.

Determination of thromboxane B_2 levels in conditioned medium
Primary rSC and T265 cells were seeded onto 60-mm culture dishes at 80–85% confluency. Cells were rinsed twice with low-glucose DMEM (primary rSC) or high-glucose DMEM (T265 cells) and held in 4 mL of serum-free DMEM medium for 24 h at 37°C in a humidified incubator (5% CO_2/95% air). Conditioned medium was collected and assayed indirectly for the presence of TXA_2 using an ELISA specific for TXB_2 (Assay Designs Inc., Ann Arbor, MI, USA); a stable metabolite of TXA_2. To determine TXA_2 levels in proliferating rSC, primary rSC were seeded onto 60-mm culture dishes as described above and stimulated with 50 ng/mL Neu-differentiation factor (NDFβ; R & D Systems), a potent mitogen for primary rSC, for 24 h. Thromboxane B_2 was not detected in stock media solutions containing 5% FBS.

Determination of intracellular cAMP levels ($[cAMP]_i$)
Primary rSC and T265 cells were seeded onto 24-well culture plates at a density of 100 000 cells/well in low-glucose DMEM (primary rSC) or high-glucose DMEM (T265 cells) and then serum deprived overnight. All treatments were performed using serum-free medium containing 200 μM 3-isobutyl-1-methylxanthine (Sigma). Solutions containing concentrations of TP receptor agonists spanning four log units (1 nM to 10 μM) were applied for 10 min at 37°C. Specificity of cAMP changes in response to U46619 was determined by pre-incubating cells with varying doses of the TP receptor antagonist BMS180,291 (10 nM to 10 μM) for 5 min followed by 10 μM U46619 for 10 min at 37°C. Following treatment, the media was aspirated completely and the cells were lysed using 200 μL of 0.1 M HCl applied for 1 h at room temperature on a rotary shaker. Lysates were collected in 500 μL centrifuge tubes, centrifuged at 500 *g* for 10 min, and used immediately. $[cAMP]_i$ were determined in triplicate using the acetylated version of a direct enzyme immunoassay kit (Assay Designs, Inc., Ann Arbor, MI, USA) according to the manufacturer's instructions. Data are expressed as fold elevation of cAMP over the basal or non-stimulated state. Mean levels of cAMP content for each condition were determined by averaging values obtained from three separate assays.

Results

Identification of TP receptor protein expression in primary rSC and T265 cells

To determine whether primary rSC and T265 cells expressed TP receptors, we performed immunocytochemical and immunoblot analyses using polyclonal antibodies raised against either the purified TP receptor protein (TxAb) or a decapeptide sequence from the first extracellular loop of the TP receptor (P2Ab; residues 89–98). Both primary rSC and T265 cells demonstrated immunoreactivity for TP receptors (Fig. 1). In T265 cells, TP receptor immunoreactivity was detected predominantly on the cytoplasmic membrane. Similar immunoreactivity was obtained in T265 cells using either TxAb (Fig. 1a) or P2Ab (Fig. 1b). In primary

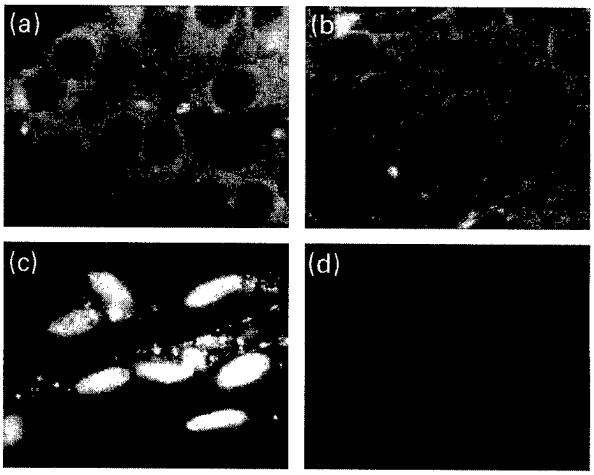

Fig. 1 Immunocytochemical detection of TP receptors. T265 cells were fluorescently labeled using either a polyclonal anti–TP receptor antibody (a, 1 : 50) or a polyclonal anti-peptide antibody (P2Ab; amino acids 89–98) (b, 1 : 50). Incubation of primary rSC with P2Ab (c, 1 : 50) also demonstrated positive immunoreactivity. Incubation of T265 cells with pre-immune IgG from the animal used to create the P2Ab anti-peptide antibody did not produce any detectable immunoreactivity (d). antibody immunoreactivity was visualized using a goat-antirabbit secondary antibody conjugated with FITC (1 : 100).

rSC, immunoreactivity for TP receptors was localized throughout the cellular cytoplasm as well as within the nuclei of the cells (Fig. 1c). Cellular immunoreactivity was not detected using a pre-immune IgG obtained from the animal used to generate P2Ab (Fig. 1d). Similar results were obtained using pre-immune IgG from the animal used to

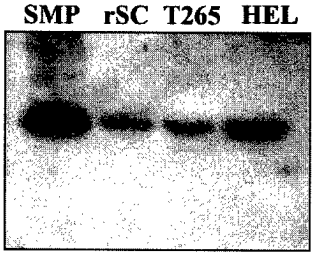

Fig. 2 Identification of TP receptor in protein lysates from primary rSC and T265 cells. Twenty micrograms of protein lysate was resolved electrophoretically on a 4–20% polyacrylamide gel and transferred to PVDF for immunoblot analysis. Incubation with TXA_2 receptor antibody (1 : 1000 dilution) revealed immunoreactivity for a 55-kDa protein in lysates from primary rSC (lane 2) and T265 cells (lane 3) that corresponded to a 55-kDa protein found in lysates obtained from human platelet membranes (SMP, 10 μg; lane 1) and human erythroleukemia cell line (HEL, 20 μg; lane 4). Incubation of PVDF membranes with pre-immune immunoglobulins from the same animal used to produce the anti-peptide antibody did not produce significant immunoreactivity in any of the lysates tested (data not shown).

generate TxAb (data not shown). To confirm that primary rSC and the T265 cells expressed TP receptor protein, we separated membrane protein extracts using SDS–PAGE and analyzed the immunoblots for the presence of TP receptor using the P2Ab. A single, prominent immunoreactive band was present at 55 kDa in both primary rSC and T265 cell extracts (Fig. 2, lanes 2 and 3). As a positive control for TP receptor immunoreactivity, a protein extract of human platelet membranes (Fig. 2, lane 1, SMP) and an extract from a human erythroleukemia cell line (Fig. 2, lane 4, HEL) were electrophoresed in parallel with Schwann cell lysates. The immunoreactive band in both primary rSC and T265 lysates co-migrated with immunoreactivity found in both SMP and HEL extracts (55 kDa). Thromboxane receptor immunoreactivity was not detected in lysates incubated with a pre-immune IgG obtained from the animal used to generate the TP receptor antibody (data not shown). Collectively, these results demonstrate that both primary rSC and T265 cells express TP receptor protein.

Radioligand binding analysis of TXA_2 binding sites in primary rSC and T265 cells

To determine whether the protein visualized by immunocytochemistry and immunoblot analysis represented functional ligand binding sites, saturation binding of the specific TP receptor antagonist [^{3}H]SQ29,548 to both primary rSC and T265 cells was performed using adherent cell cultures (Fig. 3a,b). These experiments revealed a single class of high-affinity binding sites for the ligand in both rSC and T265 cells. Primary rSC binding sites had a dissociation constant (K_D) of 3.58 ± 3.2 nM and a maximum binding (B_{max}) of 2719.63 ± 830.9 fmol/mg protein. T265 cell-binding sites were found to have a K_D of 9.69 ± 7.46 nM and a B_{max} of 196.24 ± 72.08 fmol/mg protein. The binding kinetics of both rSC and T265 cells are comparable with those obtained for the thromboxane receptor in human oligodendroglioma cells (K_D = 4.0 nM; Blackman *et al.* 1998), 1321N1 human astrocytoma cells (K_D = 10.9 nM; Nakahata *et al.* 1992) and human platelets (K_D = 7.3 nM; Hedberg *et al.* 1988).

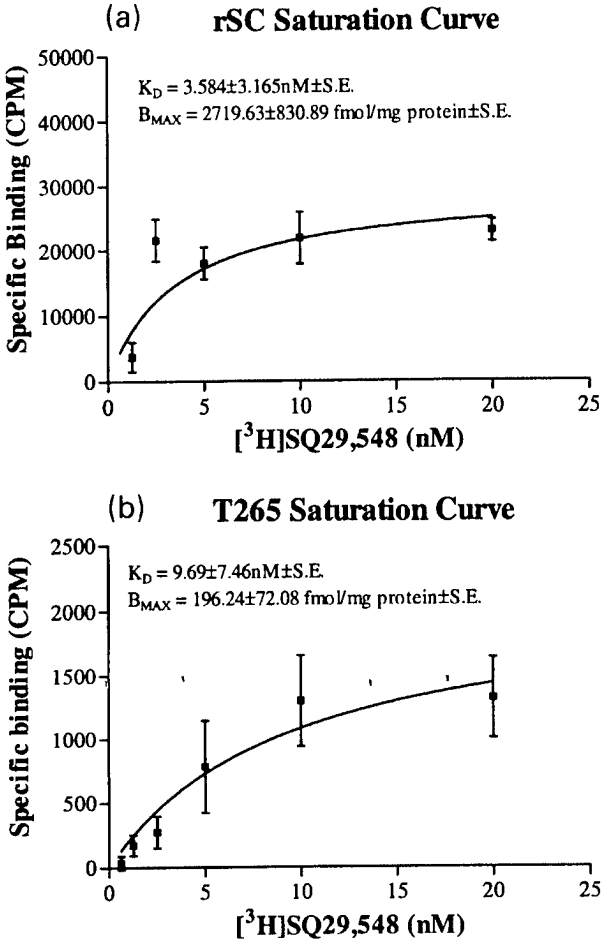

Fig. 3 Radioligand binding analysis of primary rSC and T265 cells. [^{3}H]SQ29,548 binding was measured in the absence (total binding) or presence (non-specific binding) of 20 μM unlabeled SQ29,548 for 30 min. Saturation curves demonstrate the difference between total and non-specific binding (specific binding). (a) Saturation curve for [^{3}H]SQ29,548 binding to primary rat Schwann cells. (b) Saturation curve for [^{3}H]SQ29,548 binding to T265 cells. Data are the average of two (rSC) or four (T265) experiments performed using triplicate determinations of total and non-specific binding for each experiment.

The effect of TP receptor stimulation on intracellular calcium levels

Given that both primary rSC and T265 cells demonstrated immunoreactivity for the TP receptor as well as binding of a receptor-specific antagonist, we tested the functionality of these receptors by digital fluorescence calcium imaging using the calcium-sensitive dye Fura-2. Addition of the TXA_2 mimetic U46619 (10 μM) produced a robust calcium transient in the T265 cell line (Fig. 4a). In contrast, primary rSC did not respond to 10 μM U46619 with an increase in intracellular calcium (Fig. 4a). Primary Schwann cell cultures were responsive to stimulation with 10 μM ATP. Schwann cells isolated from Lewis rats have been shown to produce TXA_2 (Constable *et al.* 1994). Thus, we hypothesized that the lack of physiological calcium response in primary rSC may have been the result of TP receptor desensitization due to endogenous TXA_2 production and release. To test this possibility, we incubated primary rSC with indomethacin (100 mM) for 24 h to inhibit any endogenous TXA_2 production. Primary rSC treated with indomethacin did not respond to U46619 stimulation with an increase in intracellular calcium (data not shown).

Determination of TXA_2 release by primary rSC and T265 cells

To determine the level of production and secretion of TXA_2 by the cells used in this study, we measured TXA_2 levels in conditioned medium from primary rSC and T265 cells after

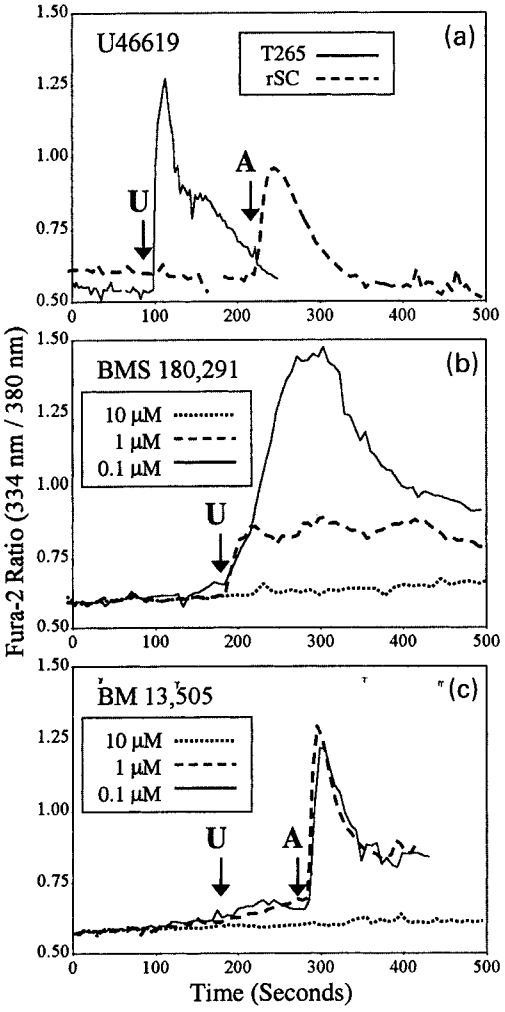

Fig. 4 Analysis of intracellular calcium levels following TP receptor stimulation. (a) Stimulation of T265 cells and primary rSC with 10 μM U46619 (arrow, U) elicited a robust calcium transient in T265 cells but not in primary rSC. Primary rSC were responsive to 10 μM ATP (arrow, A). (b) Prior treatment of T265 cells with the specific TP receptor antagonist BMS180,291 inhibited calcium transients in response to 10 μM U46619 (arrow, U) in a dose-dependent fashion. Complete response inhibition was observed following treatment with 10 μM BMS180,291 and a gradual recovery of calcium transients was observed with decreasing doses of the antagonist. In comparison to antagonist-naive T265 cells (a, solid tracing) antagonist-treated cells responded to U46619 with less synchrony resulting in a broadened calcium tracing (b, solid tracing) or several peaks (b, dashed tracing) indicative of variable response latencies. (c) Pre-treatment of T265 cells with the specific TP receptor antagonist BM13,505 inhibited calcium transients in response to 10 μM U46619 (arrow, U). Addition of 10 μM ATP (solid and dashed tracings, arrow, A) was used to obtain a physiologic response prior to terminating the experiment.

24 h. Using an ELISA specific for TXB_2, a stable metabolite of TXA_2, we found that both quiescent and actively proliferating rSC (50 ng/mL NDFβ for 24 h) did not release any detectable TXB_2 into the medium. In contrast, conditioned medium from T265 cells contained 1.1 ng/mL TXB_2. The concentration of TXB_2 in 1 mL of conditioned medium was calculated to be 2.7 pM, a level of production several orders of magnitude lower than the agonist concentrations utilized in our experiments.

Effect of TP receptor antagonists on U46619-stimulated calcium transients in T265 cells

To determine the specificity of U46619-mediated calcium elevation in T265 cells, we treated T265 cells with various doses of the TP receptor antagonists, BMS180,291 (Fig. 4b) and BM13,505 (Fig. 4c). For each individual experiment, a baseline ratio of Fura-2 fluorescence was obtained for 90 s followed by TP receptor antagonist treatment for 90 s. Following 180 s of ratio measurement, 10 μM U46619 was added to the cells (arrow, U). In the absence of a response to U46619, ATP (10 μM, arrow, A) was added in several experiments. A dose-dependent inhibition of U46619-stimulated calcium elevation was observed using BMS180,291. For the highest dose of BMS180,291 tested (10 μM), complete inhibition of calcium elevation was observed. Compared with antagonist-naive T265 cells (Fig. 4a), T265 cells treated with 1 μM BMS180,291 exhibited a moderate response that was prolonged in duration. Analysis of individual cell tracings reveals a variable response onset to U46619 stimulation (data not shown). A similar distribution of cellular responses across time was present for the lowest dose of BMS180,291 tested (0.1 μM), producing a broadened calcium transient (data not shown). However, in the case of 0.1 μM BMS180,291, no significant inhibition of U46619-stimulated calcium elevation was observed. In contrast to BMS180,291, the TP receptor antagonist BM13,505 inhibited U46619-stimulated calcium elevation for each dose tested (Fig. 4c). T265 cells remained responsive to 10 μM ATP (second arrow, A). Inhibition of calcium elevation in T265 cells following U46619 treatment was also observed using 10 μM of the TP antagonist SQ29,548 (data not shown).

Effect of TP receptor agonists on $[cAMP]_i$

In an effort to identify a functional response for TP receptors in primary rSC we measured $[cAMP]_i$ following treatment with U46619. Both primary rSC and the T265 cell line responded to U46619 treatment by an increase in $[cAMP]_i$ following 10 min of stimulation (Fig. 5a). Elevations in $[cAMP]_i$ following U46619 stimulation were dose dependent in both primary rSC (gray columns) and the T265 cells (black columns). Compared with non-stimulated conditions, the T265 cell line exhibited a 12- to 14-fold elevation in $[cAMP]_i$ at the maximum concentrations of U46619 tested (1 and 10 μM). Similarly, in primary rSC, $[cAMP]_i$ was elevated between 14- (1 μM) and 22-fold (10 μM) over basal conditions following stimulation with U46619. In both rSC and T265 cells, elevations in $[cAMP]_i$ in response to

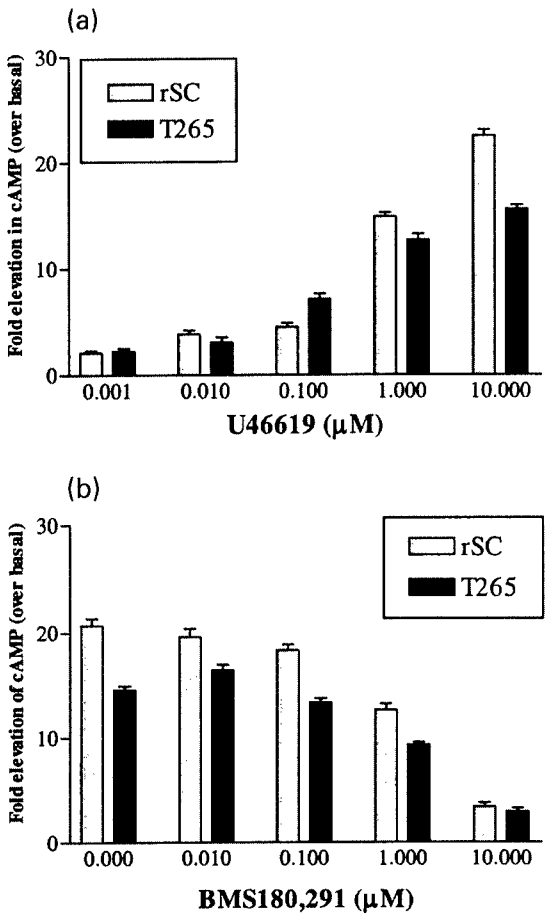

Fig. 5 Dose-dependent elevation of $[cAMP]_i$ following TP receptor stimulation. T265 cells and primary rSC treated with U46619 exhibited a dose dependent elevation in $[cAMP]_i$ following 10 min of receptor stimulation in the presence of 200 μM 3-isobutyl-1-methylxanthine (a). BMS180,298 inhibited cAMP accumulation in response to 10 μM U46619 in a dose-dependent manner in both cell types (b). For both cell types, maximum $[cAMP]_i$ were obtained using either 10 or 1 μM doses of U46619. Error bars represent the SEM of three separate experiments. Basal levels of cAMP/100 000 cells were 1.4 and 2.7 pM for primary rSC and T265, respectively.

U46619 stimulation were inhibited by the TP receptor antagonist BMS180,291 in a dose-dependent fashion (Fig. 5b). Basal levels of cAMP/100 000 cells were 1.4 and 2.7 pmol for primary rSC and T265, respectively.

Phosphorylation of CREB on Ser133 following TP receptor stimulation

To determine whether the intracellular levels of calcium and cAMP in rSC and T265 cells were sufficient to stimulate downstream signaling events to a significant degree, we performed immunoblot analyses of CREB phosphorylation following TP receptor stimulation. The addition of 10 μM U46619 produced an elevation in CREB phosphorylation on Ser133 in both primary rSC and the T265 cell line (Fig. 6).

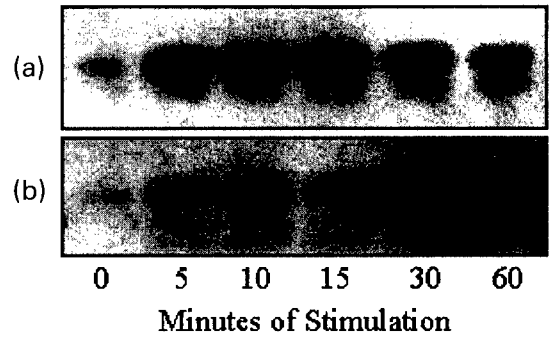

Fig. 6 Time course of CREB phosphorylation on Ser133 following TP receptor stimulation with 10 μM U46619. T265 cells and primary rSC were stimulated with 10 μM U46619 for 0, 5, 10, 15, 30 or 60 min and then lysed in preparation for immunoblot analyses of CREB phosphorylation. Immunoblot analyses demonstrate that CREB was phosphorylated within 5 min of stimulation in both T265 cells (a) and primary rSC (b).

Cyclic AMP response-element binding protein phosphorylation was strongly elevated in T265 cells following 5 min of stimulation (Fig. 6a). Cyclic AMP response-element binding protein phosphorylation was also detected in primary rSC following 5 min of treatment with maximal levels achieved following 10 min of stimulation (Fig. 6b). In both cell types, the level of CREB phosphorylation remained elevated for at least 45 min with a decrease towards basal levels after 60 min of stimulation. In T265 cells, a second immunoreactive band was detected below that corresponding to phosphorylated CREB at later time points (15–60 min). The identity of this second immunoreactive band has been shown to correspond to ATF-1, a molecule related to CREB family of transcription factors (Ginty *et al.* 1993). Interestingly, CREB was phosphorylated to a higher degree in T265 cells than in primary rSC. Using identical protein concentrations and immunoblotting conditions, immunoblots of phosphorylated CREB using T265 lysates routinely required 10-fold less exposure (30 s) than primary rSC lysates (5 min) for significant signal to develop. To further characterize the extent of CREB phosphorylation following U46619 stimulation, we performed immunocytochemistry using the T265 cell line. Compared with background levels of immunoreactivity (Fig. 7a), unstimulated T265 cells demonstrated low levels of basal CREB phosphorylation in the nuclear cytoplasm (Fig. 7b). Stimulation with 10 μM U46619 for 15 min produced a significant increase in nuclear immunoreactivity in these cells (Fig. 7c). Significant differences in nuclear staining intensity for phosphorylated CREB were not observed between non-stimulated primary rSC and primary rSC treated with U46619 (data not shown), consistent with the observation that immunoblot analyses of phosphorylated CREB in primary rSC required 10-fold longer exposures than in T265 cells.

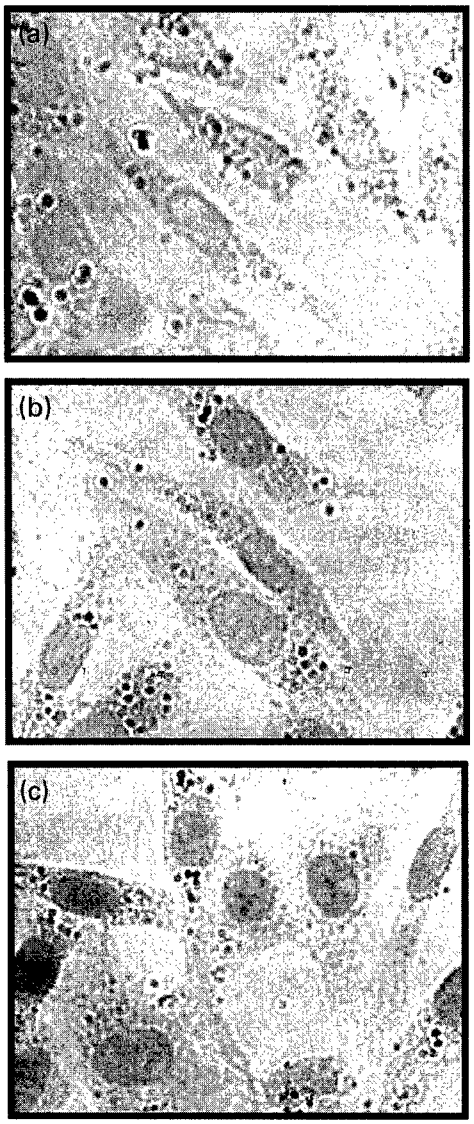

Fig. 7 Stimulation of CREB phosphorylation on Ser133 following TP receptor stimulation. Compared with labeling with secondary antibody alone (a), unstimulated T265 cells demonstrated low, basal levels of nuclear immunoreactivity for phosphorylated CREB (b, arrowheads). T265 cells stimulated with 10 μM U46619 for 15 min demonstrated increased nuclear immunoreactivity for antibodies raised against CREB phosphorylated on Ser133 (c, arrowheads).

Discussion

In this report, we demonstrate that both primary rSC and T265 cells express TP receptors using immunochemical and functional approaches. Immunoblot analyses reveal the presence of a 55-kDa protein that is reactive with an antibody raised against both a TP receptor decapeptide sequence (P2Ab) and purified human platelet TP receptor (TxAb) (Fig. 2). Immunocytochemical analysis using both of these antibodies demonstrated specific immunoreactivity (Fig. 1). Of note, although both primary rSC and T265 cells were labeled on the cytoplasmic membrane, only primary rSC demonstrated staining of both the nuclear and cytoplasmic membranes. Recent reports have identified functional EP2, EP3 and EP4 prostaglandin receptors within the nuclear envelope of HEK 293 and porcine cerebral microvascular endothelial cells (Bhattacharya *et al.* 1998, 1999). These findings, along with the data presented here, raise the interesting possibility that TP receptors may also be present within the nuclear envelope in Schwann cells and in other cell types.

Experiments were performed to evaluate the ability of intact rSC and T265 cells to bind a TP receptor ligand ([^{3}H]SQ29,548). The results demonstrated that rSC cells express 2719 fmol of receptor per mg protein with a K_D value of $\approx$ 3.6 nM. T265 cells, however, exhibit $\approx$ 196 fmol of receptor per mg protein with a K_D value of $\approx$ 9.7 nM. These data reveal a 13-fold difference in receptor density between primary rat and tumor-derived human Schwann cells. It is possible that the lower receptor density seen in T265 cells is due to altered expression of native protein secondary to transformation. Alternatively, it is possible that the T265 cell behaves as a less differentiated form of Schwann cell and that TP receptor expression varies with cell differentiation. It should be noted, however, that the K_D for both Schwann and T265 cells reported here are comparable with values observed in human platelets as well as in astrocytoma and oligodendroglioma cell lines (Nakahata *et al.* 1992; Blackman *et al.* 1998).

Functional characterization of TP receptors revealed that distinct intracellular signaling mechanisms were activated following receptor activation in these two cell types (Figs 4 and 5). Receptor stimulation with the stable TXA_2 mimetic U46619 produced a robust calcium transient in T265 cells that could be inhibited by prior treatment with several different TP receptor antagonists. In contrast to T265 cells, stimulation with U46619 did not elevate intracellular calcium in primary rSC. Interestingly, TP receptor stimulation also produced a specific, dose-dependent elevation in $[cAMP]_i$ in T265 cells as well as in primary rSC. Furthermore, a time-dependent elevation in the level of CREB phosphorylation on Ser133 was also detected in both T265 cells and primary rSC. Cyclic AMP response-element binding protein phosphorylation can be stimulated by diverse intracellular mechanisms that include both calcium- and cAMP-dependent signaling pathways (Montminy 1997; Shaywitz and Greenberg 1999). Because U46619 stimulated an elevation in intracellular calcium and $[cAMP]_i$ in T265 cells, it is possible that one or both of these signaling pathways contributed to the subsequent phosphorylation of CREB. However, because U46619 stimulation did not affect intracellular calcium levels in primary rSC, it appears that CREB was phosphorylated mainly by a cAMP-dependent mechanism in these cells. Compared with primary rSC,

CREB was phosphorylated more rapidly and to a higher degree in T265 cells (Fig. 6a), suggesting that calcium elevation following U46619 stimulation may contribute significantly to CREB phosphorylation.

Physiologic factors which stimulate cAMP in Schwann cells

It is well established that elevations in $[cAMP]_i$ in Schwann cells have profound effects on Schwann cell physiology (Sobue and Pleasure 1984). The plant diterpene forskolin, cholera toxin and non-hydrolyzable, cell-permeant analogs of cAMP are the most common pharmacological compounds used to elevate $[cAMP]_i$ in primary rSC (Yamada *et al.* 1995). However, despite the frequent application of these pharmacologic agents in Schwann cell biology, the absolute $[cAMP]_i$ that are attained by these non-physiologic means have yet to be determined and few physiologic factors that stimulate cAMP accumulation in primary rSC have been identified. Schwann cells have been shown to respond to both β-adrenergic ligands (Yasuda *et al.* 1988) and calcitonin gene-related peptide (Cheng *et al.* 1995) by an elevation in $[cAMP]_i$. Here, we identified U46619 as novel physiologic analog that is capable of stimulating intracellular cAMP accumulation and CREB phosphorylation in primary rSC and T265 cells. Activation of TP receptors has been shown to functionally couple to a wide variety of G-proteins including G_q (Knezevic *et al.* 1993; Allan *et al.* 1996) and $G_{12/13}$ (Offermanns *et al.* 1994; Allan *et al.* 1996; Djellas *et al.* 1999). In addition, TP receptors have been shown to modulate the activity of adenylyl cyclase, although the exact mechanism by which this occurs is unclear. Although both TPα and TPβ receptor isoforms activate phospholipase C to a similar extent, activation of TPα in transfected cells has been shown to elevate $[cAMP]_i$, whereas activation of TPβ in transfected cells decreases adenylyl cyclase activity (Hirata *et al.* 1996; Walsh *et al.* 1998; Cracowski *et al.* 2000). In primary rSC and T265 cells, U46619 stimulated a dose-dependent elevation of $[cAMP]_i$ suggesting that these cells may both express predominantly TPα. The levels of TPα and TPβ and the contribution of these receptors to intracellular cAMP accumulation in primary rSC and T265 cells remains to be determined as the antibodies used in this study were not devised to distinguish between the two TP receptor isoforms.

Schwann cells as a potential source of eicosanoids within peripheral nerve

In our studies, significant levels of TXB_2, a stable metabolite of TXA_2, were not detected in medium conditioned by primary rSC. In contrast, TXB_2 was detected in medium conditioned by T265 cells. Schwann cells isolated from Lewis rats have been shown to produce significant amounts of TXA_2 under both basal conditions and following an experimental elevation in intracellular calcium levels (Constable *et al.* 1994). The finding that Schwann cells isolated from Lewis rats have significantly elevated levels of TXB_2 may be species specific, suggesting that the rats used in our study may differ in some respects. Alternatively, the discrepancy may be due to the detection level of the competitive ELISA assay used in our experiments compared with the scintillation proximity assay used by Constable *et al.* (1994), which has an order of magnitude greater sensitivity.

Potential role of TP receptors in diseases affecting peripheral nerve

The identification of functional TP receptors in Schwann cells suggests that the normal or abnormal release of TP within peripheral nerve may modulate Schwann cell physiology under either normal or pathological conditions, respectively. Following peripheral nerve injury, blood-derived macrophages invade the site of injury and then differentiate into activated macrophages (Beuche and Friede 1986; Langley and Pearce 1998). Macrophages participate in the removal of degenerating axonal and myelin debris and the establishment of a local environment that is conducive for axonal regeneration (Heumann *et al.* 1987; Griffin *et al.* 1992; Avellino *et al.* 1995; Dailey *et al.* 1998). Macrophages have been shown to digest and release protein fragments of myelin basic protein from myelin phagocytized at the injury site (Baichwal *et al.* 1988). These myelin basic protein fragments have been shown to be mitogenic in the presence of experimentally elevated cAMP levels in Schwann cells (Tzeng *et al.* 1995). In addition to the production and secretion of cytokines and free radicals, macrophages have long been known to be a major source of eicosanoids including TXA_2. Our findings suggest that TXA_2 may be a physiologic factor that could operate in conjunction with myelin basic protein fragments to stimulate Schwann cell proliferation following peripheral nerve injury. The discovery of TP receptors in Schwann cells also raises the interesting possibility that these cells may express additional eicosanoid receptors (e.g. EP and IP) that may also be coupled to changes in $[cAMP]_i$.

In sum, this study is the first report of functional TXA_2 receptors in Schwann cells. The receptor was found to have an electrophoretic mobility, immunoreactivity and radioligand-binding kinetics similar to those of platelet and oligodendroglioma TXA_2 receptors. Activation of Schwann cell TP receptors stimulates elevations in $[cAMP]_i$ and the phosphorylation of CREB. Activation of TP receptors in a Schwann cell tumor line leads to elevations in both $[cAMP]_i$ and intracellular calcium. The results presented here indicate that activation of Schwann cell TP receptors leads to the mobilization of cAMP and, in a transformed cell line, both calcium and cAMP, which contributes in part to the translocation of CREB to the cell nucleus. Taken together, these findings suggest a novel pathway for by which

Schwann cells could respond to mediators released during inflammation within the PNS.

Acknowledgements

This work was supported by a grant from the Department of the Army #DAM17-98-01-860 and a grant from the Medical Research Service Department of Veterans Affairs awarded to GHDV. This work was also supported by grant #RG3054A1/1 from the National Multiple Sclerosis Society awarded to GCL. NM is the recipient of a Loyola University Graduate Fellowship from the Schmidt Foundation.

References

Allan C. J., Higashiura K., Martin M., Morinelli T. A., Kurtz D. T., Geoffroy O., Meier G. P., Gettys T. W. and Halushka P. V. (1996) Characterization of the cloned HEL cell thromboxane A_2 receptor: evidence that the affinity state can be altered by G alpha 13 and G alpha q. *J. Pharmacol. Exp. Ther.* **277**, 1132–1139.

Avellino A. M., Hart D., Dailey A. T., MacKinnon M., Ellegala D. and Kliot M. (1995) Differential macrophage responses in the peripheral and central nervous system during Wallerian degeneration of axons. *Exp. Neurol.* **136**, 183–198.

Badache A., Muja N. and De Vries G. H. (1998) Expression of Kit in neurofibromin-deficient human Schwann cells: role in Schwann cell hyperplasia associated with type 1 neurofibromatosis. *Oncogene* **17**, 795–800.

Baichwal R. R., Bigbee J. W. and DeVries G. H. (1988) Macrophage-mediated myelin-related mitogenic factor for cultured Schwann cells. *Proc. Natl Acad. Sci. USA* **85**, 1701–1705.

Beuche W. and Friede R. L. (1986) Myelin phagocytosis in Wallerian degeneration of peripheral nerves depends on silica-sensitive, *bg/bg*-negative and Fc-positive monocytes. *Brain Res.* **378**, 97–106.

Bhattacharya M., Peri K. G., Almazan G., Ribeiro-da-Silva A., Shichi H., Durocher Y., Abramovitz M., Hou X., Varma D. R. and Chemtob S. (1998) Nuclear localization of prostaglandin E_2 receptors. *Proc. Natl Acad. Sci. USA* **95**, 15792–15797.

Bhattacharya M., Peri K., Ribeiro-da-Silva A., Almazan G., Shichi H., Hou X., Varma D. R. and Chemtob S. (1999) Localization of functional prostaglandin E_2 receptors EP3 and EP4 in the nuclear envelope. *J. Biol. Chem.* **274**, 15719–15724.

Blackman S. C., Dawson G., Antonakis K. and Le Breton G. C. (1998) The identification and characterization of oligodendrocyte thromboxane A_2 receptors. *J. Biol. Chem.* **273**, 475–483.

Blackman S. C., Borg C., Yeomans D. C. and Le Breton G. C. (1999) Assessment of cellular localization of the thromboxane A_2 receptor by immunocytochemistry. *Methods Mol. Biol.* **120**, 145–171.

Borg C., Lam S. C., Dieter J. P., Lim C. T., Komiotis D., Venton D. L. and Le Breton G. C. (1993) Anti-peptide antibodies against the human blood platelet thromboxane A_2/prostaglandin H_2 receptor. Production, purification and characterization. *Biochem. Pharmacol.* **45**, 2071–2078.

Borg C., Lim C. T., Yeomans D. C., Dieter J. P., Komiotis D., Anderson E. G. and Le Breton G. C. (1994) Purification of rat brain, rabbit aorta, and human platelet thromboxane A_2/prostaglandin H_2 receptors by immunoaffinity chromatography employing anti-peptide and anti-receptor antibodies. *J. Biol. Chem.* **269**, 6109–6116.

Brock T. G., McNish R. W. and Peters-Golden M. (1999) Arachidonic acid is preferentially metabolized by cyclooxygenase-2 to prostacyclin and prostaglandin E_2. *J. Biol. Chem.* **274**, 11660–11666.

Brockes J. P., Fields K. L. and Raff M. C. (1979) Studies on cultured rat Schwann cells. I. Establishment of purified populations from cultures of peripheral nerve. *Brain Res.* **165**, 105–118.

Brück W. (1997) The role of macrophages in Wallerian degeneration. *Brain Pathol.* **7**, 741–752.

Bruner G. and Murphy S. (1993) Purinergic P_{2Y} receptors on astrocytes are directly coupled to phospholipase A_2. *Glia* **7**, 219–224.

Cheng L., Khan M. and Mudge A. W. (1995) Calcitonin gene-related peptide promotes Schwann cell proliferation. *J. Cell Biol.* **129**, 789–796.

Constable A. L., Armati P. J., Toyka K. V. and Hartung H. P. (1994) Production of prostanoids by Lewis rat Schwann cells *in vitro*. *Brain Res.* **635**, 75–80.

Cracowski J. L., Stanke-Labesque F., Chavanon O., Corompt E., Veitl S., Blin D., Bessard G. and Devillier P. (2000) Thromboxane A_2 modulates cyclic AMP relaxation and production in human internal mammary artery. *Eur. J. Pharmacol.* **387**, 295–302.

Dailey A. T., Avellino A. M., Benthem L., Silver J. and Kliot M. (1998) Complement depletion reduces macrophage infiltration and activation during Wallerian degeneration and axonal regeneration. *J. Neurosci.* **18**, 6713–6722.

Delaney C. L., Cheng H. L. and Feldman E. L. (1999) Insulin-like growth factor-I prevents caspase-mediated apoptosis in Schwann cells. *J. Neurobiol.* **41**, 540–548.

Djellas Y., Manganello J. M., Antonakis K. and Le Breton G. C. (1999) Identification of G alpha 13 as one of the G-proteins that couple to human platelet thromboxane A_2 receptors. *J. Biol. Chem.* **274**, 14325–14330.

FitzGerald G. A. (1991) Mechanisms of platelet activation: thromboxane A_2 as an amplifying signal for other agonists. *Am. J. Cardiol.* **68**, 11B–15B.

Gao Y., Tang S., Zhou S. and Ware J. A. (2001) The thromboxane A_2 receptor activates mitogen-activated protein kinase via protein kinase C-dependent Gi coupling and Src-dependent phosphorylation of the epidermal growth factor receptor. *J. Pharmacol. Exp. Ther.* **296**, 426–433.

Ginty D. D., Kornhauser J. M., Thompson M. A., Bading H., Mayo K. E., Takahashi J. S. and Greenberg M. E. () Regulation of CREB phosphorylation in the suprachiasmatic nucleus by light and a circadian clock. *Science* **260**, 238–241.

Goodrum J. F., Earnhardt T., Goines N. and Bouldin T. W. (1994) Fate of myelin lipids during degeneration and regeneration of peripheral nerve: an autoradiographic study. *J. Neurosci.* **14**, 357–367.

Griffin J. W., George R., Lobato C., Tyor W. R., Yan L. C. and Glass J. D. (1992) Macrophage responses and myelin clearance during Wallerian degeneration relevance to immune-mediated demyelination. *J. Neuroimmunol.* **40**, 153–165.

Halushka P. V., Allan C. J. and Davis-Bruno K. L. (1995) Thromboxane A_2 receptors. *J. Lipid Mediat. Cell Signal.* **12**, 361–378.

Hedberg A., Hall S. E., Ogletree M. L., Harris D. N. and Lie E. C. (1988) Characterization of [5,6-3H]SQ 29,548 as a high affinity radioligand, binding to thromboxane A2/prostaglandin H2-receptors in human platelets. *J. Pharmacol. Exp. Ther.* **245**, 786–792.

Heumann R., Lindholm D., Bandtlow C., Meyer M., Radeke M. J., Misko T. P., Shooter E. and Thoenen H. (1987) Differential regulation of mRNA encoding nerve growth factor and its receptor in rat sciatic nerve during development, degeneration, and regeneration: role of macrophages. *Proc. Natl Acad. Sci. USA* **84**, 8735–8739.

Hirata M., Hayashi Y., Ushikubi F., Yokota Y., Kageyama R.,

Nakanishi S. and Narumiya S. (1991) Cloning and expression of cDNA for a human thromboxane A_2 receptor. *Nature* **349**, 617–620.

Hirata T., Ushikubi F., Kakizuka A., Okuma M. and Narumiya S. (1996) Two thromboxane A2 receptor isoforms in human platelets. Opposite coupling to adenylyl cyclase with different sensitivity to Arg60 to Leu mutation. *J. Clin. Invest.* **97**, 949–956.

Kim S. O., Lim C. T., Lam S. C., Hall S. E., Komiotis D., Venton D. L. and Le Breton G. C. (1992) Purification of the human blood platelet thromboxane A_2/prostaglandin H_2 receptor protein. *Biochem. Pharmacol.* **43**, 313–322.

Knezevic I., Borg C. and Le Breton G. C. (1993) Identification of G_q as one of the G-proteins which copurify with human platelet thromboxane A_2/prostaglandin H_2 receptors. *J. Biol. Chem.* **268**, 26011–26017.

Langley D. and Pearce B. (1998) Pyrimidine nucleotide-stimulated thromboxane A_2 release from cultured glia. *Cell. Mol. Neurobiol.* **18**, 477–486.

Mayeux P. R., Mais D. E., Carr C. and Halushka P. V. (1989) Human erythroleukemia cells express functional thromboxane A_2/prostaglandin H_2 receptors. *J. Pharmacol. Exp. Ther.* **250**, 923–927.

Miggin S. M. and Kinsella B. T. (1998) Expression and tissue distribution of the mRNAs encoding the human thromboxane A2 receptor (TP) alpha and beta isoforms. *Biochim. Biophys. Acta* **1425**, 543–559.

Minghetti L. and Levi G. (1995) Induction of prostanoid biosynthesis by bacterial lipopolysaccharide and isoproterenol in rat microglial cultures. *J. Neurochem.* **65**, 2690–2698.

Montminy M. (1997) Transcriptional regulation by cyclic AMP. *Annu. Rev. Biochem.* **66**, 807–822.

Nakahata N., Ishimoto H., Kurita M., Ohmori K., Takahashi A. and Nakanishi H. (1992) The presence of thromboxane A_2 receptors in cultured astrocytes from rabbit brain. *Brain Res.* **583**, 100–104.

Nusing R. M., Hirata M., Kakizuka A., Eki T., Ozawa K. and Narumiya S. (1993) Characterization and chromosomal mapping of the human thromboxane A_2 receptor gene. *J. Biol. Chem.* **268**, 25253–25259.

Offermanns S., Laugwitz K. L., Spicher K. and Schultz G. (1994) G proteins of the G_{12} family are activated via thromboxane A_2 and thrombin receptors in human platelets. *Proc. Natl Acad. Sci. USA* **91**, 504–508.

Parent J. L., Labrecque P., Orsini M. J. and Benovic J. L. (1999) Internalization of the TXA2 receptor alpha and beta isoforms. Role of the differentially spliced COOH terminus in agonist-promoted receptor internalization. *J. Biol. Chem.* **274**, 8941–8948.

Pearce B., Murphy S., Jeremy J., Morrow C. and Dandona P. (1989) ATP-evoked Ca^{2+} mobilisation and prostanoid release from astrocytes: P_2-purinergic receptors linked to phosphoinositide hydrolysis. *J. Neurochem.* **52**, 971–977.

Peters-Golden M. (1997) *Lung Macrophages and Dendritic Cells in Health and Disease* (Lipscomb M. and Russell S., eds), pp. 151–182. Marcel Dekker, New York.

Raychowdhury M. K., Yukawa M., Collins L. J., McGrail S. H., Kent K. C. and Ware J. A. (1994) Alternative splicing produces a divergent cytoplasmic tail in the human endothelial thromboxane A_2 receptor. *J. Biol. Chem.* **269**, 19256–19261.

Rothwell N. J. and Hopkins S. J. (1995) Cytokines and the nervous system II: actions and mechanisms of action. *Trends Neurosci.* **18**, 130–136.

Shaywitz A. J. and Greenberg M. E. (1999) CREB: a stimulus-induced transcription factor activated by a diverse array of extracellular signals. *Annu. Rev. Biochem.* **68**, 821–861.

Smith W. L. (1992) Prostanoid biosynthesis and mechanisms of action. *Am. J. Physiol.* **263**, F181–F191.

Sobue G. and Pleasure D. (1984) Schwann cell galactocerebroside induced by derivatives of adenosine 3′,5′-monophosphate. *Science* **224**, 72–74.

Tabernero A., Stewart H. J. S., Jessen K. R. and Mirsky R. (1998) The neuron-glia signal beta neuregulin induces sustained CREB phosphorylation on Ser-133 in cultured rat Schwann cells. *Mol. Cell Neurosci.* **10**, 309–322.

Tzeng S. F., Deibler G. E., Neuberger T. J. and DeVries G. H. (1995) Two mitogenic regions of myelin basic protein interact with different receptors to induce Schwann cell proliferation in a cAMP dependent process. *J. Neurosci. Res.* **42**, 758–767.

Ushikubi F., Nakamura K. and Narumiya S. (1994) Functional reconstitution of platelet thromboxane A2 receptors with Gq and Gi2 in phospholipid vesicles. *Mol. Pharmacol.* **46**, 808–816.

Vane J. R., Bakhle Y. S. and Botting R. M. (1998) Cyclooxygenases 1 and 2. *Annu. Rev. Pharmacol. Toxicol.* **38**, 97–120.

Vezza R., Habib A. and FitzGerald G. A. (1999) Differential signaling by the thromboxane receptor isoforms via the novel GTP-binding protein, G_h. *J. Biol. Chem.* **274**, 12774–12779.

Walsh M. T., Foley J. F. and Kinsella B. T. (1998) Characterization of the role of N-linked glycosylation on the cell signaling and expression of the human thromboxane A_2 receptor alpha and beta isoforms. *J. Pharmacol. Exp. Ther.* **286**, 1026–1036.

Walsh M. T., Foley J. F. and Kinsella B. T. (2000) The α, but not the β, isoform of the human thromboxane A2 receptor is a target for prostacyclin-mediated desensitization. *J. Biol. Chem.* **275**, 20412–20423.

Yamada H., Martin P. M. and Suzuki K. (1995) Schwann cell responses to forskolin and cyclic AMP analogues: comparative study of mouse and rat Schwann cells. *Brain Res.* **681**, 97–104.

Yasuda T., Sobue G., Mitsuma T. and Takahashi A. (1988) Peptidergic and adrenergic regulation of the intracellular 3′,5′-cyclic adenosine monophosphate content in cultured rat Schwann cells. *J. Neurol. Sci.* **88**, 315–325.

Yukawa M., Yokota R., Eberhardt R. T., von Andrian L. and Ware J. A. (1997) Differential desensitization of thromboxane A2 receptor subtypes. *Circ. Res.* **80**, 551–556.

J. Biol. Chem.,submitted

Activation of the cAMP-dependent signaling cascade in primary Schwann cells by prostaglandins.

*Naser Muja and †§George H. DeVries

**Neuroscience Graduate Program and the †Department of Cell Biology, Neurobiology, and Anatomy Loyola University of Chicago, Maywood, IL 60153*
§Research Service, Edward Hines Jr. VA Hospital, Hines, IL 60141

Running title: Prostaglandins elevate cAMP in Schwann cells
Pages: 54; 44 (double spaced) + 7 figures
Figures: 7
Tables: 0
Abstract: 235 words
Introduction: 497 words
Discussion: 1497 words

Acknowledgements: This work was supported by a grant from the Medical Research Service Department of Veterans Affairs (G.H.DV.) and a Loyola University Schmidt Fellowship (N.M.). We thank Dr. Russ Hart and colleagues at Assay Designs, Inc. for their technical advice in the use of ELISA to determine intracellular cAMP levels. We thank Ian Dang for sharing his expertise in the use of RT-PCR to identify prostaglandin receptor mRNA transcripts.

Address correspondence to:
Dr. George H. DeVries
Research Service 151
Building 1, Room C432
Edward Hines Jr. VA Hospital
Hines, IL 60141
Tel: (708) 202-2262 Fax: (708) 216-5969
E-mail: gdevrie@orion.it.luc.edu

The abbreviations used are: AA, Arachidonic acid; cAMP, Cyclic adenosine 3',5'-monophosphate; $[cAMP]_i$, intracellular cAMP concentration; CGRP, Calcitonin gene related peptide; CREB, cAMP responsive element binding protein; DMEM, Dulbecco's modified Eagle's medium; D-PBS, Dulbecco's modified phosphate-buffered saline; FBS, Fetal bovine serum; G protein, GTP-binding protein; IBMX, Isobutyl methyl xanthine; NDFβ, neu differentiation factor β; PDE, Phosphodiesterase; PGE_1, PLA_2, Phospholipase A_2;Prostaglandin E1; PGE_2, Prostaglandin E_2; PGI_2, Prostaglandin I_2; PKA, Protein kinase A.

Abstract

Experimentally elevated levels of intracellular cyclic 3',5'-adenosine monophosphate levels ($[cAMP]_i$) have been shown modulate many aspects of Schwann cell physiology *in vitro*. However, few physiologic factors are known to elevate $[cAMP]_i$ in primary Schwann cells. We demonstrate that primary Schwann cells express mRNA transcripts encoding the EP2, EP4, and IP prostaglandin receptors. Prostaglandin receptor stimulation using either PGE_1, PGE_2, or PGI_2 produced a dose dependent elevation in $[cAMP]_i$ in primary Schwann cells. Peak elevations in $[cAMP]_i$ occurred within 15 minutes of stimulation and a gradual recovery of $[cAMP]_i$ towards basal levels was observed between 30 and 90 minutes of stimulation for each prostaglandin tested. Prostaglandin receptor stimulation also produced an increase in the phosphorylation of cAMP-response element binding protein (CREB) on Ser-133 within 5 minutes of exposure. Consistent with the observed decline in $[cAMP]_i$ over time, a gradual decrease in the level of CREB phosphorylation was observed following 30 minutes of stimulation with 1 μM of either PGE_1, PGE_2, or PGI_2. CREB phosphorylation in response to stimulation with PGE_1, PGE_2, or PGI_2 was inhibited by prior treatment with the specific protein kinase A inhibitor, H-89, in a dose dependent fashion. We conclude that prostaglandins are physiologic factors that potently stimulate cAMP-mediated signaling events in Schwann cells. Furthermore, we propose that macrophage-derived prostaglandins may be important modulators of Schwann cell proliferation following traumatic peripheral nerve injury.

Keywords: axotomy; cAMP; CREB; glia; macrophage; Schwann cells; peripheral nerve; prostaglandin E2; prostaglandin I2; regeneration; Wallerian Degeneration

Experimental elevation of intracellular 3',5'-cyclic adenosine monophosphate $[cAMP]_i$ using pharmacologic compounds such as forskolin and cell permeant cAMP analogues can mimic several aspects of neuron-Schwann cell interactions including proliferation (Baichwal and DeVries, 1989; Davis and Stroobant, 1990; Weinmaster and Lemke, 1990; Rahmatullah et al., 1998 Tzeng et al., 1999), and differentiation (Sobue and Pleasure, 1984; Lemke and Chao, 1988; Mokuno et al., 1988; Monuki et al., 1989; Morgan et al., 1991; LeBlanc et al., 1992; Scherer et al., 1994). Similarly, retroviral inhibition of cellular protein kinase A (PKA) inhibited myelination, but not mitosis, by Schwann cells in response to neurite contact (Howe and McCarthy, 2000). Together, these pharmacologic and genetic approaches strongly implicate cAMP-mediated signaling events as key regulators of intercellular signaling between Schwann cells and neurons. Yet, to date, no physiologic factor has been shown to reproduce the pharmacologic and physiologic effects of forskolin in primary Schwann cells. Furthermore, the putative axonal factors that elevate $[cAMP]_i$ and stimulate PKA activity in Schwann cells remain to be identified. While both norepinephrine (Yasuda et al., 1988) and CGRP (Cheng et al., 1995) produced a rapid, receptor-mediated elevation in $[cAMP]_i$, it is not known whether these physiologic factors can stimulate PKA activation, CREB phosphorylation, and subsequent physiologic effects that are similar to those produced by forskolin in Schwann cells. Furthermore, the physiologic sources of these factors for Schwann cells remain to be determined.

Following injury, monocytes infiltrate the degenerating distal nerve segment where they differentiate into resident tissue macrophages (Brück, 1997; Stoll and Müller, 1999). Upon recruitment, macrophages participate in the phagocytosis of cellular debris (Beuche and Friede, 1984; Scheidt et al., 1986; Griffin et al., 1992; Avellino et al., 1995). Selective elimination of circulating monocytes produces a significant reduction in the extent of myelin and axonal debris removal following peripheral nerve injury (van Rooijen and Sanders, 1994; Perry et al., 1995; Brück et al., 1996; Kubota et al., 1998). Similarly, blockade of macrophage activation attenuated the extent of debris clearance at the injury site even though recruitment was not affected (Brück and Friede, 1990; da Costa et al., 1997; Dailey et al., 1998; Liu et al., 1999). Impaired macrophage function also results in significantly reduced Schwann cell proliferation (Kubota et al., 1998) and reduced axonal outgrowth (Dailey et al., 1998). Thus, macrophage recruitment and activation within peripheral nerve are necessary for maximal Schwann cell proliferation and axonal regeneration to occur. However, macrophage recruitment also contributes to neuropathic pain and peripheral nerve edema (Ramer et al., 1997; Syriatowicz et al., 1999; Liu et al. 2000). The mechanisms by which macrophages influence Schwann cell physiology following peripheral nerve injury are not well understood. Macrophages have been shown to produce and release a diverse array of soluble factors upon recruitment to peripheral nerve injury sites ( ). Prostaglandins E_2 (PGE_2) and I_2 (PGI_2) are macrophage-derived factors that are known to contribute to the development of pain sensations and tissue inflammation following injury (Syriatowicz et al., 1999). Prostaglandins activate receptors coupled to heterotrimeric GTP-binding proteins (G proteins) to produce an elevation in either intracellular calcium ($[Ca^{++}]_i$) or cAMP concentration ($[cAMP]_i$) (Coleman et al., 1994). Given the role of experimentally elevated levels of $[cAMP]_i$ in Schwann cell physiology. The reduction in injury-induced Schwann cell proliferation in animals with impaired macrophage function may be due the absence of macrophage-derived prostaglandins that elevate $[cAMP]_i$ in Schwann cells and augment cell proliferation in response to mitogens. We hypothesize that Schwann cells express

prostaglandin receptors and that activation of these receptors stimulates cAMP-mediated signaling events.

These results have previously been presented in abstract form (Muja and DeVries, 1999).

Methods

Primary Schwann cell culture.

Primary Schwann cells were cultured from neonatal rat sciatic nerves. Sciatic nerves from 2 day old rat pups were extracted and enzymatically digested with 0.3 % collagenase in DMEM with low glucose and 10 mM HEPES (HE) for 45 min at 37°C and then for another 45 min in the same solution supplemented with 0.25 % porcine trypsin. Following digestion, the cells were centrifuged at 100 X *g* for 5 min, resuspended in 1 ml of HF consisting of DMEM with low glucose supplemented with 3.7 g/l $NaHCO_3$, 1 μg/ml gentamicin, and 5% fetal calf serum (FCS). Cells were gently triturated using a Pasteur pipet, and the cell suspension was then dispersed into 100 mm culture dishes (12 sciatic nerves/dish) containing HF medium.

The following day, adherent cells were rinsed with Ca^{++} and Mg^{++} free D-PBS to dilute divalent cations in preparation for differential adhesion. The medium was aspirated and fresh Ca^{++} and Mg^{++} free D-PBS (4 ml) supplemented with 0.2% EDTA was added to the cells. After 2 min, the cells were transferred to the stage of an inverted microscope. Under visual inspection, the culture plate was gently tapped until the majority of the Schwann cells were dislodged. Schwann cells in direct contact with fibroblasts were difficult to dislodge using this technique and were discarded to minimize fibroblast contamination. The media containing loose Schwann cells was collected and centrifuged in 15 ml tubes containing 5 ml of HF medium to improve pellet formation. The supernatant was discarded and the cell pellet was resuspended in HF medium for the distribution of Schwann cells to cultureware. Cultures obtained using this method consisted of greater than 99% Schwann cells according to their phase bright, narrow, bipolar morphology under microscopic view. Cells were maintained in a humidified incubator at 37°C in the presence of 5% CO_2 and 95% air.

Total RNA isolation and cDNA synthesis.

Total RNA was extracted from primary rat Schwann cells by a modification of the acid method of Chomczynski and Sacchi (1987). First strand cDNAs were synthesized from total RNA using a cocktail consisting of 2 μg total RNA, 1X PCR reaction buffer (Gibco BRL), 2.5 mM $MgCl_2$, 500 mM deoxynucleotide triphosphates (Pharmacia), 10 mM DTT, 20 U RNAsin (Promega), 200 U SuperScript II RNAase H^- reverse transcriptase enzyme (Gibco BRL), and 2 μg random hexanaucleotide primers (Perkin-Elmer). As a control for the presence of genomic DNA, some reverse transcription reactions were performed without the reverse transcriptase enzyme. Reactions were placed in a 42°C water bath for 1 hr for reverse transcription. Reactions were terminated by a 5 min incubation at 95°C.

PCR parameters.

Forward and reverse primer sequences for rat EP1, EP2, EP3, EP4, and IP receptors are as follows: EP1, forward primer 5'-TGT ATA CTG CAG GAC GTG CGC CC-3', reverse

primer 5'-GGG CAG CTG TGG TTG AAG TGA TG-3' (621 bp product); EP2, forward primer 5'-GGC TTC TTA TTC GAG AAA CCA GAC CCT AGT GGC-3', reverse primer 5'-AGG TCC CAC TTT TCC TTT CGG GAA GAG GTT TCA TC-3' (537 bp product); EP3, forward primer 5'-GCC GGG AGA GCA AAC GCA AA A-3', reverse primer 5'-ACA CCA GGG CTT TGA TGG TCG CACA GG-3' (676 bp product); EP4, forward primer 5'-CCT TCT CTT ACA TGT ACG CGG GCT TCA G-3', reverse primer 5'-TGC TTT CAG TTA GGT CTG GCA GGT ATA GGA GG-3' (537 bp product); IP, forward primer 5'-GGC ACG AGA GGA TGA AGT TTA CC-3', reverse primer 5'-GTC AGA GGC ACA GCA GTC AAT GG-3' (407 bp product). Primer sequences for EP receptors were obtained from Caggiano and Kraig (1999). The primer sequence for the rat IP receptor was obtained from Arakawa et al. (1996). PCR mixtures (50 μl) contained 1X reaction buffer, 0.7 mM deoxynucleotide triphosphates, 2.5 mM $MgCl_2$, 1.2 μM of each primer (upstream and downstream), and 2 μl of cDNA product with 1.5 U of Taq polymerase. Following one cycle of 50°C for 1 min, 94°C for 5 min, and 80°C for 3 min, cDNAs were amplified using 32 cycles of denaturation at 94°C for 45 seconds, priming at 58°C for 45 seconds, and extension at 72°C for 1 min. Reactions were completed using 1 cycle of 94°C for 1 min, 58°C for 1 min and 72°C for 5 min. Amplimers were separated on a 1.5 % agarose gel and stained with 0.5 μg/ml ethidium bromide. To confirm their identity, PCR products were recovered from agarose gels using a QuiaQuick extraction kit (Quiagen) and then sequenced (ABI Prism) using the dye-terminator method.

Determination of $[cAMP]_i$.

Primary rat Schwann cells were seeded onto 12 well culture plates at a density of $2X10^5$ cells/well in HF for 18 hr. Unless specified, all reagents for cAMP analyses were obtained from Biomol. For dose dependent studies, Schwann cells were treated with prostaglandins [BW245C (Cayman Chemical), fluprostenol, misoprostol, PGD_2, PGE_1, PGE_2, 16, 16-dimethyl-PGE_2, 17-phenyl trinor PGE_2 (Cayman Chemical), sulprostone (Cayman Chemical), $PGF_{2\alpha}$, and PGI_2; 0.001- 100 μM] prepared in HF medium (pH 7.2) containing 50 μM of the broad spectrum phosphodiesterase (PDE) inhibitor IBMX. For time dependent studies, Schwann cells were treated with 1 μM of either PGE_1, PGE_2, PGI_2, or forskolin for 5, 10, 15, 30, 60, 90, and 120 min incubations in the presence of 50 μM IBMX. Time dependent studies were also performed using either rolipram to specifically inhibit PDE IV or 8-methoxymethyl IBMX to specifically inhibit PDE I.

Following treatment, the media was completely aspirated and the Schwann cells were lysed with 400 μl of 0.1 M HCl for 1 hr at room temperature on a plate shaker (Lab Systems, WellMix; 500 RPM). The lysate was collected in 500 ml centrifuge tubes, centrifuged at 500 x *g* for 15 min, and used immediately. $[cAMP]_i$ was determined using a direct enzyme immunoassay kit (cAMP Direct; Assay Designs, Inc.), either with or without acetylation. The data are expressed as picomoles of cAMP per $2X10^5$ primary Schwann cells. Forskolin (0.001-100 μM) was used as a positive control for cAMP elevation. Basal $[cAMP]_i$ was consistently between 0.8 and 1.1 pmol cAMP/$2X10^5$ primary Schwann. Assay medium, serum conditions, and exposure to 10% ethanol, a level of vehicle 5-fold higher than those present in the highest dose of prostaglandin (2% ethanol; 100 μM dose), did not affect basal $[cAMP]_i$ in primary Schwann cells.

Immunochemical detection of phosphorylated CREB.

Primary rat Schwann cells were seeded overnight onto 12 mm glass coverslips (10,000 cells/coverslip) and stimulated with 1 μM concentrations of either PGE_1, PGE_2, PGI_2, or 10 μm misoprostol, prepared in HE medium (pH 7.2) containing 50 μM IBMX for 15 min. Following treatment, the medium was aspirated and the cells were fixed with 1% paraformaldehyde in PBS (pH 7.4) for 30 min at room temperature. Cells were rinsed (3 X 5 min) with PBS. Schwann cells were permeabilized and nonspecific immunoreactivity was inhibited by incubation with PBS containing 3% bovine serum albumin (BSA, immunoglobulin free), 0.3% normal goat serum (NGS), and 0.2% Triton X-100. Immunocytochemistry was performed using antibodies directed against phosphorylated CREB (1:500 dilution, UBI). Schwann cells were incubated with primary antibodies diluted in PBS containing 3% BSA, 0.3 % NGS, and 0.2% Triton-X100 for either 1 hr at room temperature or 18 hr at 4°C. Antibody solutions were carefully aspirated and the cells were rinsed (3 X 5 min) with PBS. Antibody reactivity was visualized using either fluorescein- or rhodamine-coupled anti-IgG $F(ab')_2$ (Pierce; 1:250) diluted in PBS with 0.2% Triton X-100. After 1 hr incubation at room temperature, secondary antibodies were aspirated and the cells were rinsed (3 X 5 min) with PBS and mounted on glass slides using VectaMount (Vector Laboratories, Burlingame, CA). Primary Schwann cells were visualized using a Leica microscope (DMRB; Wild M10) equipped for epifluorescence and photographs were taken using a Leica Photomat computer-aided imaging system (Wild MPS 48/52) mounted on this scope. Stimulation of Schwann cells with 25 ng/ml neu differentiation factor β (NDFβ) or 1 μM forskolin for 15 min was used as positive controls for CREB phosphorylation.

For immunoblot analyses of CREB phosphorylation primary rat Schwann cells were seeded onto 6 well culture clusters at a density of 500,000 Schwann cells/well. Schwann cells were treated with 1 μM concentrations of either PGE_1, PGE_2, PGI_2, or forskolin in the presence of 50 μM IBMX for either 5, 10, 15, 30, or 60 min at 37°C. Immediately following treatment, the media was aspirated completely and the cells were lysed in 200 μl of lysis buffer (5 mM Tris-HCl pH 6.8, 1% SDS, 2 mM EDTA, 2 mM EGTA, 1 μM leupeptin, 1 μM aprotinin, and 1 mM NaF) as described in Tabernero et al. (1998). Protein lysates were electrophoretically separated on a 4-20% acrylamide gel (Novex) by SDS-PAGE and transferred to a PVDF membrane (NEN; DuPont). Nonspecific binding sites were blocked by incubating PVDF membranes with PBS containing 5% non-fat dry milk (PBS-MLK) for 1 hr. Primary antibodies raised against phosphorylated CREB (Upstate Biotechnology) were diluted (1:1000) in PBS-MLK and added to PVDF membranes for 16-18 hr at 4°C. PVDF membranes were rinsed (3 X 5 min) with PBS and incubated with goat-anti-rabbit secondary antibodies conjugated with horseradish peroxidase (Transduction Laboratories; 1:4000, diluted in PBS-MLK) for 1 hr at room temperature. Immunoreactivity was visualized using ECL reagent (NEN; DuPont) according to the manufacturer protocol. To inhibit CREB phosphorylation, the specific PKA inhibitor H-89 (Biomol; 5, 10, and 20 μM concentrations) was added to stimulation medium containing 1 μM of either PGE_1, PGE_2, PGI_2, or forskolin and 50 μM IBMX. Cells were stimulated for 15 minutes and prepared as above. Stimulation of Schwann cells with 25 ng/ml NDFβ (R&D Systems) was used as a positive control for CREB phosphorylation.

Digital fluorescence calcium imaging.

Primary rat Schwann cells (2 days in vitro; DIV) were seeded overnight onto 25 mm glass coverslips (FisherBrand; #1 thickness) in HF at 37°C in the presence of 5% CO_2. Schwann cells were loaded with 3 μM Fura-2AM (Molecular Probes, Eugene, OR) for 15-20 min at 37°C in HBSS (in mM; 137.0 NaCl, 5.0 KCl, 2.0 $CaCl_2$, 1.0 $MgSO_4$, 0.44 KH_2PO_4, 0.34

$Na_2HPO_4(7H_2O)$, 20.0 Na^+ HEPES, 1.0 $NaHCO_3$, and 5.0 glucose, pH 7.4), rinsed twice, and imaged in the same medium at room temperature using the Zeiss AttoFluor RatioVision work station (Atto Instruments, Rockville, MD). This system includes a Zeiss Axiovert 135 microscope equipped for epifluorescence with a 510 nm dichroic mirror, a Fluar X40 1.3 NA oil immersion objective, and a fixed emission (520 nm) ICCD camera. Coverslips were mounted in an AttoFluor chamber with a maximum holding volume of 1 ml. The chamber was filled with 1 ml of warm HBSS and mounted onto the microscope stage for digital fluorescence microscopy. Primary Schwann cells were visualized using a 40 X oil immersion objective and a computer image of the cells was captured using the ICCD camera. Between 25 and 30 cellular regions of interest were selected and digitally monitored. Baseline values of Fura-2 fluorescence emission at 520 nm were measured at 3 second intervals during 0.5 Hz alterations of 334 nm (Ca^{++} bound) and 380 nm (Ca^{++} free) excitation filters. These values were used to compute a 334 nm/380 nm emission ratio for Fura-2. Following 1 min of baseline measurements, Schwann cells were stimulated with either 10 μM PGD_2, PGE_1, $PGF_{2\alpha}$, PGE_2, or PGI_2 prepared in HF medium containing 50 μM IBMX. Control cells were stimulated with HF medium and 50 μM IBMX alone. In the absence of a response, each individual experiment was terminated by addition of 10 μM ATP to verify that Schwann cells were capable of producing a calcium transient.

Statistical analyses.

Data are presented as means +/- SD obtained from representative experiments. All experiments were independently repeated at least three times. Statistical significance was analyzed by a Student's *t* test between stimulated and unstimulated groups. A p value of < 0.05 was interpreted as significant.

Results

Primary rat Schwann cells express RNA transcripts encoding prostaglandin receptors.

To determine whether or not primary rat Schwann cells express prostaglandin receptors capable of producing an elevation in $[cAMP]_i$, we used oligonucleotide primers designed to specifically detect cDNA encoding individual members of the rat EP prostaglandin receptor family (Caggiano and Kraig; 1999) as well as the rat IP prostaglandin receptor (Arakawa et al., 1996). PCR reactions using cDNA generated from primary rat Schwann cell total RNA resulted in products of the expected length for rat EP2 (537 bp), EP4 (537 bp), and IP (407 bp) prostaglandin receptors (Fig. 1A). Products encoding rat EP1 (621 bp) and EP3 (676 bp) prostaglandin receptors were not detected. The purified EP2, EP4, and IP PCR products were sequenced by the dye-termination technique and found to be identical to published sequences (Sasaki et al., 1994; Boie et al., 1997). An unexpected PCR product was detected using the IP primer pair (~bp). An increase in the primer hybridization temperature from 58°C to 60°C decreased the amplification of the unexpected product (Fig. 1B). While the amplification of an EP2 receptor specific PCR product was not affected by the elevation in primer hybridization temperature, the increase in hybridization temperature inhibited the ability of the EP4 primer pair to amplify an EP4 specific product. To confirm that total RNA samples were free from genomic DNA contamination, each prostaglandin receptor primer pair was tested individually with total RNA isolated from primary rat Schwann cells. In each case, no PCR products were detected (data not shown).

In addition to the PCR approach, we attempted to confirm the presence of prostaglandin receptor protein in Schwann cells using polyclonal antibodies. While EP4 receptor protein was detected in Schwann cell lysates (data not shown), appropriate reagents for the demonstration of rat EP2 and IP receptor protein were not available.

Prostaglandins elevate $[cAMP]_i$, but not intracellular $[Ca^{++}]_i$, in primary rat Schwann cells.

To determine whether the EP2, EP4, IP prostaglandin receptors expressed by primary rat Schwann cells were functional, we measured $[cAMP]_i$ in Schwann cells following a 15 minute stimulation with increasing concentrations of PGE_1 (squares) PGE_2 (circles) or PGI_2 (triangles) in the presence of the nonselective phosphodiesterase (PDE) inhibitor IBMX (50 μM). Similarly, $[cAMP]_i$ was determined in Schwann cells following a 15 minute treatment with increasing concentrations of the PGE_1 mimetic, misoprostol (open squares), and the stable EP2/EP4 specific receptor ligand, 16,16-dimethyl PGE_2 (open circles). Consistent with the finding that Schwann cells express RNA transcripts encoding EP2, EP4, and IP prostaglandin receptors, stimulation of Schwann cells with EP2/EP4 and IP selective ligands produced a dose-dependent elevation in $[cAMP]_i$ (Fig. 2A). Treatment with high ligand concentrations in the presence of IBMX resulted in a saturation of cAMP production for each ligand tested. While PGE_1 (Fig 1A, squares) was the most efficacious activator of cAMP production by primary Schwann cells, PGI_2 (Fig. 1B, triangles) was the most potent stimulator of cAMP production. The rank order potency of ligand-stimulated elevations in $[cAMP]_i$ was $PGI_2 > PGE_1 > PGE_2 = 16$, 16-$PGE_2$ > misoprostol. Stimulation of primary Schwann cells with a combination of PGE_2 and PGI_2 (squares, dashed line) produced a dose-response curve that was not significantly different from PGE_1 alone; suggesting that PGE_1 can bind to both EP2/EP4 and IP receptors to stimulate an elevation in $[cAMP]_i$. Similarly, stimulation of primary Schwann cells with either PGE_1 or a combination of PGE_2 and PGI_2 stimulated an elevation in $[cAMP]_i$ that was identical to that identical to the levels observed following stimulation with equal concentrations of forskolin (Fig. 2A, diamonds).

To confirm that additional prostaglandin receptors were not expressed by primary rat Schwann cells, we measured $[cAMP]_i$ following treatment with ligands selective for DP receptors (BW245c and PGD_2), FP receptors (sulprostone and fluprostenol), and EP1/EP3 receptors (17-phenyl-trinor PGE_2). Primary rat Schwann cells stimulated with increasing concentrations of DP, FP, and EP1/3 receptor selective ligands spanning five orders of magnitude (0.001 μM-100 μM) did not produce a significant dose dependent elevation in $[cAMP]_i$ (Fig. 2B).

In addition to stimulating adenylyl cyclase activity, activation of prostaglandin receptors has also been shown to elevate $[Ca^{++}]_i$ in a variety of cell types via an increase in phospholipase C activity. To determine whether $[Ca^{++}]_i$ was elevated in primary rat Schwann cells following prostaglandin stimulation, we monitored $[Ca^{++}]_i$ using Fura-2. An elevation in $[Ca^{++}]_i$ was not detected using a high concentration (10 μM) of any of the prostaglandin receptor ligands used in this study (data not shown). However, primary rat Schwann cells were responsive to stimulation with 10 μM ATP by an elevation in $[Ca^{++}]_i$ (data not shown).

Kinetics of cAMP production is Schwann cells stimulated with prostaglandins.

To determine the duration of intracellular cAMP elevation in primary rat Schwann cells, we measured $[cAMP]_i$ at regular time intervals from 5 mintues to 2 hours following treatment with 1 μM of either PGE_1 (Fig. 3A), PGE_2 (Fig. 3B), PGI_2 (Fig. 3C), or forskolin (Fig 3D) in the

presence of three different phosphodiesterase inhibitors. We measured $[cAMP]_i$ following treatment with prostaglandins in the presence of either a broad spectrum PDE inhibitor (circles, IBMX; 50 μM), a PDE IV-specific inhibitor (squares, rolipram; 50 μM), or a PDE I-specific inhibitor (triangles, 8-methoxymethyl IBMX; 50 μM). $[cAMP]_i$ was significantly elevated above basal levels within 5 minutes of stimulation and continued to increase over the ensuing 5-10 minutes. Maximal elevations in $[cAMP]_i$ above basal were observed between 10 and 30 minutes of stimulation beyond which $[cAMP]_i$ began to return towards basal levels. Similar recovery kinetics were observed using 50 μM of the PDE IV specific inhibitor rolipram. However, compared to 50 μM IBMX (Fig. 3, Panels A-D, circles), stimulation of primary rat Schwann cells in the presence of 50 μM rolipram (Fig. 3, Panels A-D, squares) resulted in slight, but not significant, decrease $[cAMP]_i$ with no significant difference in the kinetics of cAMP production. Stimulation of Schwann cells with PGE_1, PGE_2, PGI_2, or forskolin in the presence of the PDE I specific inhibitor, 8-methoyxmethyl IBMX, resulted in significantly less cAMP accumulation (Fig. 3, Panels A-D, triangles). This finding suggests that members of the PDE IV enzyme family effectively regulate $[cAMP]_i$ in Schwann cells. The sum of the cAMP accumulation observed for rolipram and 8-methoxymethyl IBMX was not significantly different from the level of cAMP accumulation observed using IBMX alone; suggesting that members of the PDE I and PDE IV enzyme family are the primary effectors of cAMP catabolism in Schwann cells. Compared to PGE_1, PGE_2, and PGI_2, elevations in $[cAMP]_i$ occurred more rapidly in response to stimulation with forskolin (1 μM); consistent with the ability of forskolin to act independently of G-protein activation. The recovery of $[cAMP]_i$ towards basal levels after 15 to 30 minutes of stimulation suggested that PDE activity might not have been completely inhibited for the entire duration of the assay. However, similar effects on $[cAMP]_i$ over time were observed using three different PDE inhibitors and using doses of PDE inhibitors ranging from 25 μM to 500 μM (data not shown).

Prostaglandins stimulate CREB phosphorylation on Ser-133 in primary rat Schwann cells.

To determine if the elevations in $[cAMP]_i$ were sufficient to stimulate cAMP-mediated events, we monitored CREB phosphorylation on Ser-133 in primary rat Schwann cell protein extracts obtained at regular time intervals following stimulation with 1 μM of either PGE_1, PGE_2, PGI_2, or forskolin (FSK). Prostaglandin stimulation resulted in a rapid elevation in CREB phosphorylation within 5 minutes of treatment. For each prostaglandin tested, CREB phosphorylation was maximal between 5 and 15 minutes of stimulation with a decline towards basal levels between 30 and 45 minutes of stimulation (Fig. 4). The decline in CREB phosphorylation was coincident with the observed decline in $[cAMP]_i$ over time (Fig. 4). To confirm our immunoblot findings and to detect the presence of phosphorylated CREB within individual primary Schwann cell nuclei, we performed immunocytochemistry for phosphorylated CREB. Primary rat Schwann cells treated with 50 μM IBMX alone exhibited low levels of phosphorylated CREB immunoreactivity (Fig. 5A). Stimulation with 1 μM of PGE_1 (Fig. 5), PGE_2 (Fig. 5)or PGI_2 (Fig. 5)resulted in CREB immunoreactivity within the Schwann cell nuclei, which was identical in comparison to that observed following forskolin or NDFβ stimulation. Similarly, treatment with 10 μM misoprostol (Fig. 5), which was approximately 10-fold less potent than PGE_1 at stimulating cAMP accumulation, also resulted in increased nuclear CREB immunoreactivity in Schwann cells. Primary rat Schwann cells stimulated with either 1 μM forskolin (Fig. 5) or 25 ng/ml neu differentiation factor β (NDFβ; Fig. 5) were used as positive controls for CREB phosphorylation on Ser-133.

The PKA inhibitor, H-89, inhibits CREB phosphorylation following prostaglandin stimulation in primary rat Schwann cells.

To confirm that prostaglandin receptor activation of cAMP-mediated intracellular signaling was responsible for CREB phosphorylation on Ser-133, we used the PKA inhibitor H-89 to decrease prostaglandin-stimulated PKA activation. We chose a 15 minute stimulation for analysis because the level of CREB phosphorylation was near peak levels for this duration. Cell lysates obtained from primary rat Schwann cells stimulated with 1 μM of either forskolin, PGE_1, PGE_2, or PGI_2 for 15 minutes demonstrated a significant increase in CREB phosphorylation (Fig 6, lane 3) which was inhibited in a dose dependent fashion by increasing concentrations of H-89 (5-20 μM) (Fig. 6, lanes 4-6). Similar inhibition of prostaglandin stimulated CREB phosphorylation was observed for each prostaglandin receptor ligand and for forskolin (FSK). As previously reported by Tabernero et al. (1998), protein lysates obtained from Schwann cells treated with the potent growth and survival factor NDFβ exhibited significantly higher levels of CREB phosphorylation than lysates obtained from Schwann cells treated with either forskolin or prostaglandins. Immunoblots were reprobed with an antibody raised against the catalytic subunit of PKA (PKAc) to verify equal protein loading for each condition. A representative immunoblot is shown.

Discussion

PGE_1, PGE_2, and PGI_2 are physiologic factors that stimulate cAMP-mediated signaling in primary Schwann cells.

In this study, we demonstrate that primary Schwann cells express transcripts encoding EP2, EP4, and IP prostaglandin receptors (Fig. 1). Stimulation of EP2, EP4, and IP receptors using selective ligands produced an elevation in $[cAMP]_i$ that was both dose dependent (Fig. 2) and time dependent (Fig. 3) Receptor mediated elevations in $[cAMP]_i$ were sufficient to stimulate signaling events downstream of cAMP. In particular, treatment with 1 μM concentrations of either PGE_1, PGE_2, or PGI_2 stimulated phosphorylation of the transcription factor CREB within 5 minutes of stimulation (Fig. 4). CREB phosphorylation in response to stimulation with either PGE_1, PGE_2, PGI_2, or forskolin was inhibited by the PKA inhibitor, H-89, in a dose dependent fashion (Fig. 6). Collectively, these studies demonstrate that stimulation with PGE_1, PGE_2, or PGI_2 can reproduce the each of identified intracellular signaling events that are initiated by forskolin stimulation in Schwann cells (Figs. 2-6). To date, norepinephrine (Yasuda et al., 1988) and CGRP (Cheng et al., 1995) are the only two physiologic factors that are known to elevate $[cAMP]_i$ in primary Schwann cells in a rapid, dose dependent fashion. Since their initial description, neither of these factors have been shown to stimulate intracellular signaling events downstream of cAMP in Schwann cells. In the absence of identified physiologic agents to stimulate elevations in $[cAMP]_i$ and intracellular events downstream of elevated $[cAMP]_i$, studies of the physiologic effects of cAMP in Schwann cell physiology rely almost exclusively use forskolin to stimulate adenylyl cyclase activity to a high degree. Our findings identify PGE_1, PGE_2, and PGI_2 as physiologic factors that elevate $[cAMP]_i$ and stimulate cAMP-mediated intracellular signaling events in primary Schwann cells. Schwann cells treated with either PGE_1 or a combination of equal concentrations of PGE_2 and PGI_2 stimulated elevations in $[cAMP]_i$ that were not significantly different from those observed using

identical concentrations forskolin (Fig. 2A). In addition, the kinetics of elevated $[cAMP]_i$ in response to 1 μM PGE_1, PGE_2, and PGI_2 stimulation were similar to those observed using 1 μM forskolin (Fig. 3, panels A-D). Thus, PGE_1, PGE_2, and PGI_2 are excellent physiologic factors for the study of receptor-mediated elevations in $[cAMP]_i$ and cAMP-mediated signaling events in primary Schwann cells.

By binding directly to adenylyl cyclases, forskolin stimulates rapid cAMP accumulation by a mechanism that is entirely independent of both receptors and G protein activation. In contrast, ligand-mediated elevations in $[cAMP]_i$ require ligand binding, G protein subunit dissociation, and subsequent adenylyl cyclase activation. In addition, the effects of physiologic factors such as prostaglandins are subject to ligand stability, receptor desensitization, and allosteric modulation of post-receptor signaling proteins. Furthermore, the degradation of cAMP by PDE I and PDE IV enzymes contributes significantly to the control of steady state and receptor-stimulated elevations in $[cAMP]_i$ (Bentley and Beavo, 1992). In these studies, the presence of PDE I and PDE IV inhibitors was required to detect ligand-stimulated changes in $[cAMP]_i$ and subsequent cAMP-mediated signaling events. Following peripheral nerve injury, PDE I and PDE IV activity is significantly elevated and adenylyl cyclase activity is concurrently decreased within degenerating peripheral nerve (Poduslo et al., 1995; Walikonis and Poduslo, 1998). Similarly, we demonstrate that PDE I and PDE IV are the primary PDE families involved in cAMP degradation following prostaglandin stimulation in primary Schwann cells (Fig. 4). Inhibition of PDE enzyme activity increases cAMP diffusion from the site of synthesis and may affect the spatio-temporal kinetics of PKA activation and gene expression (Jurevicius and Fischmeister, 1996). While, PGE_1, PGE_2, and PGI_2 were capable of elevating $[cAMP]_i$ in primary Schwann cells in a rapid, dose dependent fashion, $[cAMP]_i$ consistently decreased after 15 minutes of stimulation for each ligand-PDE inhibitor combination tested (Fig. 4). The mechanisms responsible for the gradual decline in $[cAMP]_i$ remain to be determined. The presence of unidentified PDE enzymes and extracellular transport of cAMP may each contribute to the observed decrease in $[cAMP]_i$ over time.

Role of prostaglandins in Schwann cell physiology.

Little is known about the role of prostaglandins in normal Schwann cell physiology and in Schwann cell responses to peripheral nerve injury. Prostaglandins are produced by the sequential actions of cyclooxygenases and various prostaglandin synthases on arachidonic acid (AA). Phospholipase A_2 (PLA_2) enzymes comprise a diverse enzyme family that is largely responsible for the generation of free AA from membrane phospholipids. Schwann cells have been shown to express PLA_2 activity within Schmidt-Lanterman incisures and paranodal membrane sites following peripheral nerve injury (Paul and Gregson, 1992); raising the possibility that Schwann cells may release AA and thus contribute to prostaglandin production. The recent finding that stimulation of the ET_B endothelin receptor subtype using either ET-1 or ET-3 increases the level AA release from Schwann cells via activation of Ca^{++}-independent PLA_2 further implicates Schwann cells as an endogenous source of AA within peripheral nerve (Berti-Mattera et al., 2000; Pomonis et al., 2001). Increased PLA_2 expression and activity has also been demonstrated in outgrowing sensory neurites *in vitro* (Smalheiser et al., 1996; Hornfelt et al., 1999) and *in vivo* (Negre-Aminou and Pfenninger, 1993), as well as in vascular endothelial cells of the blood-nerve barrier (Wong et al., 1998), and macrophages (Wightman et al., 1981; Nathan, 1987). In addition to PLA_2 protein expression and activity, most of these cell types are known to produce and release significant amounts of PGE_2 and PGI_2; particularly in response to

injury. Following peripheral nerve injury, large numbers of macrophages are recruited to the injury site via the release of inflammatory cytokines by Schwann cells (Toews et al., 1998; Rutkowski et al., 1999; Sugiura et al., 2000; Taskinen and Roytta, 2000). While the phagocytosis of cellular debris by macrophages is a salient feature of peripheral nerve injury (Beuche and Friede, 1984), little is known about the mechanisms by which macrophages, Schwann cells, and other cellular constituents of peripheral nerve communicate with one another. Following peripheral nerve injury, the presence of macrophage-derived factors, such as prostaglandins, may modulate the response of regenerating peripheral nerve fibers, perineural fibroblasts, and Schwann cells by elevating $[cAMP]_i$. In addition to the sensitization or direct activation of nociceptive sensory nerve endings (Hingtgen et al., 1995; Smith et al., 1998; Aley and Levine, 1999; Baba et al., 2001), macrophage-derived prostaglandins may influence the physiologic responses of Schwann cells to contact with regenerating axons. Macrophages have long been considered beneficial to peripheral nerve regeneration. Macrophage depletion following peripheral nerve injury reduces axonal degeneration (Sommer and Schafers, 1998) and hyperalgesia (Syriatowicz et al., 1999; Liu et al., 2000) but also decreased axonal outgrowth (Dailey et al., 1998) and Schwann cell proliferation (Kubota et al., 1998). Macrophages may affect Schwann cell proliferation following injury either directly, by releasing mitogens (Baichwal et al., 1988), or indirectly, by increasing axonal outgrowth and survival (Heumann et al., 1987; Lindholm et al., 1987). Thus, macrophages may promote peripheral nerve regeneration through their effects on Schwann cells. To that end, macrophages may also stimulate Schwann cell proliferation via the release factors such as PGE_2 and PGI_2 that elevate $[cAMP]_i$ and potentiate the proliferation of Schwann cells in response to growth factors found on regenerating peripheral nerve axons.

Conclusions

Our findings have substantial physiologic implications for the process of Wallerian degeneration and peripheral nerve regeneration following injury. These findings are also highly relevant to Schwann cell physiology under normal and pathological states. The identification of functional EP2, EP4, and IP prostaglandin receptors in primary Schwann cells more than doubles the number of known receptors that are capable of stimulating elevations in $[cAMP]_i$ in these cells. In addition to the identification of prostaglandins as a novel class of physiologic ligands for Schwann cells, this report is the first to test whether these physiologic ligands are capable of modulating Schwann cell physiology in a manner similar to the widely-used pharmacologic agent forskolin. Furthermore, data presented concerning ligand-stimulated elevations in $[cAMP]_i$ over time suggest complex, as yet characterized, regulatory mechanisms that control cAMP-mediated signaling events in Schwann cells. Finally, the data presented herein underscores the importance of PDEs in the regulation of $[cAMP]_i$ in Schwann cells. Together, these studies provide significant insights regarding the physiologic role of receptor-mediated elevations in $[cAMP]_i$ in Schwann cell biology.

References

Aley KO, Levine JD (1999) J Neurosci 19:2181-186.

Arakawa T, Laneuville O, Miller CA, Lakides KM, Wingerd BA, DeWitt DL, and Smith WL (1996) J Biol Chem 271:29569-29575.

Avellino AM, Hart D, Dailey AT, MacKinnon M, Ellegala D, Kliot M (1995). Exp Neurol 136:183-198.

Baichwal RR, Bigbee JW, DeVries GH (1988). Proc Natl Acad Sci U S A. 85:1701-1705.

Baichwal RR, DeVries GH (1989) Biochem Biophys Res Commun 164:883-888.

Bentley JK, Beavo JA (1992) Curr Opin Cell Biol 4:233-240.

Berti-Mattera LN, Wilkins PL, Harwalkar S, Madhun Z, Almhanna K, Mattera R. (2000). J Neurochem 75:2316-2326.

Beuche W, Friede RL. (1984). J Neurocytol 13:767-796.

Boie Y, Stocco R, Sawyer N, Slipetz DM, Ungrin MD, Neuschafer-Rube F, Puschel GP, Metters KM, Abramovitz M (1997). Eur J Pharmacol 340:227-241.

Bruck W (1997). Brain Path 7:741-752.

Bruck W, Friede RL. (1990). J Neuroimmunol 27:217-227.

Bruck W, Huitinga I, Dijkstra CD (1996). J Neurosci Res 46:477-484.

Caggiano AO and Kraig RP (1999). J Neurochem 72:565-575.

Cheng L, Khan M, Mudge AW (1995) J Cell Biol 129:789-796.

Chomczynski P, Sacchi N (1987) Anal Biochem 162:156-159.

Coleman RA, Smith WL, Narumiya S (1994) Pharm Rev 46:206-224.

da Costa CC, van der Laan LJ, Dijkstra CD, Bruck W (1997). Eur J Neurosci 9 2650-2657.

Dailey AT, Avellino AM, Benthem L, Silver J, Kliot M (1998) J Neurosci 18:6713-6722.

Davis JB, Stroobant P (1990). J Cell Biol 110:1353-1360.

Grafe P, Mayer C, Takigawa T, Kamleiter M, Sanchez-Brandelik R (1999) J Physiol 515:377-83

Griffin JW, George R, Lobato C, Tyor WR, Yan LC, Glass JD (1992) J Neuroimmunol 40:153-165.

Heumann R, Korsching S, Bandtlow C, Thoenen H (1987) J Cell Biol 104:1623-1631.

Hingtgen CM, Waite KJ, Vasko MR (1995) J Neurosci 5411-5419.

Hornfelt M, Ekstrom PA, Edstrom A. (1999) Neuroscience 91:1539-1547.

Howe DG, McCarthy KD (2000J Neurosci 20:3513-3521.

Jurevicius J, Fischmeister R (1996) Proc Natl Acad Sci U S A 93:295-299.

Kubota A, Komiyama A, Matsumoto M, Suzuki K (2000 Brain Res 802:254-258.

LeBlanc AC, Windebank AJ, Poduslo JF (1992). Brain Res Mol Brain Res 12:31-38.

Lemke G, Chao M (1988) Development 102:499-504.

Lindholm D, Heumann R, Meyer M, Thoenen H (1987Nature 330:658-659.

Liu L, Lioudyno M, Tao R, Eriksson P, Svensson M, Aldskogius H (1999) J Peripher Nerv Syst 4:123-33.

Liu T, van Rooijen N, Tracey DJ (2000) Pain 86:25-32.

Mokuno K, Sobue G, Reddy UR, Wurzer J, Kreider B, Hotta H, Baron P, Ross AH, Pleasure D (1988). J Neurosci Res 21:465-472.

Monuki ES, Weinmaster G, Kuhn R, Lemke G (1989) Neuron 3:783-93.

Morgan L, Jessen KR, Mirsky R (1991). J Cell Biol 112:457-467.

Muja N, DeVries GH (1999) Soc Neurosci Abstr 29: 205.

Nathan CF (1987). J Clin Invest 79:319-326.

Negre-Aminou P, Pfenninger KH (1993). J Neurochem 60:1126-1136.

Paul JA, Gregson NA (1992). J Neuroimmunol 39:31-47.

Perry VH, Tsao JW, Fearn S, Brown MC (1995). Eur J Neurosci 7:271-280.

Poduslo JF, Walikonis RS, Domec MC, Berg CT, Holtz-Heppelmann CJ (1995) J Neurochem 65:149-159.

Rahmatullah M, Schroering A, Rothblum K, Stahl RC, Urban B, Carey DJ (1998) Mol Cell Biol 18:6245-

Rutkowski JL, Tuite GF, Lincoln PM, Boyer PJ, Tennekoon GI, Kunkel SL (1999) J Neuroimmunol 101:47-60.

Sasaki Y, Usui T, Tanaka I, Nakagawa O, Sando T, Takahashi T, Namba T, Narumiya S, Nakao K (1994) 1224:601-605.

Scherer SS, Xu YT, Roling D, Wrabetz L, Feltri ML, Kamholz J (1994) J Neurosci Res 38:575-589.

Smalheiser NR, Dissanayake S, Kapil A (1996) Brain Res. 721:39-48.

Smith JA, Amagasu SM, Eglen RM, Hunter JC, Bley KR (1998) Br J Pharmacol 124:513-523.

Sobue G, Pleasure D (1984) Science 224:72-74.

Sommer C, Schafers M (1998). Brain Res 784:154-162.

Stoll G, Muller HW (1999) Brain Pathol :313-325.

Syriatowicz JP, Hu D, Walker JS, Tracey DJ (1999) Neuroscience 94:587-594.

Tabernero A., Stewart, H.J.S., Jessen R., and Mirsky R (1998) Mol Cell Neurosci 10:309-322.

Tzeng SF, Deibler GE, DeVries GH (1999) Neurochem Res 24:255-260.

Van Rooijen N, Sanders A (1994J Immunol Methods 174:83-93.

Walikonis RS, Poduslo JF (1998). J Biol Chem 273:9070-9077.

Weinmaster G and Lemke G (1990 EMBO Journal 9:915-920.

Wightman PD, Dahlgren ME, Davies P, Bonney RJ (1981) Biochem J 200:441-4444.

Wong JT, Tran K, Pierce GN, Chan AC, O K, Choy PC (1998) J Biol Chem 273:6830-6836.

Yasuda T, Sobue G, Mitsuma T, Takahashi A. (1988) J Neurol Sci 88:315-325.

Figure Legends

Figure 1. Primary rat Schwann cells express prostaglandin receptor mRNA transcripts Primary rat Schwann cells express transcripts encoding the EP2 (537 bp, lane 2), EP4 (537 bp, lane 4), and IP (407 bp, lane 5) receptors. Primers specific for EP1 (607 bp, lane 1) or EP3 (657 bp, lane 3) receptors did not detect transcripts encoding these receptors. An elevation in primer hybridization temperature from 58°C to 60°C reduced the amplification of non-specific products by the IP primer pair. Whereas the EP2 primer pair yielded a specific PCR product at the higher hybridization temperature, the EP4 primer pair did not produce a PCR product. The ΦX174 restriction digest (Life Technologies, lane 6) was used to estimate base pair lengths.

Figure 2. Prostaglandins elevate $[cAMP]_i$ in primary rat Schwann cells in a dose dependent fashion. (A) Stimulation of primary rat Schwann cells with either EP2/EP4 and IP receptor selective ligands (PGE_1, PGE_2, PGI_2, 16,16 dimethyl PGE_2, or misoprostol) in the presence of 50 μM IBMX produced a significant, dose-dependent elevation in $[cAMP]_i$. Compared to EP2/EP4 and IP selective ligands, (B) stimulation with DP receptor ligands (BW245C and PGD_2), EP1/EP3 receptor ligands (17-phenyl-trinor PGE_2), or FP receptor ligands (sulprostone and fluprostenol) did not produce elevation in $[cAMP]_i$. Treatments were prepared in DMEM low glucose containing 5% FBS. Primary Schwann cells were stimulated with ligand for 15 minutes and then lysed as described in Methods. Stimulation of primary rat Schwann cells with forskolin (A) was included as a positive control for cAMP elevation. Assays were performed in triplicate (n= 3) for each ligand. Standard deviations were less than 10% for each treatment concentration tested.

Figure 3. Prostaglandins stimulate a time dependent elevation $[cAMP]_i$ in Schwann cells. Primary rat Schwann cells were treated with 1 μM concentration of either PGE_1, PGE_2, PGI_2, or forskolin in the presence of either a broad spectrum PDE inhbitor (50 μM IBMX), a PDE IV specific inhibitor (50 μM rolipram), or a PDE I specific inhibitor (50 μM 8-methoxymethyl IBMX).

Figure 4. Prostaglandins stimulate CREB phosphorylation on Ser-133 in primary rat Schwann cells. Primary rat Schwann cells were treated with 1 μM concentrations of either PGE_1, PGE_2, or PGI_2, for 0, 5, 10, 15, 30, or 60 minutes in the presence of 50 μM IBMX. Schwann cell protein extracts were analyzed for increased CREB phosphorylation on Ser-133 by immunoblot analysis using an antibody specific for phosphorylated CREB. Immunoblot analyses of primary Schwann cell extracts (20 μg/lane) reveal that PGE_1, PGE_2, and PGI_2 each stimulate CREB phosphorylation within 5 minutes of addition and that CREB phosphorylation was sustained for at least 30 minutes. Primary Schwann cells stimulated with 1 μM forskolin were used as a positive control for CREB phosphorylation.

Figure 5. Immunocytochemical detection of CREB phosphorylation on Ser-133 in primary rat Schwann cells following prostaglandin stimulation. Primary rat Schwann cells (1 $X10^5$ cells/cover glass) were treated with a 1 μM concentration of either, PGE_1 (E), Misoprostol (F), PGE_2 (G), or PGI_2 (H) in the presence of 50 μM IBMX for 15 minutes and then fixed with 1 % paraformaldehyde in preparation for immunocytochemistry. Primary Schwann cells treated with 50 μM IBMX alone (B) were used to identify basal levels of CREB phosphorylation on Ser-133. As positive controls for CREB phosphorylation on Ser-133, primary rat Schwann cells were stimulated with 25 ng/ml NDFβ (C) and 1 μM forskolin (D). Fluorescent signal was not detected in the absence of primary antibody (A).

Figure 6. Inhibition of PKA activity in primary rat Schwann cells inhibits CREB phosphorylation following prostaglandin stimulation. Primary rat Schwann cells (1 $X10^6$ cells/well) were treated for 15 minutes with 1 μM concentrations of PGE_1, PGE_2, PGI_2, or forskolin either alone or in the presence of increasing concentrations of the specific PKA inhibitor H-89 (5, 10, and 20 μm). Protein extracts from primary Schwann cells treated with 50 μM IBMX (Untreated) were used to identify basal levels of CREB phosphorylation. Stimulation of primary Schwann cells with 25 ng/ml NDFβ was used as an internal positive control for CREB phosphorlyation for each ligand analysis. Immunoblots were reprobed for the catalytic subunit of PKA (PKAc) to verify equal protein loading in each lane. A representative immunoblot for the catalytic subunit of PKA is included for comparison.

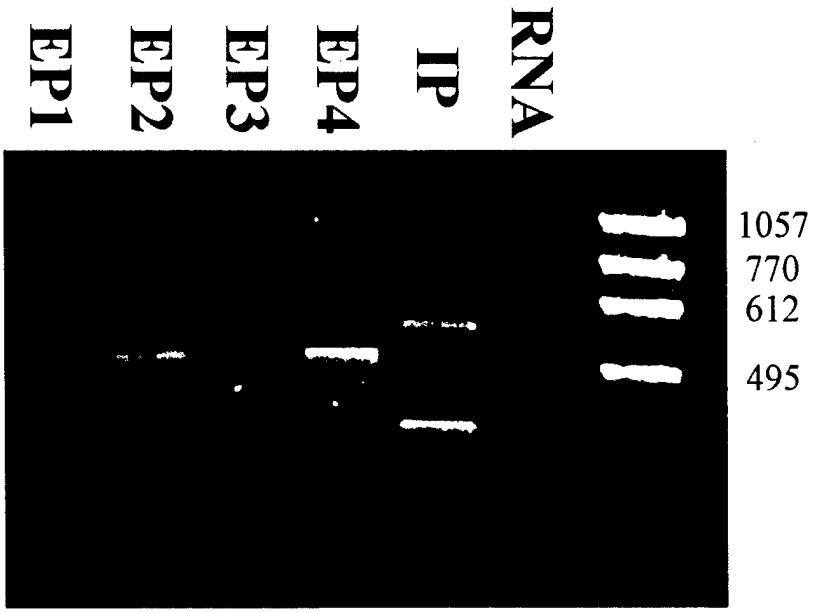

Fig 1

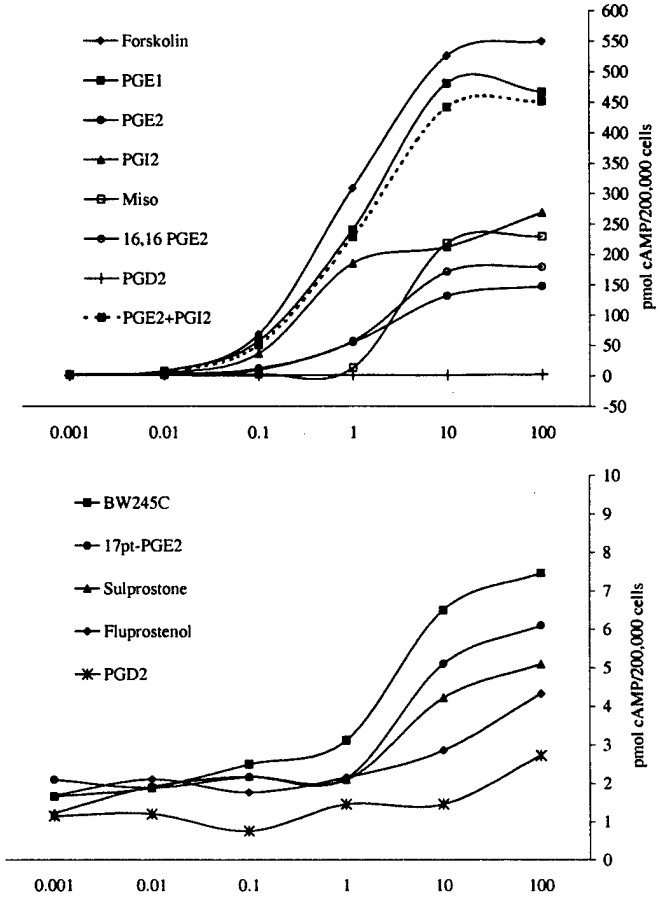

Ligand Concentration (μM)

Fig 2

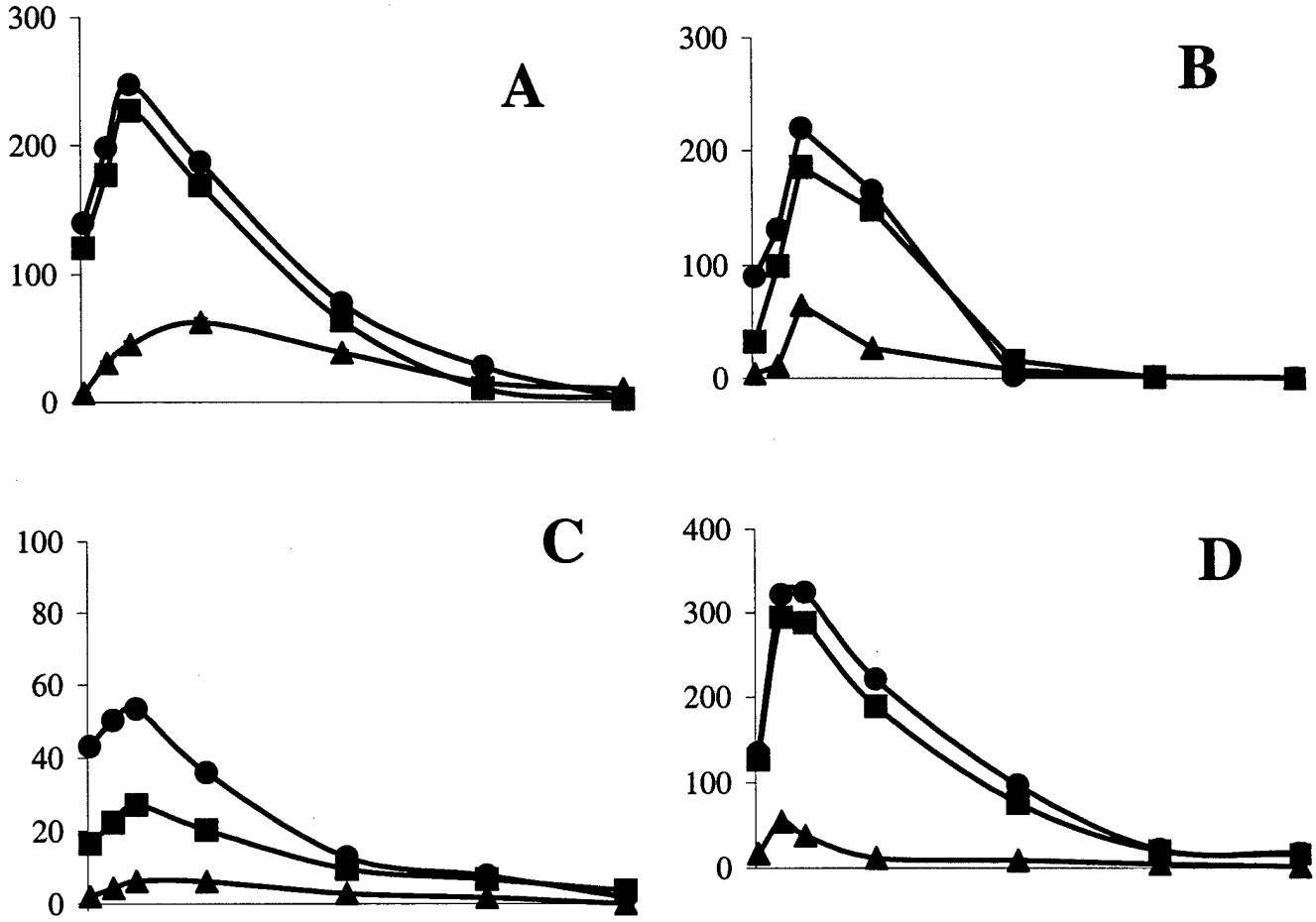

Fig 3

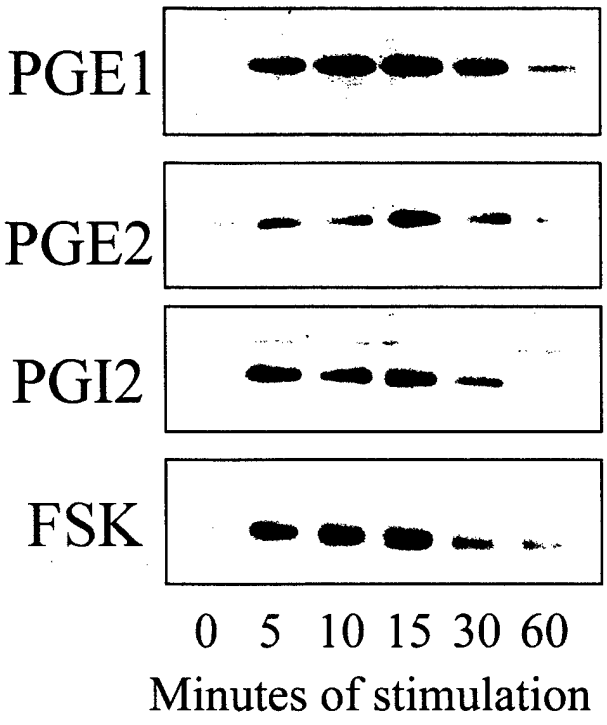

Fig 4

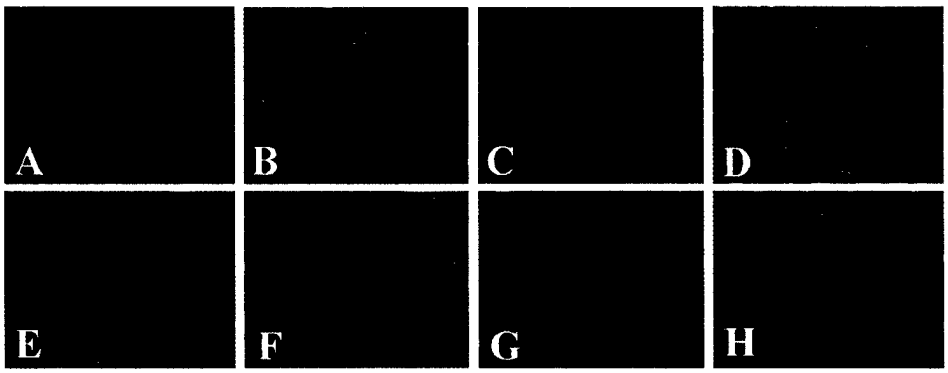

Fig 5

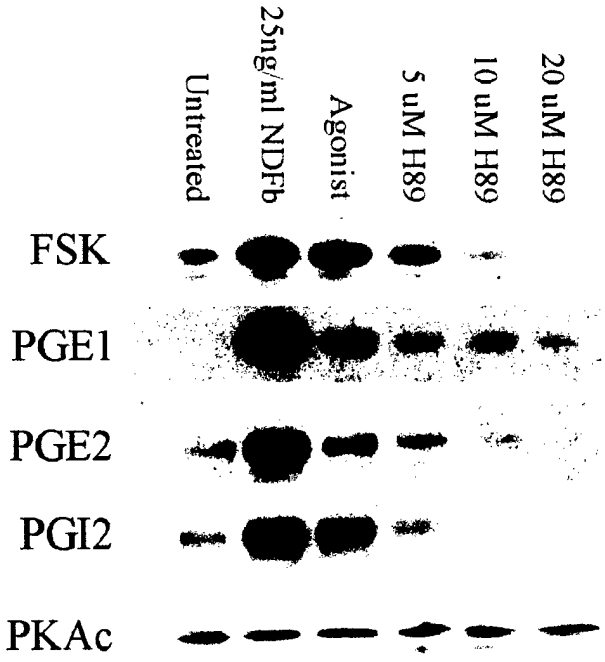
Untreated
25ng/ml NDFb
Agonist
5 uM H89
10 uM H89
20 uM H89
FSK
PGE1
PGE2
PGI2
PKAc

Fig 6

c-Kit Receptor Expression in Normal Schwann Cells and Schwann cell Lines derived from NF1 Tumors

Ian Dang and George H. DeVries
Research Service
Edward Hines Jr. VA Hospital
Hines, IL 60141
Department of Cell Biology, Neurobiology and Anatomy
Loyola University of Chicago
Maywood, IL 60153

Abstract

Neurofibromatosis type 1 (NF1) is a genetic disorder characterized by Schwann cell tumors called neurofibromas, which can potentially become malignant to form neurofibrosarcomas. Previously, our laboratory has reported that Schwann cells derived from neurofibromas abnormally express high levels of the receptor tyrosine kinase c-kit, which contributes weakly to Schwann cell proliferation (Badache et al, 1998a). It is possible that c-kit plays an important role during development and that its aberrant re-expression by adult NF1 cells contributes to the development of Schwann cell tumors. We now report that neurofibromin expression and c-kit expression are inversely regulated in rat sciatic nerves during development. Normal adult Schwann cells contain neurofibromin and do not express c-kit, while human Schwann cell lines derived from NF1 tumors express c-kit but do not express neurofibromin. In neonates, c-kit is expressed by cultured Schwann cells. Its activation by SCF prevents programmed cell death via the activation of Akt but does not induce Schwann cell proliferation or differentiation.

Introduction

Many growth factors interact with specific cell surface receptors belonging to the receptor tyrosine kinase (RTK) superfamily. Members of the RTK superfamily possess both shared and unique structural subdomains (Yarden and Ullrich, 1988). The proto-oncogene, c-kit, belongs to the RTK superfamily and is a member of the same receptor subfamily as the platelet-derived growth factor (PDGF) and colony-stimulating factor-1 (CSF-1) receptors (Yarden et al, 1987 and Qui et al, 1998). This RTK subfamily is

characterized by the presence of five immunoglobulin-like motifs in the extracellular domain and an insert that splits the cytoplasmic kinase domain into an adenosine triphosphate (ATP)-binding region and a phosphotransferase domain (Ullrich et al, 1987 and Yarden et al, 1998). C-kit and its ligand, stem cell factor, constitute an important signal transduction system regulating cell growth and differentiation in hematopoiesis, gametogenesis, melanogenesis (for review see Broudy 1997), and they possibly play a role in the pathogenesis of neurofibromatosis type 1.

Neurofibromatosis type 1 (NF1) is a genetic disorder affecting approximately 1 in 3000 individuals that manifests with various phenotypic features including neurofibromas, café-au-lait spots, axillary freckling, Lish nodules, optical gliomas, and learning disabilities (Friedman, 1999). Neurofibromas are benign peripheral nerve sheath tumors that consist of a majority of Schwann cells, but also contains fibroblasts, perineurial cells, and mast cells embedded in an abundant extracellular matrix. Most importantly, Schwann cells are responsible for the formation of malignant neurofibromas in up to 5% of NF patients (Friedman, 1999).

In hematopoietic cells, abnormal proliferation of both immature and lineage restricted progenitor populations occurs in response to SCF Nf1-/- progenitors (Zhang et al., 1998). In addition, mast cells derived from Nf1+/- mice display increased cell proliferation, survival, colony formation in response to SCF (Ingram et al., 2000). Interestingly, mast cells are present in neurofibromas and have been implicated in promoting Schwann cell growth through the release of various factors (Ricardi et al., 1992). These studies may explain hematopoietic disorders associated with the loss of neurofibromin. Children with NF1 are predisposed to juvenile chronic myelogenous

leukemia (JCML) and other malignant myeloid disorders, and heterozygous Nf1 knockout mice spontaneously develop a myeloid disorder resembling JCML (Shannon et al., 1994; Jacks et al., 1994). Taken together, c-kit and its activation by SCF are important during development for numerous cell types, such as progenitor cells, mast cells, and possibly Schwann cells. Neurofibromin is a protein that regulates signal transduction pathways during development, and its loss in embryonic stages or in the adult results in the development of tumors and leukemia.

We have observed that Schwann cells derived from neurofibromas abnormally express high levels of the receptor tyrosine kinase c-kit, which contributes to Schwann cell proliferation (Badache et al, 1998a). It has been found in a number of cancers that tumor forming cells inappropriately synthesize proteins that are normally only produced during development. Based on our previous studies (Badache et al., 1998), we postulated that c-kit is inappropriately re-expressed by Schwann cells present in neurofibrosarcomas; however during normal development of Schwann cells the receptor may play an important role. We now report that c-kit is developmentally regulated in rat sciatic nerves and helps prevent Schwann cell apoptosis during development. The SCF induced activation of c-kit expressed in cultured Schwann cells results in the phosphorylation of the downstream effector Akt known to be activated in an anti-apoptotic pathway.

Materials and Methods

Cell lines and Reagents

Recombinant stem cell factor (SCF) was a gift from Amgen (Thousand Oaks, CA). Forskolin was from Calbiochem (La Jolla, CA). The cell lines ST88-14, T265, STS 26T used in this study have been previously described (Badache et al., 1998). The 90-8 and 88-3 cell lines were obtained from Dr. Jeff DeClue and have been previously described (DeClue et al. 1992).

Schwann cell culture

Primary Schwann cell cultures were established essentially as described by Brockes and colleagues (1979). Sciatic nerves were removed from 3-day rat pups, digested for 2 hours in 0.03% collagenase (Serva) at 37°C, and triturated thoroughly to achieve dissociation. Cells were cultured as monolayers in low glucose Dulbecco's Modified Eagle's Medium (DMEM) supplemented with 10% FBS, 100 units/ml penicillin and 100ug/ml streptomycin, and maintained at 37°C in a humid atmosphere of 10% CO2/90%air. Contaminating fibroblasts were inhibited by 72 hours treatment with 10uM cytosine arabinoside.

Human Schwann cells

Primary human Schwann cell cultures were established as described by Wood et al., (2000) (Miami Project, University of Miami, Miami, Fla). Fresh human peripheral nerves (cauda equina) were obtained from Dr. Wood from transplant patients. For ten days, the nerve fragments were placed in DMEM containing 10% heat inactivated fetal

bovine serum (Hyclone, Logan, UT), 2uM forskolin, 10nM NDF β1 (Amgen Inc., Thousand Oaks, CA), 50U/ml penicillin and 0.05 mg/ml streptomycin (Sigma, St Louis, MO). Then the fragments were dissociated in DMEM containing 10% heat inactivated fetal bovine serum, 2uM forskolin, 10nM NDF, 50U/ml penicillin and 0.05 mg/ml streptomycin, 0.05% collagenase (Worthington Biochemicals, Freehold, NJ) and 0.25 % dispase (Boehringer Mannheim, Indianapolis, IN) in a erlenmyer flask. The nerve fragments were incubated at 37C in a 5% CO2 incubator in the enzyme solution for 18h. After centrifugation, the cells were resuspended in fresh media and were plated in 100mm culture dishes in DMEM containing 10% heat inactivated fetal bovine serum, 2uM forskolin, and 10nM NDFβ1. In Schwann cells cultured without forskolin, the nerve fragments were incubated with DMEM containing 10% serum for 3 days. Then the nerve fragments were worked up as previously described in media containing 10% serum with no forskolin or NDF β1. The cells were harvested 24 hours after plating.

Sciatic nerves

Rat sciatic nerves were extracted from neonatal and adult animals. The nerves were lysed in RIPA buffer (1% triton X-100, 0.5% sodium deoxycholate, 0.1% sodium dodecylsulfate, SDS, in phosphate buffered saline, PBS, pH 7.2) containing 1mM sodium orthovanadate and a cocktail of protease inhibitors. Protein concentration was determined by the DC protein assay (Bio-Rad, Hercules, CA).

MTT assay

This assay involved a spectophotometric analysis of the degradation of the bromide salt MTT (3-[4,5-dimethythiazol-2-yl]-2,5 diphenyl tetrazolium bromide) by mitochondrial dehydrogenase enzymes yielding purple formazan crystals as a by-product of this reaction. After the incubation treatment, MTT labeling reagent (0.5 mg/ml) were added to cell cultures for 4 hours (humidified atmosphere, 5% CO_2, 37° C). Following overnight incubation with a solubilization solution (10% SDS in 0.01 M HCL), the amount of solubilized formazan crystals were quantified at 505 nm using an automated microplate reader EL311sx (Bio-Tek Instruments, Inc., Winooski, VT). Increases in absorbance correlated with the number of cells.

Western blotting

Cells cultured in DMEM supplemented with 10% FCS were lysed in RIPA (1% triton X-100, 0.5% sodium deoxycholate, 0.1% SDS in phosphate buffer saline) containing a cocktail of protease inhibitors, PMSF, leupeptin, aprotinin (Calbiochem). Protein lysates were separated by electrophoresis in a 4 to 10% gradient polyacrylamide gel (In Vitrogen) and transferred onto a PVDF membrane (Dupond, NEN, Boston, MA) for 1 hour at 80 V. After blocking with a 5% nonfat dry milk solution for 30 minutes, the PVDF membrane were incubated in the presence of the primary antibody overnight at 4C. Following 4 washes in PBS containing 1% Tween 20 for 20 minutes, the membrane was incubated with a horseradish peroxidase-conjugated secondary antibody for 1 hour at room temperature (Transduction Systems, San Diego, CA).

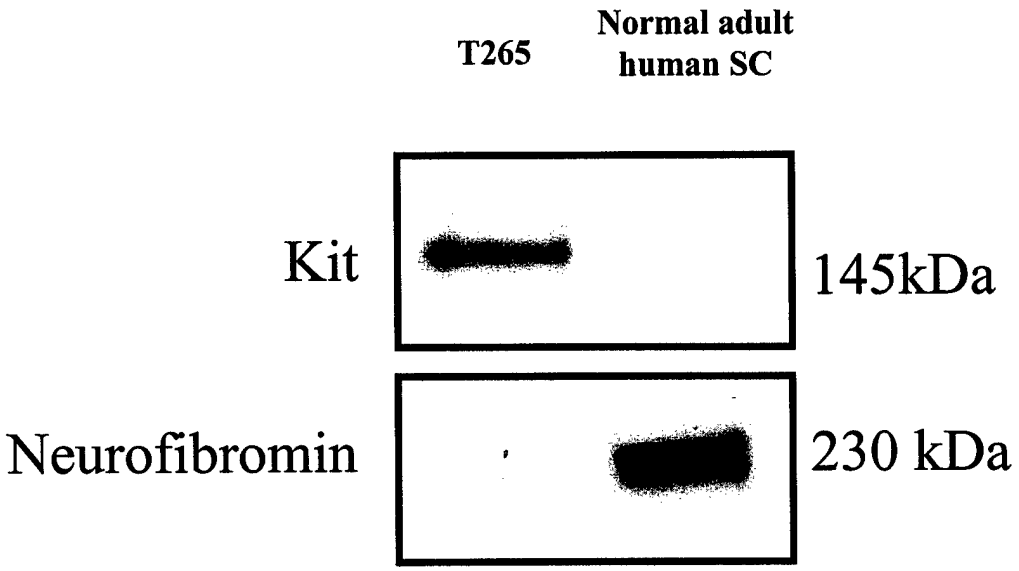

Figure 4. Normal human Schwann cells do not express c-kit but express neurofibromin. Cells were lysed and 25ug of proteins were analyzed by immunoblotting with c-kit (A) and neurofibromin (B) antibodies. These immunoblots are a representative experiment repeated 3 times with similar results.

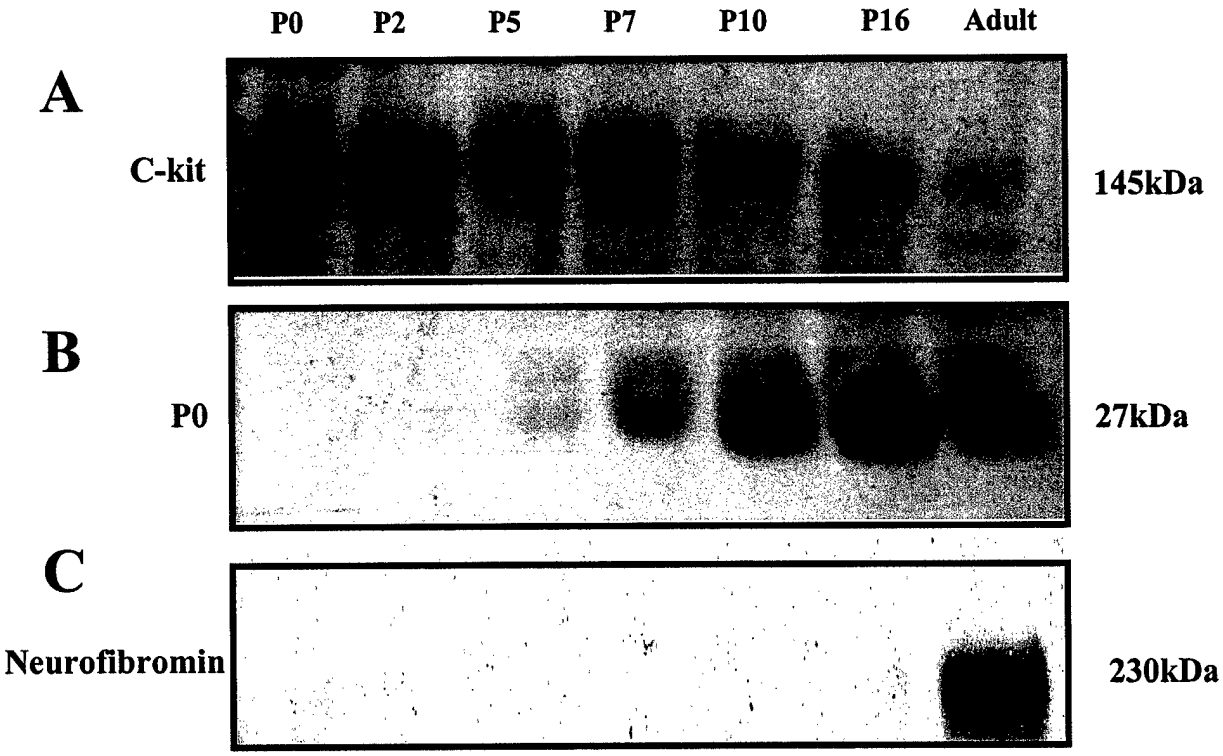

Figure 5. Developmental analysis of c-kit, P0, and neurofibromin protein in rat sciatic nerves, postnatal day 0, postnatal day 2 (P2), postnatal day 5 (P5),postnatal day 7 (P7), postnatal day 10 (P10), postnatal day 16 (P16), and adult. Rat sciatic nerves were homogenized with lysis buffer, and 100ug of proteins were analyzed by immunoblotting with c-kit (A), P0 (B), or neurofibromin (C) antibodies. These immunoblots are a representative experiment repeated 3 times with similar results.

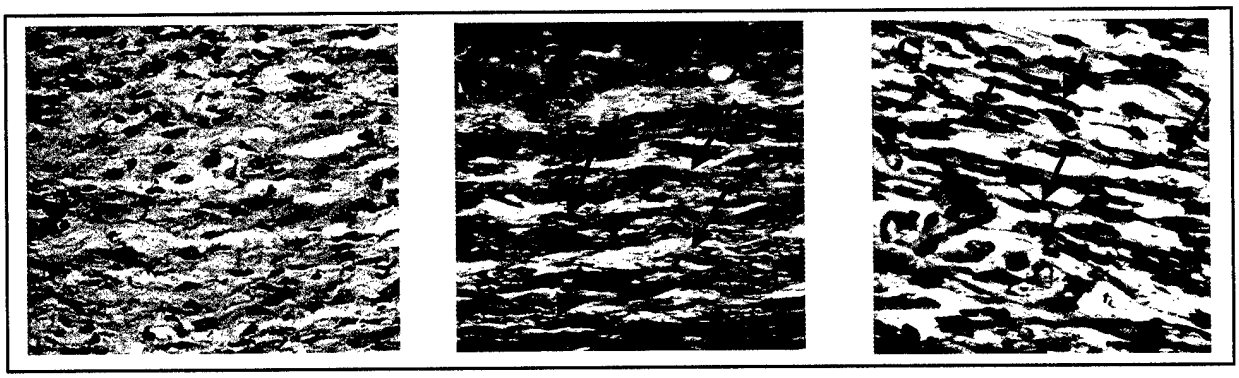

Figure 6. Expression of c-kit in neonatal rat sciatic nerves. Studies were carried out to determine c-kit and S100 expression in fresh frozen sections of postnatal day 2 rat sciatic nerves. In the nerve, the control section incubated with the absence of primary antibody showed no staining (panel A). Cells (arrows) display strong immunoreactivities to S100 antibody. The spindle shaped-cells present in the sciatic nerve are immunoreactive to the kit antibody as illustrated by the arrows (panel C). These stained sections are a representative experiment repeated 3 times with similar results.

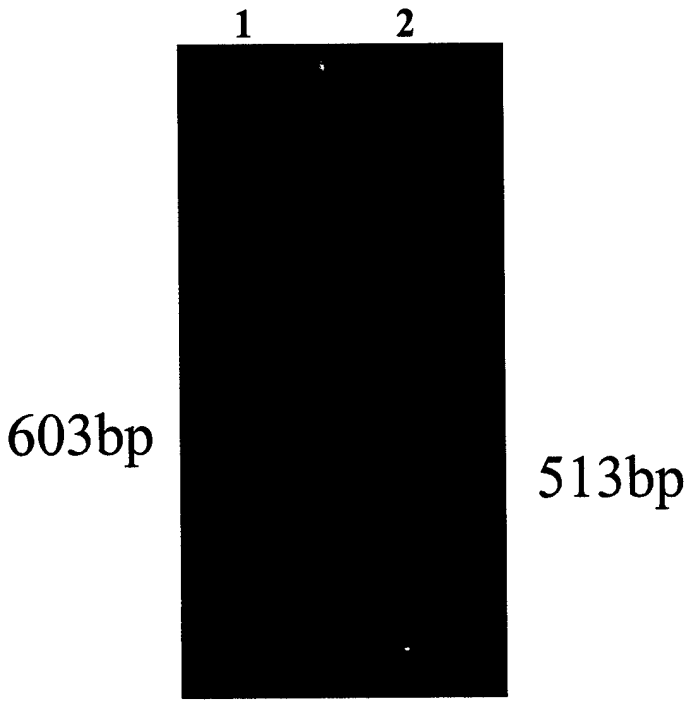

Figure 7. Cultured neonatal rat Schwann cells express c-kit mRNA. RT/PCR amplification of c-kit mRNA in cultured neonatal rat Schwann cells. Photograph of c-kit products, 513 base pairs (lane 2) separated on a 2% agarose gel stained with ethidium bromide. Molecular weight markers are derived from Hae III digest of $\phi\chi$-174 viral DNA as shown in lane 1. This PCR product is a representative experiment repeated 3 times with identical results.

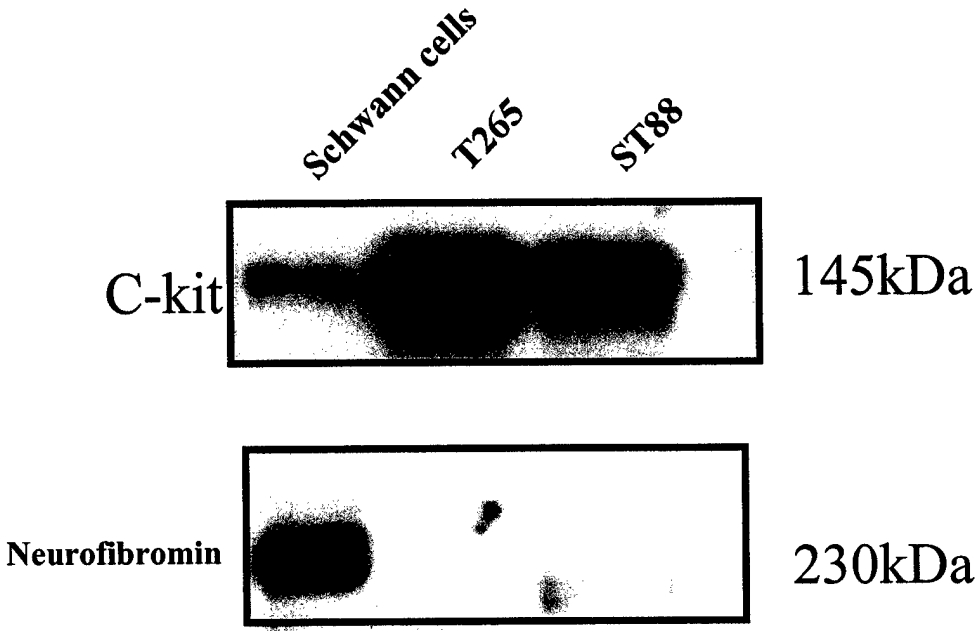

Figure 8. Neonatal rat Schwann cells express low c-kit levels but high neurofibromin levels. Cells were lysed and 25ug of proteins were analyzed by immunoblotting with c-kit and neurofibromin antibodies. These immunoblots are a representative experiment repeated 3 times with similar results.

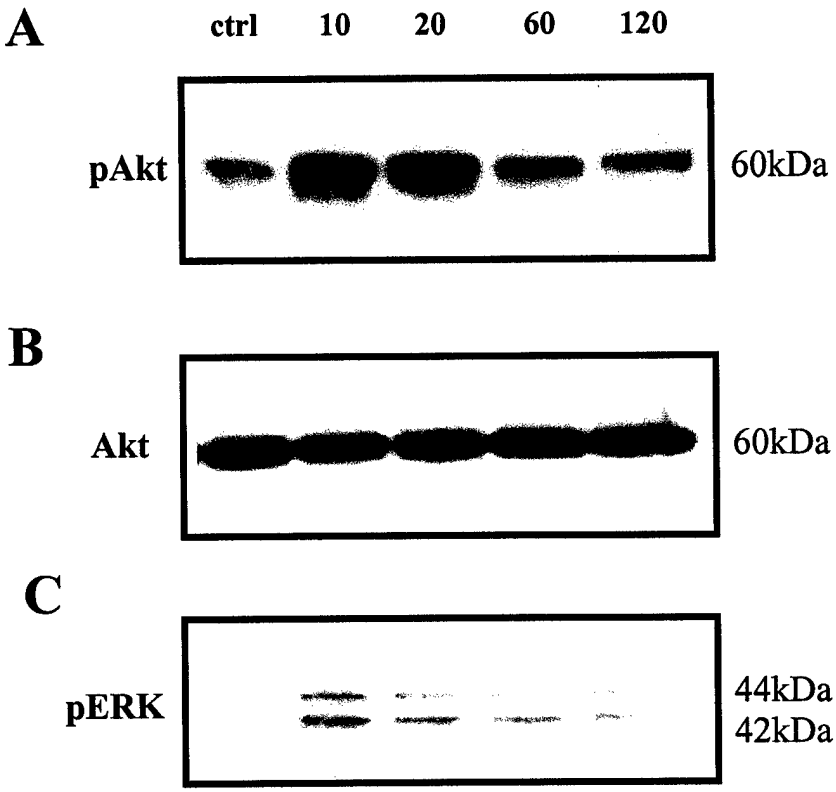

Figure 9. SCF induces weak ERK phosphorylation but strong Akt phosphorylation in neonatal rat Schwann cells. Schwan cells were cultured with 50ng/ml of SCF for up to 120 minutes. Schwann cells were lysed and 25ug of proteins were analyzed by immunoblotting with a phosphorylated specific Akt antibody (panel A), the Akt antibody (panel B), or the phosphorylated specific ERK antibody (panel C). These immunoblots are a representative experiment repeated 3 times with similar results.

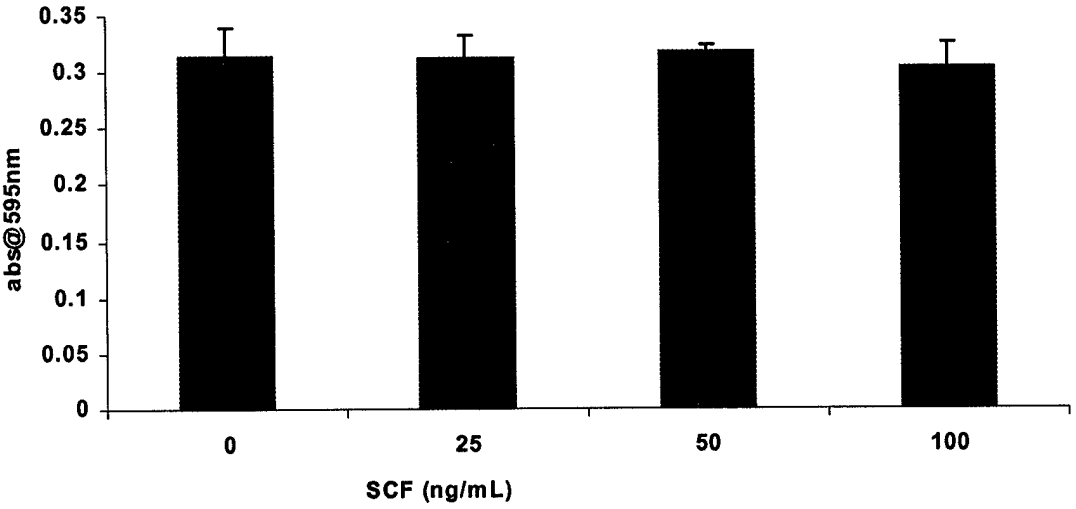

Figure 10. SCF does not induce neonatal rat Schwann cell proliferation. Schwann cells were cultured in the presence of increasing concentrations of SCF for 96 hours. Cell number was evaluated by the colorimetric MTT assay after 96 hours in culture. Values are expressed as mean of at least 3 replicates from a representative experiment repeated 3 times. Error bars represent standard deviations. The data were statistically analyzed using One Way Analysis of Variance (ANOVA) and no statistical significance was found ($F=0.990$).

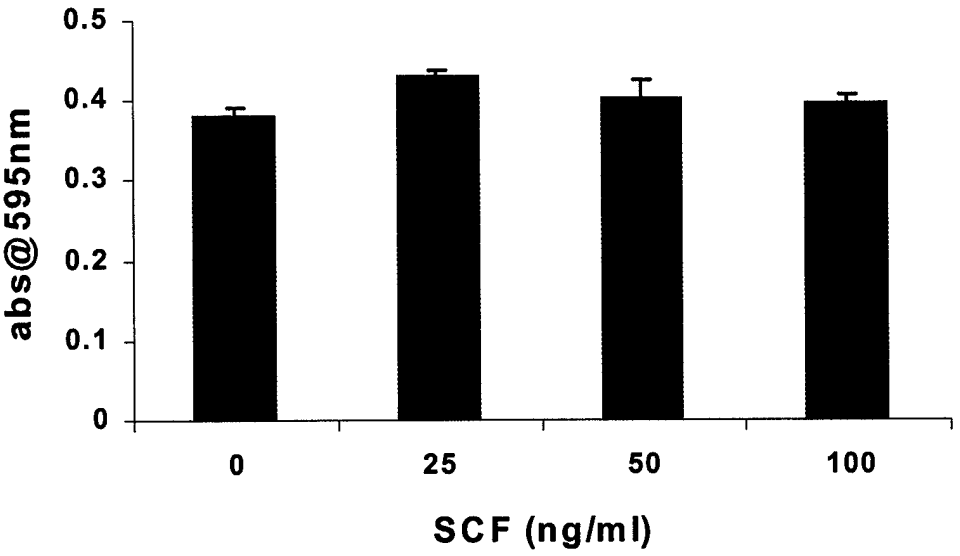

Figure 11. SCF does not synergize with NDF to increase Schwann cell proliferation. Schwann cells were cultured in the presence of 20ng/ml of NDF and increasing concentrations of SCF for 96 hours. Cell number was evaluated by the colorometric MTT assay after 96 hours in culture. Values are expressed as mean of at least 3 replicates from a representative experiment repeated 3 times. Error bars represent standard deviations. The data were statistically analyzed using One Way Analysis of Variance (ANOVA) and no statistical significance was found (F=0.962).

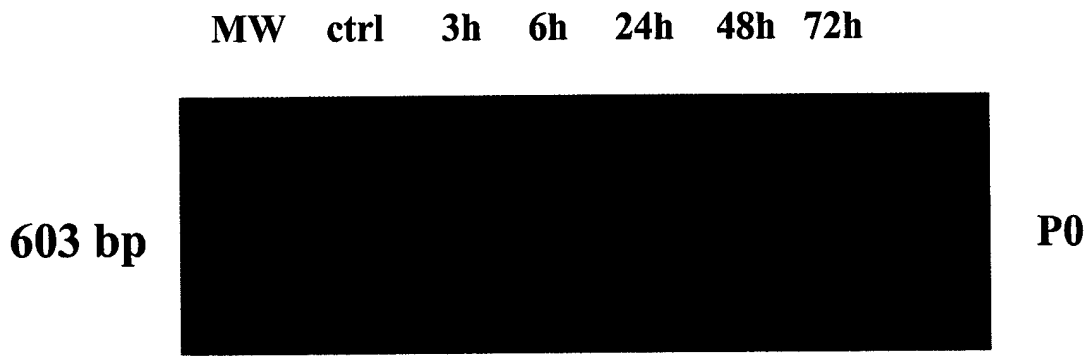

Figure 12. SCF does not induce Schwann cell differentiation. Schwann cells were cultured in the presence of 100ng/mlof SCF up to 72 hours. RT/PCR amplification of P0 mRNA were performed for each time point. Photograph of P0 products, 603 base pairs were separated on a 2% agarose gel stained with ethidium bromide. Molecular weight markers (MW) are derived from Hae III digest of $\phi\chi$-174 viral DNA. These PCR products are a representative experiment repeated 3 times with similar results.

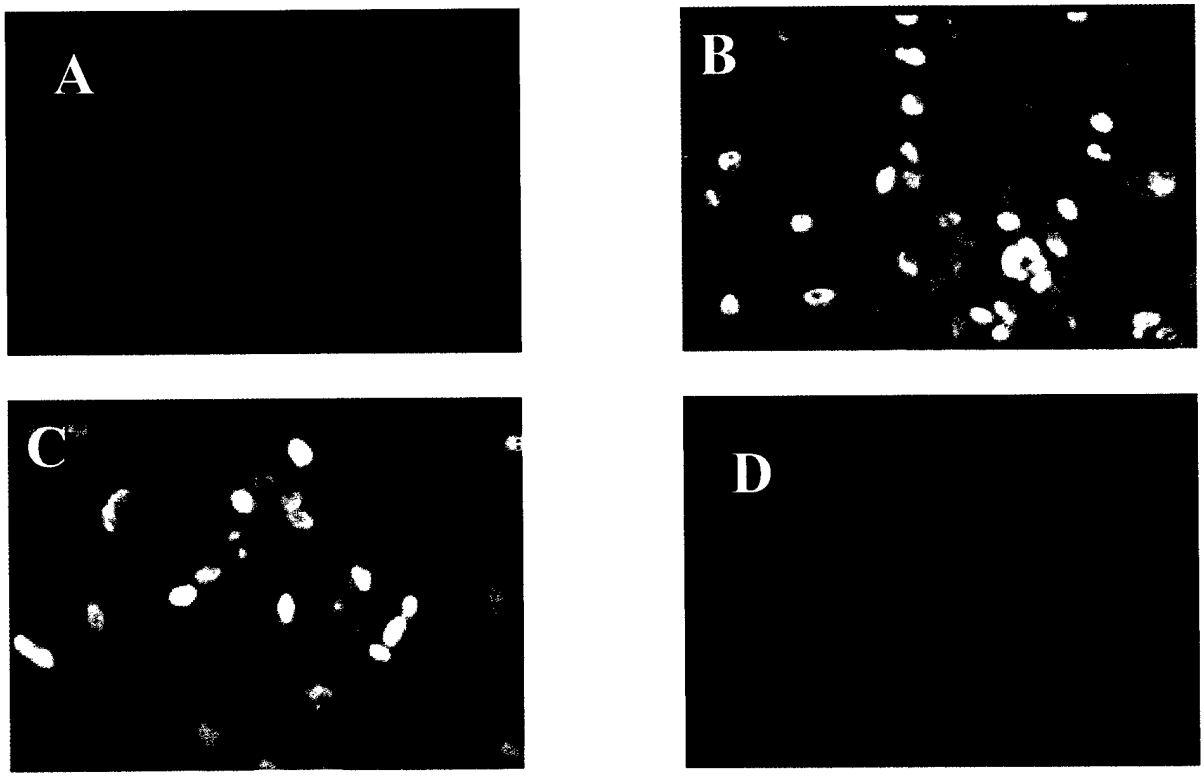

Figure 13. SCF promotes Schwann cell survival. Schwann cells were cultured in the presence of SCF for 72 hours. Using the TUNEL assay, apoptotic cells display fluorescent nuclei. Control cells without TdT (A), serum free medium (B), Schwann cells in serum free medium with SCF (50ng/ml) (C), and Schwann cells in serum free medium with neuregulin (50ng/ml) (D). These photographs are a representative field of an experiment for repeated 3 times with similar results.

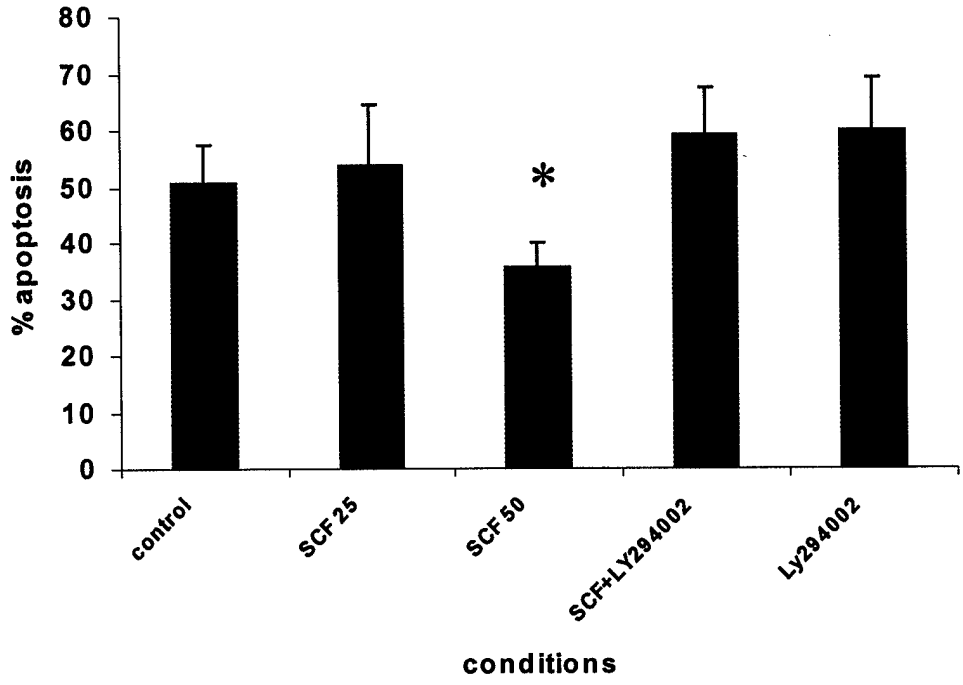

Figure 14. SCF promotes Schwann cell survival. Schwann cells were cultured in serum free media, in the presence of SCF (25 or 50ng/m), or in the presence of SCF (50ng/ml) with LY294002 (10uM) for 72 hours. Apoptotic cells were determined using TUNEL assays. Values are the mean percentage of apoptotic cells of an experiment repeated 3 times. Error bars represent +/- standard error of the mean. 2 fields of 120-150 cells were counted for each experiment at each condition. The data were determined to be statistically significant using ANOVA ($F(3,8)=13.992$). Post-hoc comparisons were determined using Tukey's LSD (*, significantly different from control, $P<0.05$).

Discussion

In this study, we have shown that c-kit is developmentally regulated in rat sciatic nerves. C-kit expression is at its highest level during postnatal development and at its lowest level in the adult. C-kit expression is inversely related to that of P0 expression. In intact sciatic nerves neurofibromin expression is present in the adult but absent in neonatal rats. Using immunohistochemistry, c-kit receptors have been localized to Schwann cells in sciatic nerves. In addition, cultured neonatal rat Schwann cells express c-kit mRNA and c-kit protein. Upon the addition of SCF, c-kit activation results in the phosphorylation of Akt and not ERK. Functionally, the activation of c-kit with SCF prevents Schwann cell apoptosis and neither proliferation nor differentiation. C-kit activation in NF1 Schwann cells results in the activation of Akt and ERK, which is not the case in cultured neonatal Schwann cells. Interestingly, normal human adult Schwann cells do not express c-kit while NF1 Schwann cells overexpress c-kit.

Receptor expression in the development of sciatic nerves

Schwann cells expressed many growth factor receptors on their surface. The PDGF receptor has been well studied in Schwann cells, but it is not developmentally regulated. Its expression is as high in neonate as in the adult (Eccleston et al., 1993). The erb-B receptor family is another type of Schwann cell surface growth factor receptor that is regulated during development. Similar to c-kit, Erb 2 expression is high in neonatal sciatic nerves but is low in the adult (Cohen et al., 1992). In addition, ErbB3 is developmentally regulated similar to erbB2 (Dang, unpublished observations). Furthermore, NGF is another growth factor receptor, which is regulated during

development (Lemke et al., 1988). The developmental regulation of c-kit expression is similar to that of p75 expression. Both receptors expressions are high in rat sciatic nerves until postnatal day 6 and decrease to low levels at postnatal day 14 and in the adult (Tikoo et al., 2000). At the time when both receptor expressions decrease, P0 expression increases to maximal level in the adult. Interestingly, neurofibromin is absent in neonatal sciatic nerves, but is present in the adult. Its expression is high in the neonatal stages and disappears in the adult. These results suggest that the lack of neurofibromin expression correlates with the proliferation of Schwann cells. Similar to other growth factor receptors, c-kit activation contributes to the development of Schwann cells. Both Erb-B2 and p75 receptor expressions are inversely correlated with that of P0 protein. In neonates c-kit expression is high during the proliferating stages of Schwann cells, but is low during the differentiating stages of Schwann cells in the adult. Taken together, c-kit expression may be important during the survival phase of Schwannn cells during development.

c-kit expression in Schwann cells

In this study, we report that c-kit is expressed by 2 additional NF cell lines, the 90-8 and 88-3, which are missing neurofibromin (Badache et al., 1998; DeClue et al., 1992). The expression of c-kit correlates with the absence of neurofibromin in Schwann cells derived from NF tumors. These observations are consistent with those in studies performed by Ryan et al. (1994) and Badache et al. (1998). However, we report that neonatal rat Schwann cells express low c-kit receptor levels on their surface compared to that of NF Schwann cells overexpressing c-kit. These results are in contrast to the findings reported by Ryan and co-workers, who did not detect any c-kit mRNA or c-kit

protein expression in normal Schwann cells (Ryan et al., 1994). The difference may be explained by the use of primers with higher affinities for mRNA detection and FACS analysis instead of immunoblots. In addition, Badache and co-workers did not detect c-kit in normal Schwann cells, since the amount of protein analyzed was two fold less and autoradiography not sufficiently long enough for detection. In conclusion, increased proteins loaded for immunoblotting and longer exposure during autoradiography may explain the discrepancies observed between reports.

Schwann cells and apoptosis

Schwann cells undergo apoptosis when incubated in serum free media over 3 days (Syroid et al., 1998; Delaney et al., 1999). Schwann cell apoptosis is mediated by caspase activities, and the cells can be rescued by IGF (Delaney et al., 1999). Salzer et al. (2000) reported that neuregulins promote Schwann cell survival through the phosphorylation of Akt. Similarly, our results show that SCF is able to rescue Schwann cells from programmed cell death via the activation of Akt. However, SCF is not as potent as neuregulins that have already documented effects on Schwann cell survival (Syroid et al., 1996; Maurel et al., 2000). The difference between the two growth factors may be that neuregulins activate several signaling pathways, including MAPK and PI3K, while SCF only activates PI3K. Taken together, the activation of c-kit by SCF prevents Schwann cell death during development and contributes to the survival of NF1 Schwann cells.

Schwann cells and neurofibromin expression

Several studies have reported that neurofibromin regulates Ras due to its homologous sequence to GTPase activating protein, GAP, (DeClue et al., 1992). This sequence represents only a small fraction of the neurofibromin protein, while the majority of the Nf1 gene product has yet to be characterized. It is possible that neurofibromin may play a role in the proliferation of Schwann cells during development. Wrabetz et al., (1995) reported the lack of regulation for NF1 mRNA expression but did not investigate neurofibromin protein in rat sciatic nerves. In this study we report that neurofibromin is developmentally regulated and expressed only in adult sciatic nerves. Our findings suggest that neurofibromin is translationally regulated in Schwann cells. Neurofibromin expression is absent in human fetal Schwann cells but present in adult human Schwann cells (Dang, unpublished observations). These observations are consistent with the idea that neurofibromin plays a role of a suppressor of proliferation. It is absent during the proliferating stages of Schwann cells but is present when Schwann cells stop proliferating. The loss of neurofibromin in combination with other factors results in the transformation of adult Schwann cells leading to the development of neurofibromas.

Interestingly, neonatal sciatic nerves do not express neurofibromin, but cultured neonatal rat Schwann cells express high levels of neurofibromin. During Schwann cell isolation, the Schwann cells lose axonal contact and cease to proliferate. Concomitantly, they increase the expression of neurofibromin, which correlates with the normal non-proliferative stage of Schwann as in the adult. Numerous reports have shown that Schwann cells freshly isolated from neonatal rat sciatic proliferate minimally unless

cultured with forskolin and growth factors, such as neuregulins. Similar to our findings, Wrabetz et al. (1995) reported that cultured neonatal rat Schwann cells express neurofibromin. In contrast to our studies, they investigated the regulation of neurofibromin mRNA expression and not neurofibromin protein expression in rat sciatic nerves.

As shown previously, the loss of neurofibromin in adult Schwann cells leads to abnormal cell proliferation. It is possible that the loss of neurofibromin in Schwann cells induces the aberrant expression of c-kit. However, the molecular mechanism for this abnormal expression of this growth factor receptor is still under investigation. As it is in a number of cancers, c-kit may be a receptor involved in the development of Schwann cells and due to a series of mutations, such as the loss of neurofibromin, c-kit is inappropriately re-expressed in NF1 Schwann cells.

c-kit expression in tumor cells

The expression of c-kit has been associated with several types of tumors including gliomas, melanomas, myeloid leukemias, small cell lung cancer, and breast cancer (Krystal et al., 1996; Tuner et al., 1993). In humans, series of gain-of-function mutations in the c-kit juxtamembrane region have been found in gastrointestinal stromal cell tumors (Hirota et al., 1998). C-kit is also aberrantly expressed in approximately 70% of all small cell carcinomas in the lung (SCCL), as well as in breast, cervical and ovarian tumors (Tuner et al., 1993; Hines et al., 1995; Hines et al., 1996). Schwann cells derived from NF1 tumors have high levels of c-kit expression contributing to Schwann cell neoplasia (Badache et al., 1998). Coexpression of c-kit and SCF in NF1 Schwann cells generates

an autocrine loop that may play a role in the etiology of these diseases (Badache et al. 1998; Ryan et al., 1994). Our results report that additional cell lines, the 90-8 and 88-3, express c-kit as well. In contrast to NF1 Schwann cells, normal adult human Schwann cells expressing neurofibromin do not have c-kit on their surfaces. Taken together, the loss of neurofibromin in Schwann cells may induce aberrant expression of growth factor receptors, such as c-kit, contributing to Schwann cell transformation and the development of NF tumors.

c-kit and glial cells

C-kit expression has been detected in many glial cells, but the normal function of the c-kit receptor differs depending on the cell type. For instance, high c-kit expression levels induced by HIV are associated with astrocyte apoptosis (He et al., 1997). In the case of oligodendrocytes, c-kit expression is increased between postnatal days 10 and 12, suggesting that c-kit and its ligand may play a role during oligodendrocyte development (Ida et al., 1993). Similarly, c-kit expression is developmentally regulated in Schwann cells. Our results suggest that activation of c-kit prevents Schwann cell apoptosis in the embryonic and neonatal stages of development to obtain the appropriate Schwann cell numbers needed for the myelination of a segment of the axon. Previous reports have shown that the ligand for c-kit, SCF, may be secreted by axons (Young et al., 1998) or may also be secreted from mast cells (De Paulis et al., 1999). Taken together, SCF may be a growth factor important for the survival Schwann cell during development.

Conclusion

In summary, c-kit is important for Schwann cell development and its expression is inversely correlated with that of neurofibromin. In addition, we have shown that normal human adult Schwann cells do not express c-kit, but all NF1 cell lines aberrantly express c-kit. Although we do not know the functions of neurofibromin during development, our results indicate its expression increases in the adult. Interestingly, an inverse correlation exists between neurofibromin and c-kit expression. Activation of c-kit with SCF prevents Schwann cell apoptosis in the neonates and contributes to the increased survival of NF1 Schwann cells (summarized in figure 15). The loss of neurofibromin is the first event in a long series of events that leads to the re-expression of c-kit contributing to the development of NF1 tumors. These results may provide a better understanding of the molecular mechanisms leading to the abnormal proliferation of Schwann cells in patients with NF1.

Stimulation of intracellular Signaling Pathways in Response to PDGF BB I NF1 Schwann Cells

Ian Dang and George H. DeVries
Research Service
Edward Hines Jr. VA Hospital
Hines, IL 60141
Department of Cell Biology, Neurobiology and Anatomy
Loyola University of Chicago
Maywood, IL 60153

Abstract

Neurofibromatosis type 1 (NF1) is a genetic disease characterized by the loss of neurofibromin leading to the formation of either benign Schwann cell tumors (neurofibromas) or highly invasive and metastatic Schwann cell tumors (neurofibrosarcomas). Our laboratory has studied growth factor receptor expression and signal transduction pathways in Schwann cells to better understand the molecular basis of hyperplasia in NF1. We now report that the ERK and PI3K pathways are both activated in response to PDGF BB in normal human adult Schwann cells and Schwann cells derived NF1 tumors. Inhibition of the PI3K pathway leads to the decreased proliferation of NF1 Schwann cells. Interestingly, PDGF BB induces increases in intracellular calcium levels only in NF1 Schwann cells. In addition, PDGF BB induces phosphorylation of calmodulin kinase II (CAMKII) in NF1 Schwann cells, and the CAMKII inhibitor, KN62, decreases the proliferation of NF1 Schwann cells stimulated by PDGF BB. Overall, these results indicate that the aberrant activation of the calcium signaling pathway in Schwann cells contributes to the formation of NF1 tumors.

Introduction

Neurofibromatosis type 1 (NF1) is an inherited disease, which is diagnosed by many symptoms including neurofibromas, café-au-lait spots, and learning disabilities (Friedman et al., 1999). Among the numerous hallmarks of NF1 are the formation of either benign Schwann cell tumors of peripheral nerve sheath called neurofibromas or sometimes lethal malignant peripheral nerve sheath tumors, which are

neurofibrosarcomas. The tumors of this genetic disease are caused by defects of the NF1 gene resulting in the absence of its protein product, neurofibromin. Although the function of neurofibromin is not known, its loss leads to the elevated levels of the activated form of Ras (Ras-GTP). Past studies have shown that Ras-GTP levels are elevated in neurofibrosarcoma tumors from NF1 patients and Schwann cells derived from mice lacking NF1 (Feldkamp et al., 1999; Kim et al., 1995). However, the link between the development of Schwann cells tumors and the loss of neurofibromin has not yet been clearly established.

As it is the case with several types of cancer, aberrant expression of growth factor receptors may play a role in cellular transformation. Schwann cell lines derived from NF1 tumors expressed aberrant growth factor receptor expression. Badache et al.(1998) have previously reported that Schwann cells overexpress c-kit and PDGF receptors. In addition, the aberrant expression of the EGF receptors has been documented on the surface of NF1 Schwann cells (DeClue et al., 2000). Interestingly, NF1 Schwann cells lack Erb-B2 receptors (Badache et al., 1998), which are activated in response to neuregulin, the most potent growth factor for normal Schwann cells (Morrisey et al., 1995). Taken together, these results implicate aberrant growth factor receptor expression in the development of Schwann cell tumors in NF1 patients.

The activation of PDGF receptors in NF1 cells may lead to abnormal activation of intracellular signaling pathways contributing to increased NF1 Schwann cell proliferation compared to normal human adult Schwann cells. In this study we report that both the PI3 kinase pathway and the calcium pathway mediate NF1 Schwann cell proliferation induced by PDGF BB. The ERK pathway was activated in response to PDGF BB.

Materials and Methods

Cell lines and Reagents

Recombinant platelet derived growth factor BB (PDGF BB) was purchased from R&D (Minneapolis, MN). Thapsigargin was from Biomol (Plymouth Meeting, PA), rapamycin (Calbiochem), KN62 (Biomol), PD98059 (Calbiochem), LY294002 (Calbiochem). PDGF receptor beta (Santa Cruz), Neurofibromin (Santa Cruz), pERK (Cell signaling), pAkt (Cell Signaling), Akt (Cell Signaling), CAMK II (Promega).

The cell lines ST88-14, T265, STS 26T used in these studies were previously described (Badache et al., 1998). The 90-8 and 88-3 cell lines were obtained from Dr. Jeff DeClue have been previously described (DeClue et al. 1992). Cells were cultured as monolayers in low glucose Dulbecco's Modified Eagle's Medium (DMEM) supplemented with 10% FBS, 100 units/ml penicillin and 100ug/ml streptomycin, and maintained at 37°C in a humid atmosphere of 10% CO2/90%air. For proliferation assay and western blotting, cells were serum starved overnight and were cultured in serum free media with PDGF BB alone or in combination with inhibitors.

Human Schwann cells

Primary human Schwann cell cultures were established as described by Wood et al., (2000) (Miami Project, University of Miami, Miami, Fla). Fresh human peripheral nerves (cauda equina) were obtained from Dr. Wood from transplant patients. For ten days, the nerve fragments were placed in DMEM containing 10% heat inactivated fetal bovine serum (Hyclone, Logan, UT), 2uM forskolin, 10nM NDF β1 (Amgen Inc.,

Thousand Oaks, CA), 50U/ml penicillin and 0.05 mg/ml streptomycin (Sigma, St Louis, MO). Then the fragments were dissociated in DMEM containing 10% heat inactivated fetal bovine serum, 2uM forskolin, 10nM NDF, 50U/ml penicillin and 0.05 mg/ml streptomycin, 0.05% collagenase (Worthington Biochemicals, Freehold, NJ) and 0.25 % dispase (Boehringer Mannheim, Indianapolis, IN) in a erlenmyer flask. The nerve fragments were incubated at 37C in a 5% CO2 incubator in the enzyme solution for 18h. After centrifugation, the cells were resuspended in fresh media and were plated in 100mm culture dishes in DMEM containing 10% heat inactivated fetal bovine serum, 2uM forskolin, and 10nM NDFβ1. In Schwann cells cultured without forskolin, the nerve fragments were incubated with DMEM containing 10% serum for 3 days. Then the nerve fragments were worked up as previously described in media containing 10% serum with no forskolin or NDF β1. The cells were harvested 24 hours after plating.

NF1 tumors

NF1 tumors were obtained from patients diagnosed with NF1 and were removed by Dr. John Shea at Loyola University Medical Center.

MTT assay

This assay involved a spectophotometric analysis of the degradation of the bromide salt MTT (3-[4,5-dimethythiazol-2-yl]-2,5 diphenyl tetrazolium bromide) by mitochondrial dehydrogenase enzymes yielding purple formazan crystals as a by-product of this reaction. After the incubation treatment, MTT labeling reagent (0.5mg/ml) were added to cell cultures for 4 hours (humidified atmosphere, 5% CO_2, 37°C). Following overnight incubation with a solubilization solution (10% SDS in 0.01 M HCL), the

amount of solubilized formazan crystals were quantified at 595 nm using an automated microplate reader EL311sx (Bio-Tek Instruments, Inc., Winooski, VT). Increases in absorbance correlated with the number of cells.

Western blotting

Cells cultured in DMEM supplemented with 10% FCS were lysed in RIPA (1% triton X-100, 0.5% sodium deoxycholate, 0.1% SDS in phosphate buffer saline) containing a cocktail of protease inhibitors, PMSF, leupeptin, aprotinin (Calbiochem). Tumors lysates were obtained by homogenizing the tissue in RIPA. Protein lysates were separated by electrophoresis in a 4 to 10% gradient polyacrylamide gel (InVitrogen) and transferred onto a PVDF membrane (Dupont, NEN, Boston, MA) for 1 hour at 80V. After blocking with a 5% nonfat dry milk solution for 30 minutes, the PVDF membrane were incubated in the presence of the primary antibody overnight at 4°C. Following 4 washes in PBS containing 1% Tween 20 for 20 minutes, the membrane was incubated with a horseradish peroxidase-conjugated secondary antibody for 1 hour at room temperature (Transduction Systems, San Diego, CA). After 3 washes with PBS-T for 10 minutes each, the immunoreactivity was detected by enhanced chemiluminescence (Dupont-NEN, Boston, MA).

Digital fluorescence ratio imaging of intracellular calcium

NF1 Schwann cells and normal human human Schwann cells were seeded onto 25mm coverslips in DMEM low glucose with 10%FBS. Following serum starvation overnight, cells were loaded with 0.5 to 1uM of with the Ca^{2+} sensitive indicator fura-

2/AM (Molecular probes, Eugene, OR) in DMEM or HBSS (Gibco BRL, Gaithersburg, MD) for 20 minutes at 37°C. After washing the cells twice with PBS or HBSS, the coverslip was fitted in a holder with a maximum holding volume of 1ml. The holder was filled with 1 ml of warm HBSS or PBS and mounted onto the microscope stage of a Zeiss Axiovert 135 inverted microscope equiped with digital fluorescence microscopy. Fields of at least 20 cells were selected for Ca^{2+} measurements using a fluor x40 oil objective. Computer images of at the cells were captured and digitally monitored using a ICCD camera. Recordings measured changes in fluorescence intensity in Schwann cells in a Hepes-buffered balanced salt solution (pH 7.2) or in PBS at room temperature. The excitation light from a xenon lamp alternated between 340nm (Ca^{2+} bound) and 380nm (Ca^{2+} free) band excitation filters, and the emission was measured at 520nm. Following 60-90s of baseline measurements, PDGF BB or thapsigargin were added at the indicated time into the 1 ml holding volume and assayed for a change in Fura-2 ratio. Fluorescence signals of at least 20 cells were acquired, stored, and analyzed using the Zeiss Attofluor RatioVision system; increases in intracellular calcium were determined using the ratio method.

STATISTICS

Statistics were determined using the Sigma Plot 2.0 software.

Results

PDGF receptor β and neurofibromin expression in NF1 cell lines, non-NF1, and normal Schwann cells.

We reported that PDGF receptor β was overexpressed in 2 neurofibrosarcoma cell lines: ST88 and T265 (Badache et al., 1998). We extended this observation to the 90-8 and 88-3 NF1 cell lines. To investigate the expression of PDGF receptor in MPNST cell lines, 25ug of cell lysates were analyzed by immunoblotting using a PDGF receptor β antibody. All NF1 cell lines (T265, ST88, 90-8, and 88-3) expressed high levels of PDGF receptor compared to the non-NF1 cell line (STS26T), which expressed low levels of this tyrosine kinase receptor (**figure 16A**). The high levels of PDGF receptor β in NF1 cells are associated with the absence of neurofibromin (**figure 16B**). Interestingly, normal human adult Schwann cells isolated from human peripheral nerves had comparable PDGF receptor expression to the T265 NF1 cell line as shown in **figure 16A**. These high receptor levels in normal adult Schwann cells are not related to the chronic elevation of intracellular cAMP due to the forskolin since the PDGF receptor is still present in cells not treated with forskolin as shown in **figure 16A**. In addition, the normal human Schwann cells express normal levels of neurofibromin (**figure 16B**).

PDGF receptor β expression in NF1 tumors

We have shown that NF1 cells expressed PDGF receptor, but we wanted to investigate the expression of PDGF receptor tumors directly in the tumors. To determine PDGF growth factor receptor expression in NF1 tumors, lysates from 4 different NF1 tumors were analyzed by immunoblotting using a PDGF receptor β antibody. Most

tumors express high levels of PDGF receptor as illustrated in **figure 17**. These results confirm that cells present inside the tumor expressed the receptor. Most cells present in the tumor are Schwann cells; however, other cells within the tumor expressing PDGF receptor cannot be ruled out. As we have previously reported (Badache et al., 1998) cell lines derived from NF1 tumors express PDGF receptors as well.

PDGF BB and downstream effectors in T265 cells

We wanted to study effectors downstream of the PDGF receptor when activated by PDGF BB, such as the phosphorylation of ERK and Akt. To investigate ERK or Akt phosphorylation induced by PDGF BB, NF1 cells were cultured in serum free medium with 20 ng/ml PDGF BB for up to 120 minutes. NF1 cell lysates were analyzed by immunoblotting using a phospho-specific ERK or Akt antibody. PDGF BB induced phosphorylation of ERK1 and ERK2 within 10 minutes of stimulation (**figure 18A**). After 120 minutes, ERK1 and ERK2 phosphorylation decreased to basal levels. When the cells were preincubated with the MEK inhibitor PD98059 for 120 minutes, ERK1 and 2 phosphorylation was not inhibited with the inhibitor concentration as high as 10 uM (**figure 18E**). We used a non-phosphorylated ERK1 antibody to determine that protein levels were similar for each time point, as shown in **figure 18C**.

In addition, PDGF BB induced phosphorylation of Akt within 10 minutes of stimulation as shown in **figure 18B**. After 60 minutes, Akt phosphorylation decreased to basal levels. We confirmed equal protein loading for each time point with an antibody against the non-phosphorylated form of Akt **(figure 18D)**. To determine if Akt phosphorylation was mediated by PI3K, an upstream effector molecule of Akt, we

preincubated the cells with different concentrations (0 to 20uM) PI3K inhibitor LY294002 for 120 minutes. As shown in **figure 18F**, Akt phosphorylation was decreased in a dose dependent manner, and using the inhibitor a concentration of 20uM resulted in the maximal decrease in phosphorylation.

Overall, these results suggest that the growth factor PDGF BB induces the activation of Akt and ERK in the ERK pathway and Akt of the PI3K pathway in NF1 Schwann cells. Next we wanted to known if these 2 pathways are also activated in normal human adult Schwann cells.

PDGF BB and downstream effectors in normal human adult Schwann cells

We postulated that PDGF BB does not phosphorylate the same downstream effectors in normal human adult Schwann cells as those in NF1 Schwann cells. To investigate the ERK and Akt phosphorylation, normal human adult Schwann cells were cultured in serum free medium with 20ng/ml PDGF BB for up to 120 minutes. Normal Schwann cell lysates were analyzed by immunoblotting using a phospho specific ERK and Akt antibody. PDGF BB induced phosphorylation of ERK after 10 minutes and the activation decreased to basal levels after 60 minutes (**figure 19A**). Similarly, the addition of PDGF BB to normal human adult Schwann cells resulted in Akt phosphorylation after 10 minutes. Akt phosphorylation remained above basal levels after 120 minutes, as illustrated in **figure 19B**. Overall, these results suggest that PDGF BB induces phosphorylation of ERK and Akt in normal human adult Schwann cells similar to NF1 Schwann cells. The loss of neurofibromin in Schwann cells does not cause signaling abnormalities in the ERK and the PI3K pathway.

Despite activation of similar signaling molecules to NF1 Schwann cells by PDGF BB stimulation, human adult Schwann cells did not proliferate to the extent of NF1 Schwann cells in response to PDGF BB. After 72 hours, PDGF BB induces almost a 2 fold increase in NF1 Schwann cell proliferation (Badache et al., 1998b), while human adult Schwann respond at a much slower rate, around a 1.2 fold increase (**figure 20**). This difference in proliferation may be due to the activation of additional signaling pathways in NF1 Schwann cells compared to human Schwann cells.

NF1 cell proliferation stimulated by PDGF BB is mediated by Akt

Since the inhibitor PD98059 did not have any effects of NF1 cell proliferation induced by PDGF BB, we decided to investigate the role of Akt in the PI3K pathway using 2 inhibitors to the PI3K pathway: wortmannin and LY294002. NF1 cells were cultured in serum free medium with 20ng/ml of PDGF BB in combination with PI3 kinase inhibitors for 72 hours. The results show that both inhibitors decreased cell proliferation induced by PDGF BB compared to cells treated with vehicle (**figure 21**). In addition, the decrease in cell proliferation was dose dependent, and the LY294002 compound had a more profound effect in slowing NF1 cell proliferation than the wortmannin compound. Overall, these results show that NF1 cell proliferation induced by PDGF BB is strongly dependent on the PI3K pathway.

PDGF BB increases intracellular calcium levels in NF1 Schwann cells

Another downstream effector of the PDGF receptor is the divalent cation calcium, which can be released from intracellular storage in response to the formation of IP3

induced by PLCγ upon receptor stimulation. To determine intracellular calcium levels in Schwann cells, cells were incubated with 1uM of Fura 2/AM and changes in relative fluorescence of the 380/340 ratio were monitored for increases in calcium levels. The individual recording of at least 20 cells are illustrated in **figure 22A**. The average recording of NF1 Schwann cells showed a rise in intracellular calcium levels in response to PDGF BB (**figure 22B**). The influx of calcium peaked 100 seconds after adding PDGF BB (**figure 22B**). However, the levels of calcium in normal human adult Schwann cells remain unchanged in response to PDGF BB but responded to the addition of a 1uM of ionomycin, a Ca^{2+} elevating agent (**figure 23**). The increase in calcium is due to intracellular calcium, since in media depleted of calcium cells still responded similarly to those in calcium containing media (data not shown). To confirm these findings, we use thapsigargin, an ATPase calcium pump inhibitor, to block the reuptake of intracellular calcium. The addition of 1uM of thapsigargin to the cells resulted in an increase Ca^{2+} levels and inhibited further releases of intracellular calcium when PDGF BB was added subsequently (**figure 24A**). Cells treated with vehicle did not affect the release of calcium from intracellular storage in response to PDGF BB added subsequently (**figure 24B**). Thus, the source of the PDGF BB-evoked calcium in NF1 Schwann cells is from the intracellular calcium storage.

PDGF BB increases phosphorylation of CAM KII

The increase in intracellular calcium levels in Schwann cells may lead to activation of calcium dependent proteins, such as CAM KII, contributing to the aberrant proliferation of NF1 Schwann cells. To investigate phosphorylation of CAM KII, T265

cells were cultured with serum free medium with 20ng/ml PDGF BB for up to 6 hours. Schwann cell lysates were analyzed by immunoblotting using a phospho specific a CaM KII antibody. PDGF BB induced phosphorylation of CAM KII after 5 minutes and results in maximum phosphorylation after 120 minutes (**figure 25**). These results suggest that the activation of the PDGF receptor with its ligand PDGF BB induces the phosphorylation of the CaM KII.

The proliferation of NF1 Schwann cells stimulated by PDGF BB is mediated by CAMKII

We investigated the role of CAMKII in the proliferation of NF1 Schwann cells in response to PDGF BB. NF1 cells were cultured in serum free medium with 20ng/ml of PDGF BB in combination with the CAMK II inhibitor KN62 for 72 hours. The results show that the CAMKII inhibitor decreased cell proliferation induced by PDGF BB in a dose dependent manner with a maximal inhibition at 4uM (**figure 26**). These results show that NF1 cell proliferation induced by PDGF BB is mediated by CAMKII of the Ca signaling pathway.

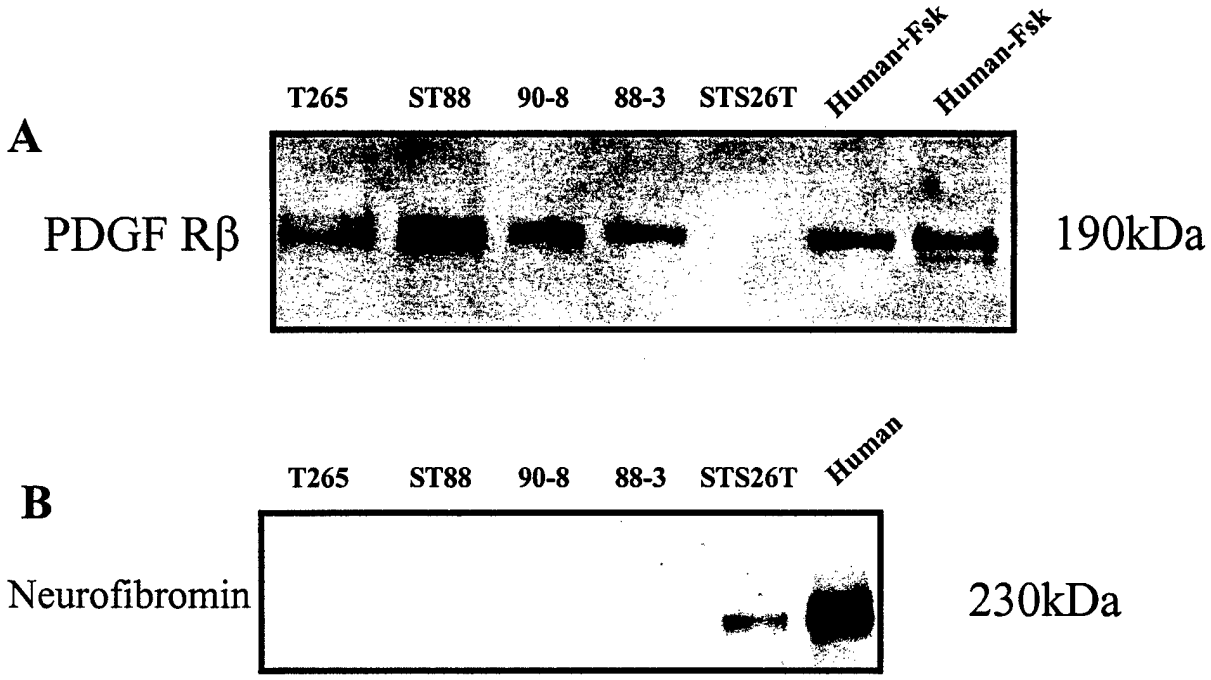

Figure 16. Western blot analysis of PDGF Receptor β and neurofibromin expression in NF1 Schwann cells and normal Schwann cells. Cells were lysed and 50ug of proteins were analyzed by immunoblotting with PDGF Receptor β (A) and neurofibromin (B) antibodies. These immunoblots are a representative experiment repeated 3 times with similar results.

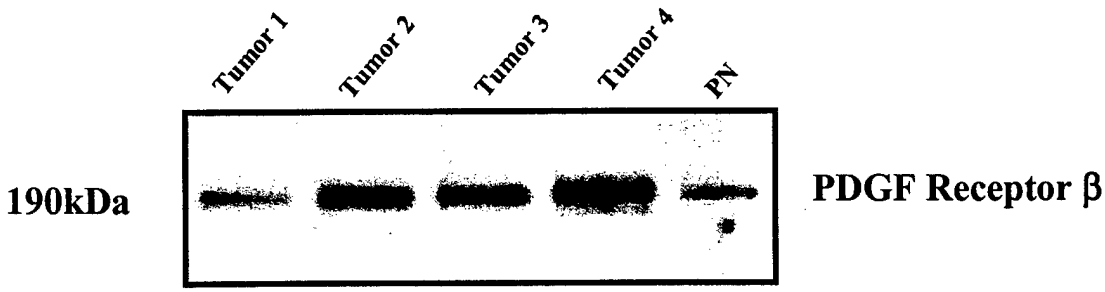

Figure 17. Western blot analysis of PDGF Receptor β in NF1 tumors. 4 fresh NF1 tumors and 1 human peripheral nerve samples were lysed with RIPA and 25ug of proteins were analyzed by immunoblotting with a PDGF Receptor β antibody. This immunoblot is a representative experiment repeated twice with similar results.

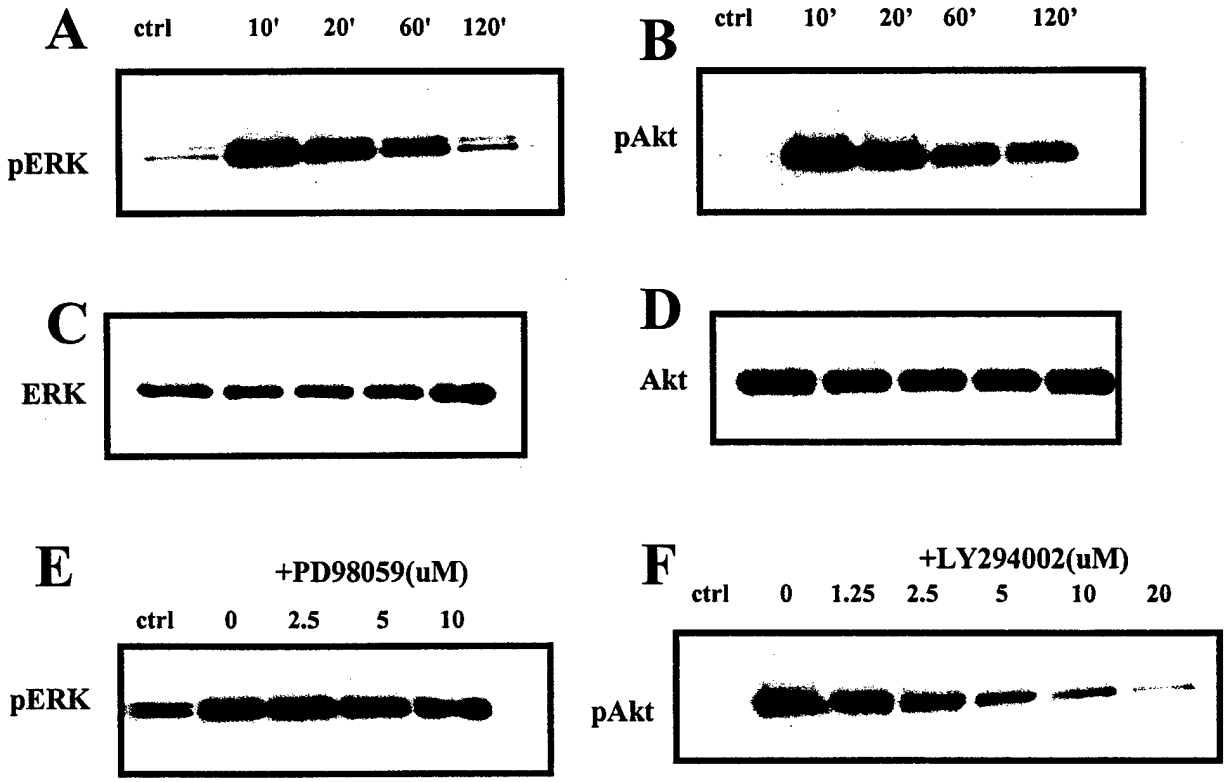

Figure 18. PDGF BB induces phosphorylation of ERK and Akt in NF1 Schwann cells. The NF1 Schwann cells were cultured with 20ng/ml of PDGF BB for up to 120 minutes. Cells were lysed and 25ug of proteins were analyzed by immunoblotting with an antibody specific for the phosphorylated form of ERK (A) or ERK (C),and the phosphorylated form of Akt (B) or Akt (D). Cells were incubated with increasing concentrations of PD980509 (E) or LY294002 (F) for 2 hours prior to adding 20ng/ml of PDGF BB for 10 minutes. These immunoblots are a representative experiment repeated 3 times with similar results.

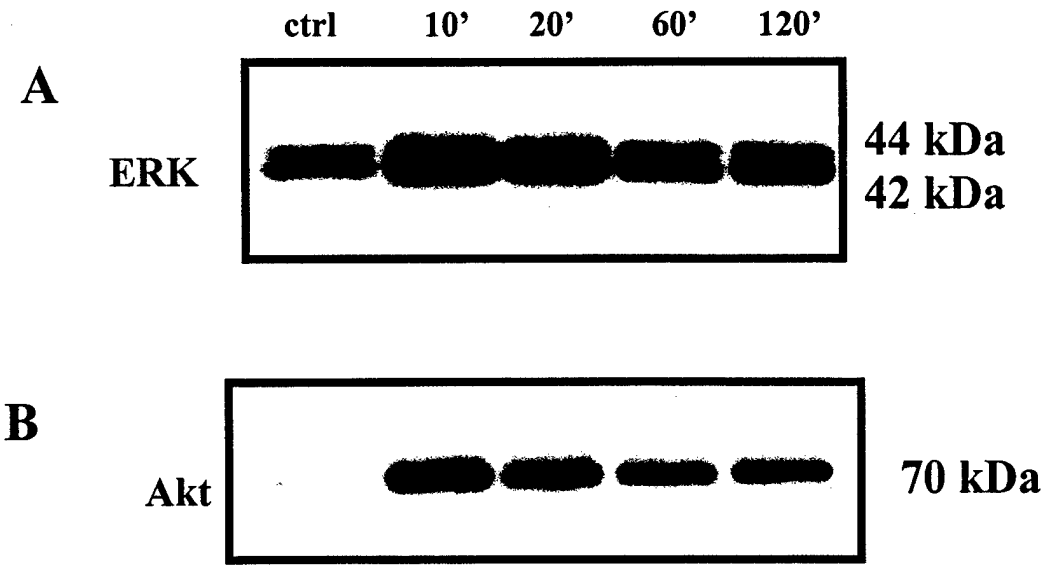

Figure 19. PDGF BB induces phosphorylation of ERK and Akt in normal human adult Schwann cells. T265 cells were cultured with 20ng/ml of PDGF BB for up to 120 minutes. Cells were lysed and 25ug of proteins were analyzed by immunoblotting with a phospho specific ERK antibody (A), a phospho specific Akt antibody (B). These immunoblots are a representative experiment repeated 3 times with similar results.

3

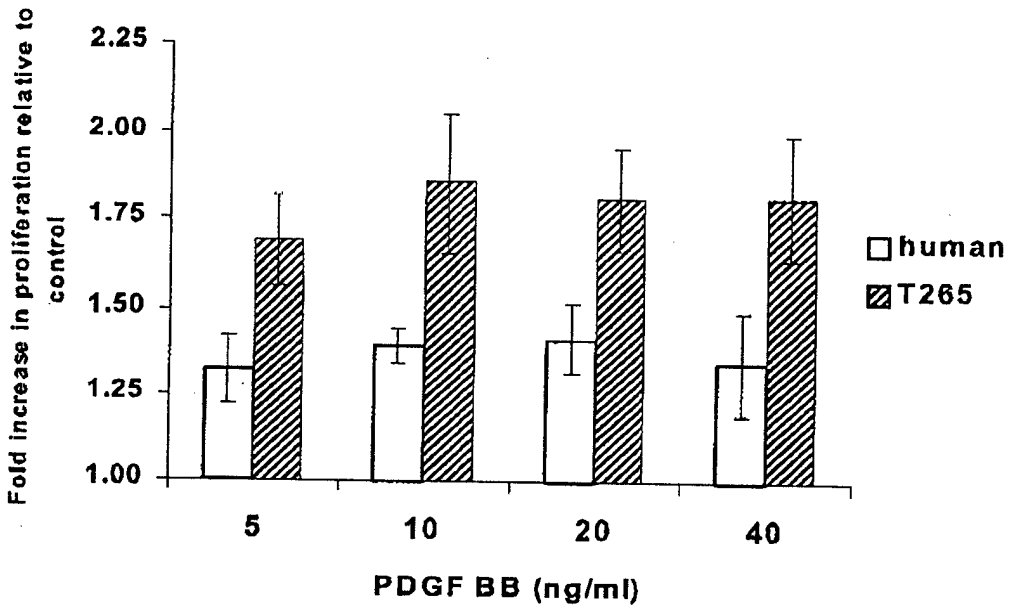

Figure 20. PDGF BB induces higher levels of proliferation in NF1 Schwann cells than in normal human adult Schwann cell. Normal human Schwann cells were cultured in serum free medium the presence of increasing concentrations of PDGF BB (5 to 40ng/ml) for 72 hours. Cell number was evaluated by the colorimetric MTT assay after 72 hours in culture. The values are a representative experiment repeated 3 times with similar results. Values are expressed as average fold increase over controls. Error bars represent the standard deviation of 3 replicates.

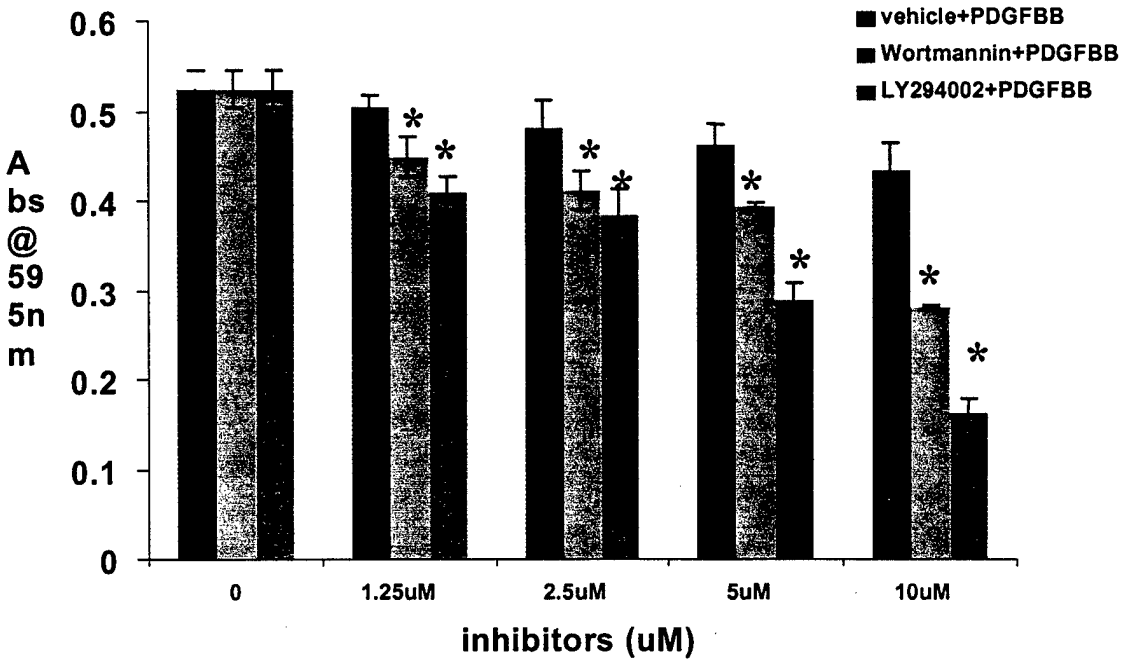

Figure 21. PDGF BB stimulated NF1 Schwann cell proliferation is mediated by PI3K. T265 cells were cultured in serum free medium the presence of 20ng/ml of PDGF BB with vehicle or increasing concentrations of 2 PI3K inhibitors, wortmannin and LY294002, for 72 hours. Cell number was evaluated by the colorimetric MTT assay after 72 hours in culture. Values are expressed mean of at least 3 replicates from a representative experiment repeated 3 times. Error bars represent +/- standard deviation of 3 replicates. The data were determined to be statistically significant using ANOVA: LY294002 ($F(4,10)=105.313$), Wortmannin ($F(4,10)=63.34$). Post-Hoc comparisons were determined using Tukey's LSD (*, significantly different from control, $P<0.05$).

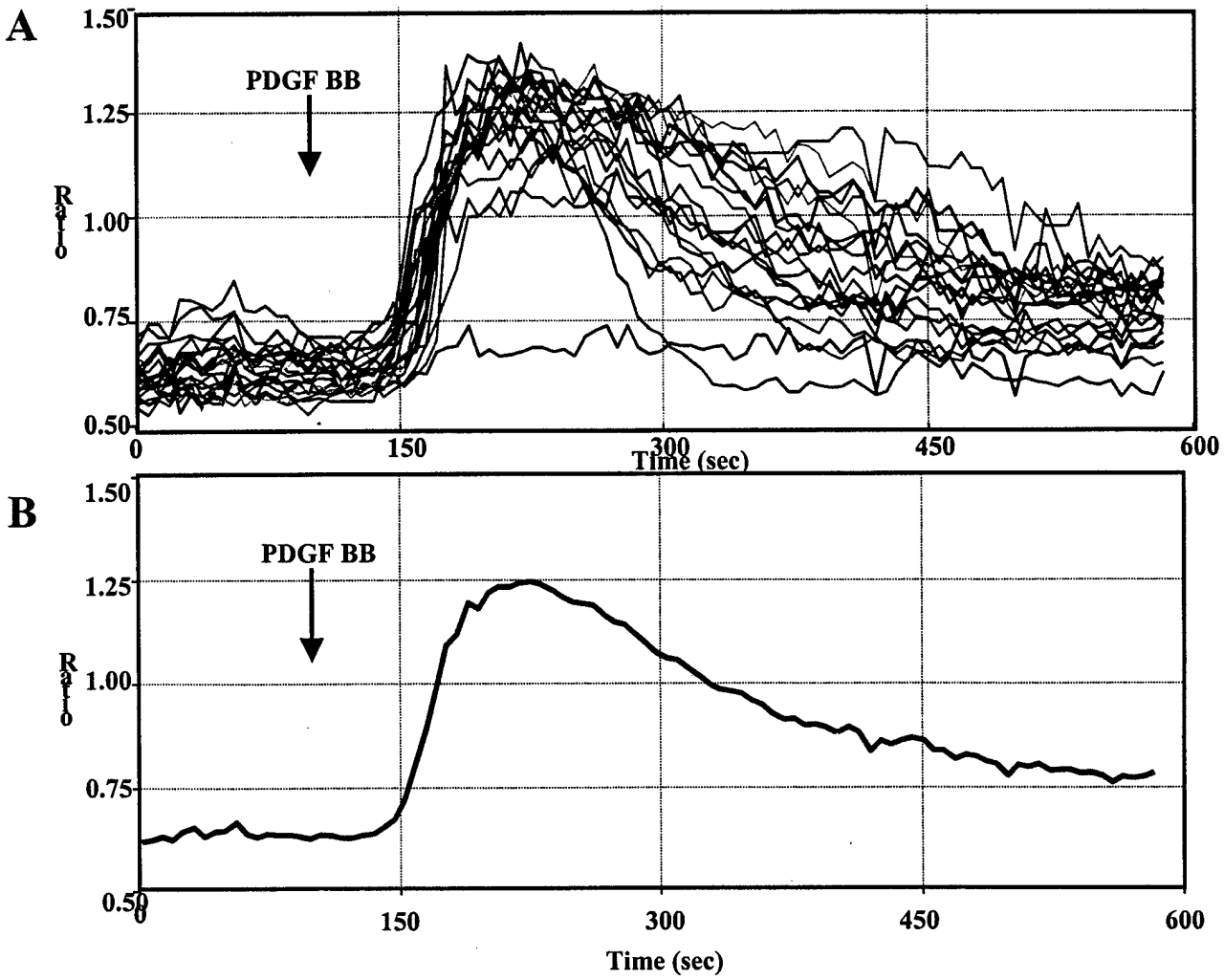

Figure 22. PDGF BB elevates intracellular calcium in NF1 Schwann cells. Schwann cells were loaded with Fura-2/AM for 20 minutes and levels of intracellular calcium were measured using the 340/360 ratio. Individual cell responses are depicted in (A) and the average of 20 cells were depicted in (B). These calcium ratio tracings are a representative experiment repeated 4 times with similar results.

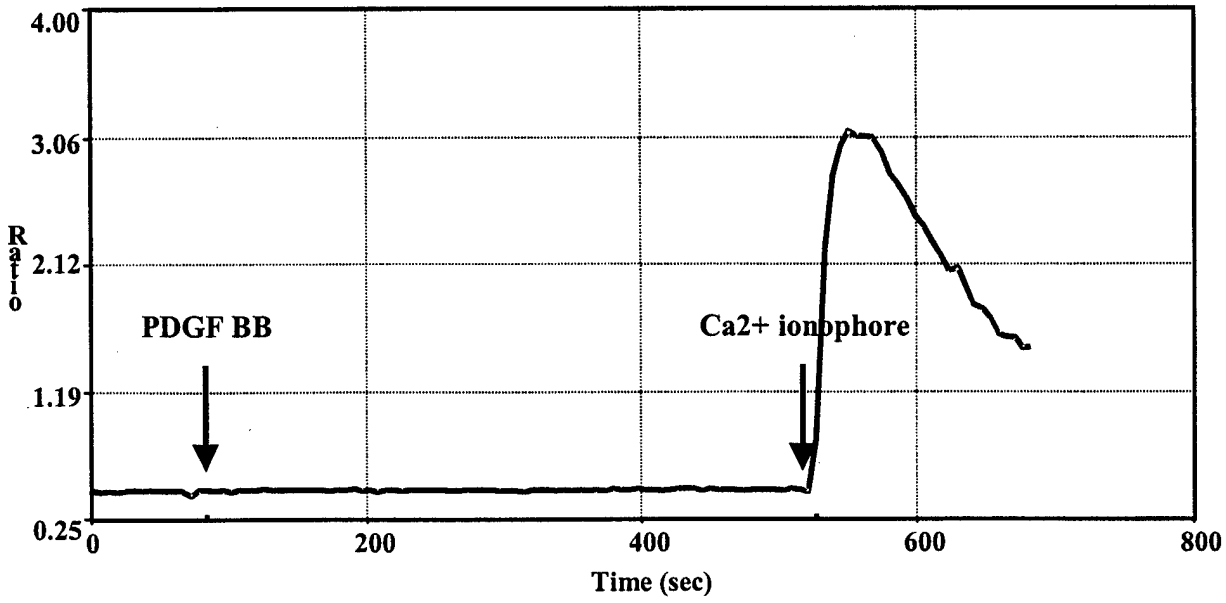

Figure 23. PDGF BB does not elevate intracellular calcium in normal human adult Schwann cells. Schwann cells were loaded with 1uM Fura-2/AM for 20 minutes and levels of intracellular calcium were measured using the 340/360 ratio. 20ng/ml of PDGF BB was added to cells and a calcium ionophore (1uM ionomycin) was added subsequently. This calcium ratio tracing is a representative experiment repeated 3 times with similar results.

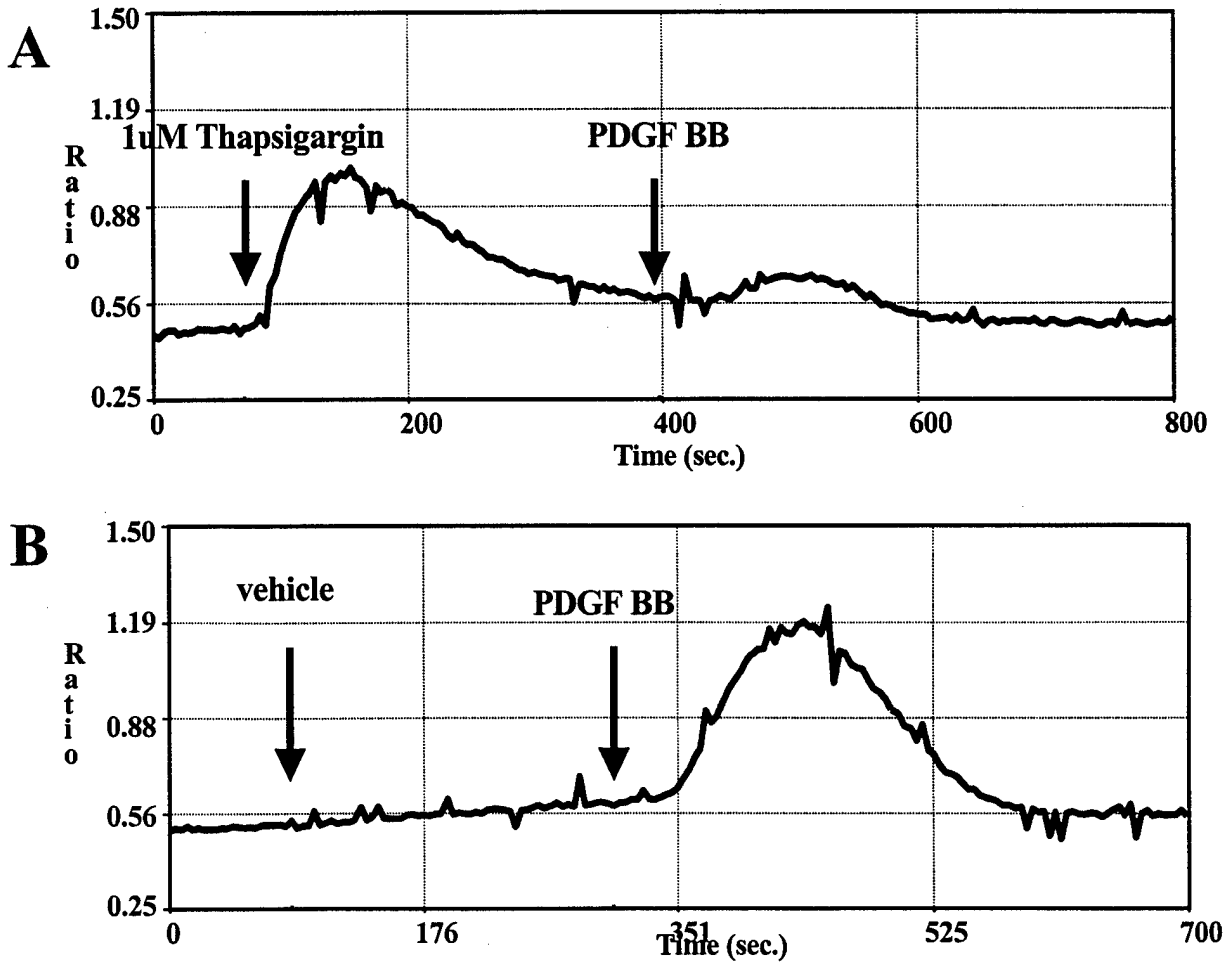

Figure 24. Increases in intracellular calcium levels are due to the release of calcium from the cell internal storage. Schwann cells were loaded with 1uM of Fura-2/AM for 20 minutes and levels of intracellular calcium were measured using the 340/360 ratio. Calcium responses with 1uM thapsigargin and 20ng/ml PDGF BB added subsequently are depicted in (A). Calcium responses with vehicle control and 20ng/ml PDGF BB added subsequently are illustrated in (B). These calcium ratio tracings are a representative experiment repeated 3 times with similar results.

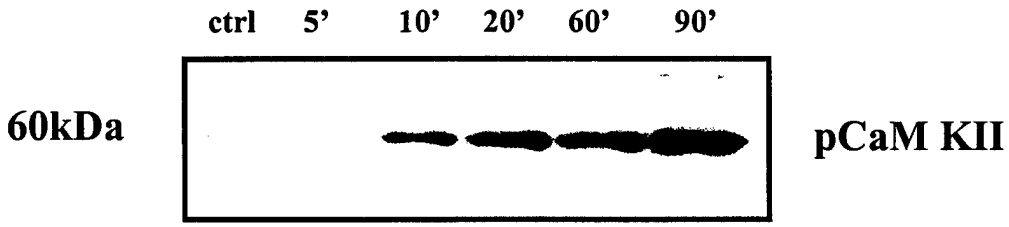

Figure 25. PDGF BB induces phosphorylation of CAM KII in NF1 Schwann cells. The NF1 derived Schwann cells were incubated with 20ng/ml of SCF for up to 90 minutes. Cells were lysed and 25ug of proteins were analyzed with an antibody specific for the phosphorylated form of CAMKII. This immunoblot is a representative experiment repeated 3 times with similar results.

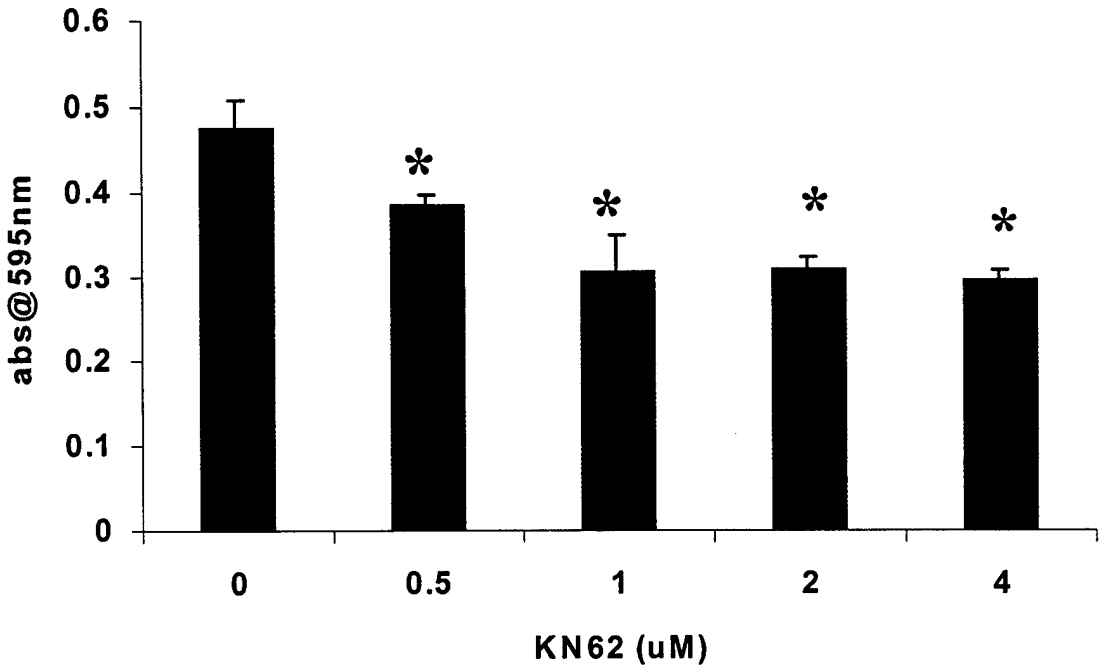

Figure 26. PDGF BB induced NF1 Schwann cell proliferation is mediated by the CAMKII. T265 cells were cultured in serum free medium the presence of 20ng/ml of PDGF BB with increasing concentrations of the CAMKII inhibitor, KN62, for 72 hours. Cell number was evaluated by the colorimetric MTT assay after 72 hours in culture. Values are expressed as mean of 5 replicates from a representative experiment repeated 3 times with similar results. Error bars represent +/- standard deviation. The data were determined to be statistically significant using ANOVA ($F(4,20)=46.238$). Post-hoc comparisons were determined using Tukey's LSD (*, significantly different from control, $P<0.05$).

Discussion

Summary of Results

We report that freshly isolated NF1 tumors express PDGF receptors. In addition, we show that 2 additional Schwann cell lines derived from NF1 tumors expressed PDGF receptor β. Interestingly, normal adult Schwann cells express PDGF receptor and neurofibromin, which is absent in NF1 Schwann cells. The phosphorylation of both receptors results in the activation of ERK and Akt. The proliferation of Schwann cells induced by PDGF BB is mediated by Akt of the PI3K pathway. Inhibitors of signaling molecules of the PI3K pathway, LY294002 and wortmannin, decreased the proliferation of NF1 cells. Interestingly, activation of the PDGF receptor is associated with in an intracellular increase in calcium levels and phosphorylation of CAMKII in NF1 Schwann cells. Inhibition of the CAMKII with KN62 resulted in decreased cell proliferation.

NF1 cell signaling

Numerous growth factor receptors are aberrantly expressed on NF1 Schwann cells. Our laboratory reported that NF1 cells aberrantly express c-kit and overexpress PDGF receptor (Badache et al., 1998a,b). However, we report that NF1 Schwann cells expressed comparable levels of PDGF receptor as normal human adult Schwann cells. Badache et al. (1998b) compared the expression of PDGF receptor in NF1 Schwann cells with the receptor expression in a non-NF1 Schwann cell line (STS26T). Normal Schwann cells isolated from human adult peripheral nerves expressed PDGF receptors in the presence or in the absence of forskolin. The condition for Schwann cell isolation did not increase PDGF receptor expression, since Weinmaster and co-workers (1990)

reported that Schwann cells with chronic elevations of cAMP results in increased PDGF receptor expression levels. Thus the increased proliferation of NF1 Schwann cells is due to aberrant intracellular signaling in NF1 Schwann cells.

It is interesting to note that the expression of other growth factor receptors are affected by the loss of neurofibromin. Our laboratory reported that NF1 Schwann cells aberrantly express c-kit (Badache et al., 1998a). In addition, DeClue et al., have reported that NF1 Schwann cells aberrantly express EGF receptors. These 3 growth factor receptors contribute to the aberrant proliferation of NF1 cells. Interestingly, the Erb-B receptors, which contribute to proliferation of normal Schwann, cells are absent in the transformed state (Badache et al., 1998; DeClue et al., 2000).

ERK and PI3K signaling pathway in Schwann cells

We have shown that PDGF BB stimulates the phosphorylation of Akt an the PI3 K pathway in NF1 Schwann cells and in normal human adult Schwann cells. Inhibition of the PI3K pathway with compounds such as LY294002 decreases phosphorylation of Akt, resulting in the decrease in the proliferation of NF1 Schwann cells. These results suggest that the loss of neurofibromin in NF1 Schwann cells does not affect the PI 3K pathway. A recent study reported that the activation of Akt is important for Schwann cell proliferation and survival (Maurel et al., 2000). Maurel and co-workers reported that neuregulins promote Schwann cell survival and proliferation through the PI 3-kinase. Similarly, IGFI prevents Schwann cell apoptosis through the PI 3-kinase (Delaney et al., 1999). The Akt protein has been shown to mediate important physiological function in normal Schwann cells and the proliferation of NF1 Schwann cells. Thus, the PI3 kinase

signaling is not aberrantly regulated in NF1 Schwann cells. The activation of the PI3K pathway is equally critical for normal human adult Schwann cell proliferation and NF1 Schwann cell proliferation contributing to the development of Schwann cell tumors NF1.

We investigated if the ERK pathway was aberrantly regulated in NF1 Schwann cells. We showed that PDGF BB induces ERK phosphorylation in NF1 Schwann cells and in normal human adult Schwann cells as well. No differences between the two cell types were observed in the ERK pathway. Interestingly, the MEK inhibitor did not have any effect on ERK phosphorylation. It may be that the NF1 Schwann cells have such high basal activation levels of ERK that the inhibitor was not able to significantly decrease ERK phosphorylation due to the elevated levels of activated Ras. Numerous studies have demonstrated that the loss of neurofibromin in NF1 Schwann cells results in increased Ras activity (DeClue et al., 1992; Sherman et al., 2000). These results suggest that PDGF BB activates the PI3K and ERK pathway in a similar manner in both the normal human adult Schwann cells and NF1 Schwann cells in response to PDGF BB. The loss of neurofibromin expression in Schwann cells does not affect the signaling of these 2 pathways, and the cause for the increased proliferation of NF1 Schwann cells in response to PDGF BB may be due to the abnormal signaling of other pathways, such as the cAMP or the calcium pathway.

Schwann cells and calcium

The elevation in intracellular calcium in response to PDGF BB is the major transduction signaling difference between normal and NF1 Schwann cells. The release of calcium from internal storage was observed in two cell lines (T265 and ST88). Calcium

may mediate the proliferation of NF1 Schwann cells induced by PDGF BB. In addition, the downstream effector of calmodulin CAM KII activated by the release of calcium was phosphorylated in response to PDGF BB. Taken together, these results suggest that calcium plays a role in NF1 Schwann cell proliferation. Interestingly, PDGF BB did not elevate calcium in normal Schwann cells. In fact only 2 other compounds, ATP and serotonin, increase intracellular calcium in Schwann cells. ATP was the first compound to increase calcium levels in normal Schwann cells (Lyons et al., 1995; Ansselin et al., 1994). The neurotransmitter serotonin increases calcium levels through HT2a receptors (Yoder et al., 1996). The physiological role of calcium elevations in response to ATP has been elucidated in a recent report. Using an in *vitro* model, Stevens and co-workers used the Schwann cell and DRG co-culture model to show that ATP is released from neurons following electrical stimulation (Stevens et al., 2000). Upon binding to the purinergic receptor on Schwann cells, ATP induces elevations of calcium levels resulting Schwann cell differentiation (2000). Interestingly, calcium is involved in proliferation in NF1 Schwann cells, but it is not involved in normal Schwann cell differentiation.

Numerous studies have shown that calcium has a variety of physiological effects including proliferation and apoptosis (for review see Berridge et al., 1998). For instance, calcium mediates the proliferation of T and B cells, but also plays a role in apoptosis in neurons. In addition, oscillations of Ca^{2+} in neuronal cells may be involved with long term potentiations. These different physiological functions of calcium may be related to the different downstream effectors activated by calcium and the activation of other pathways in conjunction with calcium. In NF1 Schwann cells, PDGF BB increases the levels of intracellular calcium and its downstream effectors, such as CAMKII. But

PDGF BB also induces the signaling of other pathways, such as the PI3K and ERK pathways. The increases in intracellular calcium levels in conjunction with the activation of the PI3K or the ERK signaling pathway may result in the proliferation of NF1 Schwann cells. However, increases in intracellular calcium levels result in the differentiation of normal Schwann cells. In the case of NF1 Schwann cells, the loss of neurofibromin expression switches the cellular function of calcium from differentiation in normal Schwann cells to proliferation in NF1 Schwann cells. These findings suggest that neurofibromin regulates signaling pathways and its loss results in aberrant intracellular signaling in Schwann cells leading to the development of NF1 tumors.

Conclusion

In this study, we report that NF1 Schwann cells aberrantly elevate intracellular calcium levels in response to PDGF BB. However, the Akt and ERK transduction pathways signal in NF1 Schwann cells similarly to normal human adult Schwann cells in response to PDGF BB (summarized in **figure 27**). The elevation of calcium and the subsequent phosphorylation of CAM KII mediates Schwann cell proliferation. The loss of neurofibromin in NF1 Schwann cells induces changes in intracellular signaling pathways resulting in aberrant cell proliferation. The mechanism leading to the aberrant elevation of calcium due to the loss of neurofibromin is under investigation at the present time.

NF1 Schwann Cells have Elevated cAMP levels and Increased Secretion of Prostaglandin PGE_2

Ian Dang and George H. DeVries
Research Service
Edward Hines Jr. VA Hospital
Hines, IL 60141
Department of Cell Biology, Neurobiology and Anatomy
Loyola University of Chicago
Maywood, IL 60153

Abstract

Neurofibromatosis Type 1 (NF1) is a human genetic disorder affecting approximately 1 in 3000 individuals. Characteristics of this disease are benign neurofibromas and malignant neurofibrosarcomas primarily made up of Schwann cells. Although the lack of neurofibromin leads to elevated Ras activities contributing to Schwann cell hyperplasia, it has recently been appreciated that Schwann transformation requires additional intracellular abnormalities. We now report that NF1 Schwann cells have 2 fold higher cAMP levels than normal human adult Schwann cells. PCR analysis of normal adult human Schwann cells reveals adenylyl cyclase (AC) mRNA for types III, IV, and IX. Similar analysis of NF1 Schwann cells shows all the isoforms in normal adult human Schwann cells, but additionally the NF1 Schwann cells express AC mRNA of types II, V, VII, and VIII. Increased cAMP levels may be the results of prostaglandins secreted by Schwann cells themselves. In support of this view, we find that NF1 Schwann cells express higher levels of $cPLA_2$ and Cox-2 than control cells. PCR analysis reveals that NF1 Schwann cells express mRNA for EP2 and EP4 prostaglandin receptors while normal human Schwann cells only express the EP2 receptor. Interestingly, the addition of exogenous prostaglandins to NF1 Schwann cells induces further increases of cAMP levels and also induces the proliferation NF1 Schwann cells. The proliferation of NF1 Schwann cells in response to PDGF BB decreased by Cox-2 and PKA inhibitors. These results are consistent with the view that aberrant cAMP signaling and elevated prostaglandin metabolism in NF1 Schwann cells contribute to tumor

formation in NF1 patients. (Supported by US Army Medical Research and Material Command; Contact grant number: DAMD17-98-8607).

Introduction

Neurofibromatosis type 1 (NF1) is an inherited disease, which is diagnosed by many symptoms including neurofibromas and café-au-lait spots (Friedman et al., 1999). A prominent feature of NF1 is the formation of benign Schwann cell tumors of peripheral nerve sheath called neurofibromas. In some instances, NF1 patients develop lethal malignant peripheral nerve sheath tumors, which are neurofibrosarcomas. The tumors of this genetic disease are caused by defects of the NF1 gene resulting in the absence of its protein product, neurofibromin. Although the function of neurofibromin is not known, its loss leads to the elevated levels of the activated form of Ras (Ras-GTP) (DeClue et al., 1992). It has been previously reported that Ras-GTP levels are elevated in neurofibrosarcoma tumors from NF1 patients and Schwann cells derived from mice lacking NF1 (Feldkamp et al., 1998; Kim et al., 1997). However, the link between the development of Schwann cells tumors and the loss of neurofibromin has not been clearly established.

As is the case with several types of cancer, aberrant expression of growth factor receptors may play a role in cellular transformation. Schwann cell lines derived from NF1 tumors express growth factor receptors that are not present in normal human Schwann cells. Badache et al. (1998a) have previously reported that Schwann cells overexpress c-kit receptors. In addition, the aberrant expression of the EGF receptors has

been documented on the surface of NF1 Schwann cells (DeClue et al., 2000). Interestingly, NF1 Schwann cells lacks Erb-B2 receptors, which are activated in response to neuregulin, the most potent growth factor for normal Schwann cells (Badache et al., 1999). Taken together, these results implicate aberrant growth factor receptor expression in the development of Schwann cell tumors in NF1 patients.

Since cAMP can regulate growth factor receptor expression in Schwann cells (Weinmeister et al., 1990) and cAMP is also a Schwann cell mitogen, intracellular levels of cAMP may play an important role in the proliferation of NF1 Schwann cells. Increased levels of intracellular cAMP brought about by forskolin stimulation of adenylyl cyclase causes enhanced Schwann cell proliferation when used in combination with growth factors such as, neuregulin β1 and PDGF (Rahmatullah et al., 1998; Davis et al., 1990). It has been reported that sustained high levels of cAMP increase growth factor receptor expression leading to aberrant Schwann cell proliferation (Weinmaster et al., 1990). In this study, we report that NF1 Schwann cells express additional adenyly cyclase isoforms and have higher basal levels of cAMP than that of normal Schwann cells. In addition, NF1 Schwann cells secrete higher levels of PGE_2 and express more EP receptors than normal adult Schwann cells. The addition of exogenous PGE_2 results in further elevation of intracellular cAMP and increased cell proliferation. Finally, we present evidence that the proliferation of NF1 Schwann cells stimulated by PDGF BB is mediated by Cox-2 and PKA.

Materials and Methods

Cell lines and Reagents

Recombinant platelet derived growth factor BB (PDGF BB) was purchased from R&D (Minneapolis, MN). H89, NS-398, and PGE_2 were purchased from Biomol (Plymouth Meeting, PA), indomethacin from Sigma (St Louis, MO). Forskolin was purchased from Calbiochem (La Jolla, CA).

The cell lines ST88-14, T265, STS 26T used in these studies were previously described (Badache et al., 1998). The 90-8 and 88-3 cell lines were obtained from Dr. Jeff DeClue have been previously described (DeClue et al. 1992). Cells were cultured as monolayers in low glucose Dulbecco's Modified Eagle's Medium (DMEM) supplemented with 10% FBS, 100 units/ml penicillin and 100ug/ml streptomycin, and maintained at 37°C in a humid atmosphere of 10% CO2/90%air. For proliferation assay and western blotting, cells were serum starved overnight and were cultured in serum free media with PDGF BB alone or in combination with inhibitors.

Human Schwann cells

Primary human Schwann cell cultures were established as described by Wood et al., (2000) (Miami Project, University of Miami, Miami, Fla). Fresh human peripheral nerves (cauda equina) were obtained from Dr. Wood from transplant patients. For ten days, the nerve fragments were placed in DMEM containing 10% heat inactivated fetal bovine serum (Hyclone, Logan, UT), 2uM forskolin, 10nM NDF β1 (Amgen Inc., Thousand Oaks, CA), 50U/ml penicillin and 0.05 mg/ml streptomycin (Sigma, St Louis, MO). Then the fragments were dissociated in DMEM containing 10% heat inactivated

fetal bovine serum, 2uM forskolin, 10nM NDF, 50U/ml penicillin and 0.05 mg/ml streptomycin, 0.05% collagenase (Worthington Biochemicals, Freehold, NJ) and 0.25 % dispase (Boehringer Mannheim, Indianapolis, IN) in a erlenmyer flask. The nerve fragments were incubated at 37C in a 5% CO2 incubator in the enzyme solution for 18h. After centrifugation, the cells were resuspended in fresh media and were plated in 100mm culture dishes in DMEM containing 10% heat inactivated fetal bovine serum, 2uM forskolin, and 10nM NDFβ1. In Schwann cells cultured without forskolin, the nerve fragments were incubated with DMEM containing 10% serum for 3 days. Then the nerve fragments were worked up as previously described in media containing 10% serum with no forskolin or neuregulin β1. The cells were harvested 24 hours after plating.

NF1 tumors

NF1 tumors were obtained from patients diagnosed with NF1 and were removed by Dr. John Shea at Loyola University Medical Center.

Schwann cell culture

Primary Schwann cell cultures were established essentially as described by Brockes and colleagues (1979). Sciatic nerves were removed from 3-day rat pups, digested for 2 hours, in 0.03% collagenase (Serva) at 37°C, and triturated thoroughly to achieve dissociation. Cells were cultured as monolayers in low glucose Dulbecco's Modified Eagle's Medium (DMEM) supplemented with 10% FBS, 100 units/ml penicillin and 100ug/ml streptomycin, and maintained at 37°C in a humid atmosphere of

10% CO2/90%air. Contaminating fibroblasts were inhibited by 72 hours treatment with 10uM cytosine arabinoside.

MTT assay

This assay involved a spectophotometric analysis of the degradation of the bromide salt MTT (3-[4,5-dimethythiazol-2-yl]-2,5 diphenyl tetrazolium bromide) by mitochondrial dehydrogenase enzymes yielding purple formazan crystals as a by-product of this reaction. After the incubation treatment, MTT labeling reagent (0.5mg/ml, Sigma, St Louis, MO) were added to Schwann cell cultures for 4 hours (humidified atmosphere, 5% CO_2, 37°C). Following overnight incubation with a solubilization solution (10% SDS in 0.01M HCL), the amount of solubilized formazan crystals were quantified at 595 nm using an automated microplate reader EL311sx (Bio-Tek Instruments, Inc., Winooski, VT). The increase in absorbance correlated with the number of cells.

Western blotting

Cells cultured in DMEM supplemented with 10% FCS or rat sciatic nerves were lysed in RIPA buffer (1% triton X-100, 0.5% sodium deoxycholate, 0.1% SDS in phosphate buffer saline) containing a cocktail of protease inhibitors. Tumor lysates were obtained by homogenizing tumor samples in RIPA. Protein lysates were separated by electrophoresis in a polyacrylamide gel (Invitrogen) and transferred onto a PVDF membrane (Dupont, NEN, Boston, MA). After blocking with a 5% nonfat dry milk solution (5% milk in PBS containing 1% Tween, PBS-T) for 30 minutes, the PVDF

membrane was incubated overnight in the presence of the primary antibody (anti-cPLA$_2$ from Santa Cruz Biotechnology or anti-Cox-2 from Transduction laboratory) at 4°C. After several washes in PBS-T, the membrane was incubated with a horseradish peroxidase-conjugated secondary antibody (Transduction Laboratories, San Diego, CA). Following additional washes with PBS-T, the immunoreactivity was detected by enhanced chemiluminescence (Dupont-NEN, Boston, MA).

REVERSE TRANSCRIPTION PCR

Total cellular RNA isolation and quantitation

Total RNA was isolated from cultured Schwann cells by a modification of the acid-method of Chomczynski and Sacchi (1987). Briefly, cells were washed with PBS and solubilized using Trizol reagent (Gibco-BRL). For each sample, 0.2 ml of chloroform were added per 1 ml of Trizol. After the samples were subjected to centrifugation at 12,000 x g for 15 min. at 4°C, the aqueous phase of each sample were transferred to a fresh tube. The RNA in the aqueous phase was precipitated by mixing 0.5 ml of isopropyl alcohol per 1 ml of Trizol reagent (used for the initial solubilization of cells). To enhance recovery of small amounts of RNA, 20 μg of glycogen were added as a carrier prior to isopropanol precipitation. Samples were subjected to centrifugation at 12,000 x g for 10 min. at 4°C and the RNA pellet obtained were redissolved in sterile water.

First strand cDNA synthesis by reverse transcriptase

Total cellular RNA were converted to cDNA in 20 μl reactions consisting of 1 μg RNA, 1xPCR buffer (Gibco BRL), 2.5 mM $MgCl_2$, 500mM dNTPs (Pharmacia), 10 mM DTT, 20 U RNAsin (Promega), 200 U Superscript II Rnase H^- reverse transcriptase (RT), and 2 μg random hexamer primers (Perkin-Elmer). Reactions were incubated at room temperature for 5 min. for primer annealing, then at 42°C for 60 minutes for reverse transcription. Reactions were terminated by a 5 min. incubation at 95°C, and RT products were used immediately.

Primer design for polymerase chain reaction (PCR)

Oligonucleotides of 21 base pairs were designed with the Oligo IV software using the gene sequence for each AC obtained from GenBank. The sofware was utilized for the analysis and design of the best upstream and downstream primers according to specific conditions, such as annealing temperatures, secondary structures, and several other factors. Oligonucleotides were synthesized for our laboratory by Gibco BRL.
Sizes and sequences for the upstream (UP) and downstream (DWN) each AC primers are as following:

ACI (1044bp):UP 5'-GGG GCT GCG TTT CTC TTG CTG-3'; DWN 5'-CAG GGC AAA AGC AAA CTC CAC-3'; ACII (581bp):UP 5'-GAG TTT GCT TTT GCC CTG GTA-3'; DWN 5'-GCG CTC CTT TTC CCT TTT GCT-3'; ACIII (774bp): UP 5'-CCT GGC GTC CCG TCT TTG ATG-3'; DWN 5'-CAG CCA GAA CCC CGC CTT TGT-3'; ACIV (559bp): UP 5'-TCG GGG ACT GTG AGA ACC TCT-3'; DWN 5'-TCA GCG

TCC TCA TCA CCT ATG-3'; ACV (301bp):UP 5'-TGG GGC AAA ACT GTG AAC CTG-3'; DWN 5'-GCT GCT TCT GCC TTT GCC TAT-3'; ACVI (774bp): UP 5'-GCA CGG CTG TTG GAG TCT TCT-3'; DWN 5'-CAT TGT TGC CCT CCA GTT CCA-3'; ACVII (772bp):UP 5'-TCG CCT GCT CGG TCT TCC TGA-3'; DWN 5'-AGG CGG AAG GAG TTG AAG GAG-3';ACVIII (781):UP 5'-GCG GCT CGT GCT TTC TGT GCT-3'; DWN 5'-ATT ATC AAA GGG CAG TTC AGG-3'; ACIX(469): UP 5'-GGA GAA AAC GGA CGC CCA CTT-3'; DWN 5'-TGC GGG AAG CGA CAC CAG GAT-3'.

PCR conditions

After reverse transcription, PCR reactions were carried out in volumes of 50 μl, using bulk mixes for multiple samples. PCR master mix consisted of 1xPCR buffer (Gibco BRL), 2.5 mM $MgCl_2$, 0.4 mM dNTPs, 3 U per final reaction Taq polymerase (Gibco BRL), and 0.3 μM of each primer. Each sample consisted of 48 μl of master mix and 2μl (50ng) of each completed RT reaction added to 0.7 ml microcentrifuge tubes. PCR reactions took place in a Hybaid thermocycler. The PCR profile was one cycle of 95°C for 5 min. for initial denaturation of cDNA/RNA hybrids, and one cycle of 80°C for 3 min. for the addition of Taq Polymerase; 32 cycles of 95°C for 45 sec., 62°C for 45 sec. and 72°C for 60 sec.; then a final extension cycle at 72°C for 5 min. to ensure complete synthesis of amplimers.

PCR product detection

Following PCR amplification, equivalent amount (10 μl) of reaction products were separated by gel electrophoresis using 2% agarose gels in TAE buffer for 30 minutes. Amplimers were visualized following exposure of the gel to 2% ethidium bromide solution and were photographed under trans-illumination with a Polaroid MP4+ Camera system.

Cyclic AMP ELISA

Schwann cells were seeded onto 6 well culture plates at a density of 300,000 cells/well in DMEM with 10% FCS. Cells were serum deprived for 24 hours. Before treatment, Schwann cells were incubated with serum free media containing 250uM isobutyl methyl xanthine (IBMX) for 20 to 30 min to inhibit phosphodiesterase activity. After the media was aspirated, the cells were lysed with 0.1M HCl for 1 hour at room temperature on a rotary shaker. The lysate was collected in 1.5 ml centrifuge tubes and used immediately. Concentrations of cAMP were determined using the acetylated version of direct enzyme immunoassay kit (Assay Designs, Inc) according to the manufacturers instructions. The data are expressed as picomoles of cAMP per mg of protein. The concentrations of cAMP were determined in triplicate.

PGE_2 ELISA

Schwann cells were seeded onto 6 well culture plates at a density of 300,000 cells/well in DMEM with 10% FCS. Cells were serum deprived for 24 hours. After incubating the cells for 1 hour in fresh DMEM, the cells were lysed to determine protein

concentrations for each condition and supernatants were collected into a 96 well-plate. Levels of PGE_2 were determined using the direct enzyme immunoassay kit (Assay Designs, Inc) according to the manufacturers instructions. Concentrations of PGE_2 were determined in triplicate wells and were normalized to protein levels. The levels of PGE_2 are expressed in pmole/ml/mg.

STATISTICS

Statistics were determined using the Sigma Plot 2.0 software.

Results

Intracellular cAMP levels in NF1 and non-NF1 Schwann cell lines

Previous reports have shown that elevation of cAMP levels in normal Schwann cells lead to increase growth factor receptor expression, such as PDGF receptor (Weinmaster et al., 1990). Based on this observation, we wanted to investigate the basal levels of intracellular cAMP in NF1 derived Schwann cells, since elevated intracellular cAMP may lead to high PDGF receptor expression in NF1 cells. To determine basal levels of cAMP in Schwann cells, cells were incubated in serum free medium with a phosphodiesterase inhibitor (200uM IBMX). After a 20-minute incubation, cAMP concentrations measured by ELISA. The results show that three of the four NF1 cell lines expressed about 10pmoles of cAMP per mg of protein (**figure 28**). The normal rat Schwann cells expressed 2pmoles cAMP/mg and the adult human Schwann cells

expressed 5 pmoles/mg. These results demonstrate that NF1 cells have higher basal cAMP levels than control cells.

Determination of adenylyl cyclases in Schwann cells

The higher cAMP levels of NF1 cells compared to the levels of normal Schwann cells may be related to the different subtypes of adenylyl cyclases each cell type expresses. We set out to determine the subtypes of adenylyl cyclases expressed by both NF1, non-NF1, and normal human adult Schwann cells. We performed RT/PCR using specific primers for each 9 different subtypes of adenylyl cyclases. Normal human adult Schwann cells express mRNA for AC types III, IV, VII (weakly), and IX (**figure 29A**). A similar analysis conducted with NF1 Schwann cells revealed that they express the same AC isoforms as normal Schwann cells plus 3 additional AC subtypes: II, V, and VIII (**figure 29B**). Interestingly, the non-NF1 Schwann cells (STS26T) express similar AC subtypes as NF1 Schwann cells plus one additional AC subtype VI (data not shown). The AC mRNA expressed by Schwann cells are summarized in Table 1. The increased AC isoforms expressed by NF1 Schwann cells may result in higher basal levels of cAMP than in normal human adult Schwann cells.

Table 1. Adenylyl cyclase isoform expression in NF Schwann cells, non-NF Schwann cells, and normal human Schwann cells.

AC Isoforms	Normal Human	NF1 cells	Non-NF1
ACI	-	-	-
ACII	-	+	-
ACIII	+	+	+
ACIV	+	+	+
ACV	-	+	-
ACVI	-	-	+
ACVII	+/-	+	-

ACVIII	-	+	-
ACIX	+	+	-

Prostaglandin E_2 secretion in NF1 and non-NF1 Schwann cell lines

We postulated that the high levels of cAMP in Schwann cells could be sustained by PGE_2 secretion by the Schwann cells themselves. In many cell types, PGE_2 stimulates a specific adenylyl cyclase linked recetpor leading to increased intracellular cAMP. To determine the levels of PGE_2 secreted from NF1 cells, serum free media from 300,000 cells was conditioned for 3 hours and were analyzed by ELISA. The results show that the 2 NF1 cell lines, T265 and ST88, secreted the most PGE_2 with 250pg/ml/mg (**figure 30**). Neonatal rat Schwann cells and normal human adult Schwann cells produced the least amount of PGE_2 with 90pg/ml/mg. The non-NF1 cell line secreted less PGE_2 than the 2 NF1 cell lines. Interestingly, the 90-8 and 88-3 cell lines secreted at least 5fold more PGE_2 than that of the ST88 and T265 levels (data not shown). Overall these results show that NF1 cells secrete the highest levels of PGE_2. The levels of PGE_2 secretion do not correlate with the levels of intracellular cAMP.

Expression of $cPLA_2$ and Cox-2 in Schwann cells

We wanted to determine if Schwann cells express enzymes relating to the secretion of PGE2, such as cPLA2 and Cox-2. To investigate expressions of cPLA2 and Cox-2 receptor in Schwann cells, 25ug of cell lysates were analyzed by immunoblotting using $cPLA_2$ and Cox-2 antibodies. The immunoblotting analysis revealed that NF1 Schwann cells expressed elevated levels of $cPLA_2$ compared to normal human adult Schwann cells (**figure 31A**). Similarly, levels of Cox-2 expression were much higher in

NF1 cells than in normal Schwann cells as illustrated in **figure 31B**. Overall, the increased expression of cPLA2 and Cox-2 in NF1 Schwann cells correlate with high levels of prostaglandin secretion.

Prostaglandin secretion by NF1 tumors

We established the secretion of PGE_2 by NF1 Schwann cells *in vitro*, and we wanted to extend our findings *in vivo* by analyzing levels of PGE_2 in fresh NF1 tumors. To determine the levels of PGE_2 in fresh NF1 tumors, serum free media was conditioned with tissue samples for 12 hours and levels of PGE_2 were normalized to the volume and weight of each sample. The analysis of the conditioned media revealed that 2 tumors expressed 6 and 5 pg/ml/mg of PGE_2 respectively, while 2 other tumors secreted only 1 and 1.5 pg/ml/mg respectively **(figure 32)**. Controls obtained from conditioned media of human peripheral nerve had 1 pg/ml/mg. Levels of PGE_2 in NF1 tumors are somewhat variable; 2 tumors have higher PGE_2 levels than control while 2 NF1 tumors have similar levels as control. Overall, the results suggest that cells present in NF1 tumors secrete PGE_2.

Determination of prostaglandin receptor subtypes in Schwann cells

PGE_2 affects cells through a receptor mediated mechanism. PGE_2 binds preferably to the E class prostanoid (EP) receptor family, which has 4 isoforms: EP1, EP2, EP3, and EP4. (Coleman et al., 1994). To determine the EP receptors expressed by NF1, non-NF1, and normal human adult Schwann cells, RT/PCR reactions were performed using specific primers for each of the 4 receptors. PCR analysis revealed that

all NF1 cells expressed both EP2 (602bp) and EP4 (553bp) receptor mRNA (**figure 33A**). However, non-NF1 Schwann cells expressed only EP2 receptor mRNA (**figure 33B**) and normal human adult Schwann cells have only the EP4 receptor mRNA (**figure 33C**). Overall, NF1 Schwann cells express a different prostaglandin receptor profile from normal and non-NF1 Schwann cells. Interestingly, EP2 and EP4 receptors are both AC coupled so that their activation can lead to increases in cAMP metabolism (Coleman et al., 1994).

Effects of PGE_2 on intracellular cAMP levels in Schwann cells

To determine the increase of cAMP levels in NF1 cells as a function of PGE_2 concentration, cells were cultured in serum free medium with increasing concentrations of PGE_2 (0.01 to 10uM) in the presence of phosphodiesterase inhibitor (200uM IBMX). After 20 minutes, cell lysates were analyzed by ELISA to determine cAMP levels. Levels of cAMP were normalized with control levels and are reported as fold increase over controls. Within 20 minutes, cells cultured with 0.01 uM of PGE_2 increased their cAMP synthesis 100-fold relative to basal levels within 20 minutes (**figure 34A**). At concentrations of 1uM or greater, the increase in cAMP levels reached a maximum of 180 fold. These results show that the NF1 cells respond to PGE_2 by increasing intracellular cAMP.

Next, using a fixed concentration of PGE2 (1uM), we compared the increase of cAMP levels in NF1 Schwann cells to that of normal human adult Schwann cells and non-NF1 Schwann cells (**figure 34B**). Cells were cultured in serum free medium with 1uM PGE_2 and 200uM IBMX. After 20 minutes, cell lysates were analyzed by ELISA to

determine cAMP levels. Levels of cAMP were normalized with control levels and are reported as fold increase over controls. The results showed that 1uM of PGE_2 induces cAMP a 40 fold increase in normal human adult Schwann cells and a 60 fold increase in non-NF1 Schwann cells **(figure 34B)**. These increases are much smaller than the 200 fold increase observed with the NF1 Schwann cells. These results show that PGE_2 induce a larger increase in cAMP response in NF1 Schwann cells than in normal human adult Schwann cells and non-NF1 Schwann cells.

Effects of PGE_2 on NF1 cell proliferation

Previous studies have shown that increased levels of cAMP induce Schwann cell proliferation. We wanted to determine if increased cAMP levels stimulated by PGE_2 would increase NF1 Schwann cell proliferation. Previously, we had already determined to which extent PGE_2 increases cAMP in Schwann cells. To investigate the effects of PGE_2 on the proliferation of Schwann cells, cells were cultured in serum free medium with increasing concentrations PGE_2 (0.01 to 10uM) for 72 hours. The proliferation assay showed that PGE_2 increases in cell proliferation of NF1 Schwann cells **(figure 35)**. Overall, increased cAMP levels with PGE_2 induced the proliferation of NF1 Schwann cells. Interestingly, the PGE_2 did not potentiate the proliferation of NF1 Schwann cells cultured with PDGF BB.

PDGF BB induced cell proliferation and cox inhibitors

We have shown that the T265 NF1 cell line secretes high levels of PGE_2 and decided to determine if the secreted PGE_2 mediates NF1 cell proliferation. It is possible

that the use of cyclooxygenase inhibitors (indomethacin and NS398) would decrease the production of PGE_2 and decrease NF1 Schwann cell proliferation induced by PDGF BB. For the analysis of the production of PGE_2, serum free media from 300,000 cells was conditioned for 3 days with or without indomethacin (50uM). After 72 hours the media were analyzed by ELISA for the presence of PGE_2, and the values were normalized to protein levels. The results show that 50 uM of indomethacin reduces prostaglandin secretion of approximately 40% compared to control **(figure 36A)**. Similar to indomethacin, we also found that 50uM of NS-398 decreases prostaglandin secretion by 40% as shown in **figure 36B.** Thus both inhibitors have similar effects.

For the proliferation assay, NF1 cells preincubated with NS-398 or indomethacin for 12 hours, then were cultured in serum free medium with 20ng/ml of PDGF BB alone or in combination with increasing concentrations of inhibitors for 72 hours. As shown in **figure 37A**, these results showed that indomethacin significantly decreased NF1 cell proliferation, but the inhibitor itself was not toxic to the cells. The decrease in cell number was dose dependent, with significant inhibition with 50uM and 100uM of indomethacin compared to control (**figure 37A**). Indomethacin does not discriminate between Cox-1 and Cox-2. To determine the specific cyclooxygenase enzyme contributing to the NF1 cell proliferation, NS-398, a specific inhibitor of Cox-2, was used in the proliferation of NF1 cells induced by PDGF BB (**figure 37B**). Similarly to indomethacin, NS-398 decreased the proliferation of NF1 cells in a dose dependent manner (**figure 37A**). We concluded that NF1 cell proliferation is mediated by Cox-2. However, the inhibition is not complete, since other signaling pathways are involved in the proliferation of NF1 cells.

PDGF BB induced cell proliferation and PKA inhibitor

Previously, we have shown that NF1 cells have elevated cAMP levels, which may contribute to the aberrant proliferation of NF1 cells. Since the downstream effector of cAMP is PKA, we evaluated the extent to which cAMP mediates NF1 cell proliferation induced by PDGF BB by using the PKA inhibitor H89. To investigate the effect of H89 on NF cell proliferation, NF1 cells were cultured in serum free medium with 20ng/ml of PDGF BB in combination with increasing concentration of the H89 inhibitor for 72 hours. As shown in **figure 38**, the PKA inhibitor H89 decreased NF1 cell proliferation in a dose dependent manner. This data is consistent with the viewpoint that NF1 cell proliferation induced by growth factor, such as PDGF BB, is mediated by PKA.

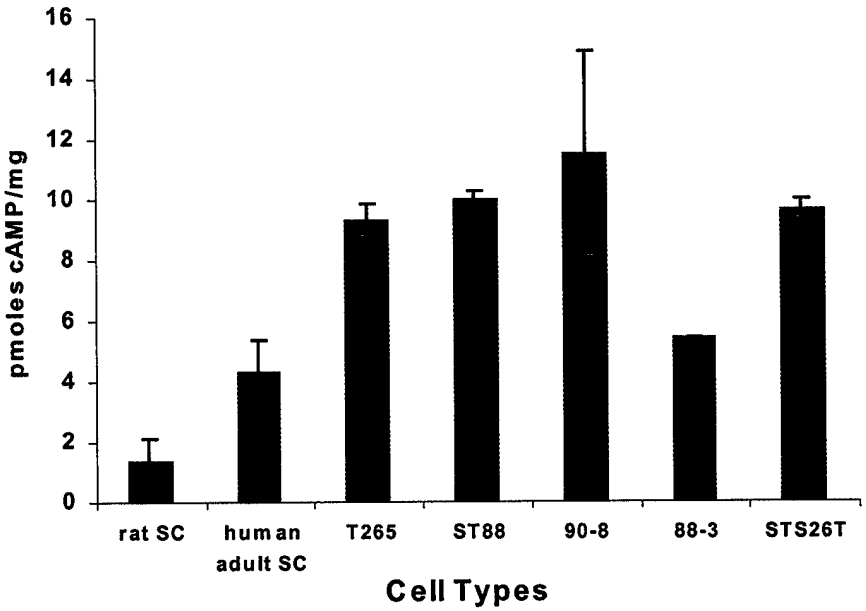

Figure 28. NF1 Schwann cells have higher basal cAMP levels than normal Schwann cells. Schwann cells were incubated in serum free medium with the phosphodiesterase inhibitor, IBMX (200uM), for 30 minutes. Cells were lysed and concentrations of cAMP were determined by ELISA in duplicate. Values are mean of 3 different experiments. Error bars represent +/- standard error deviation.

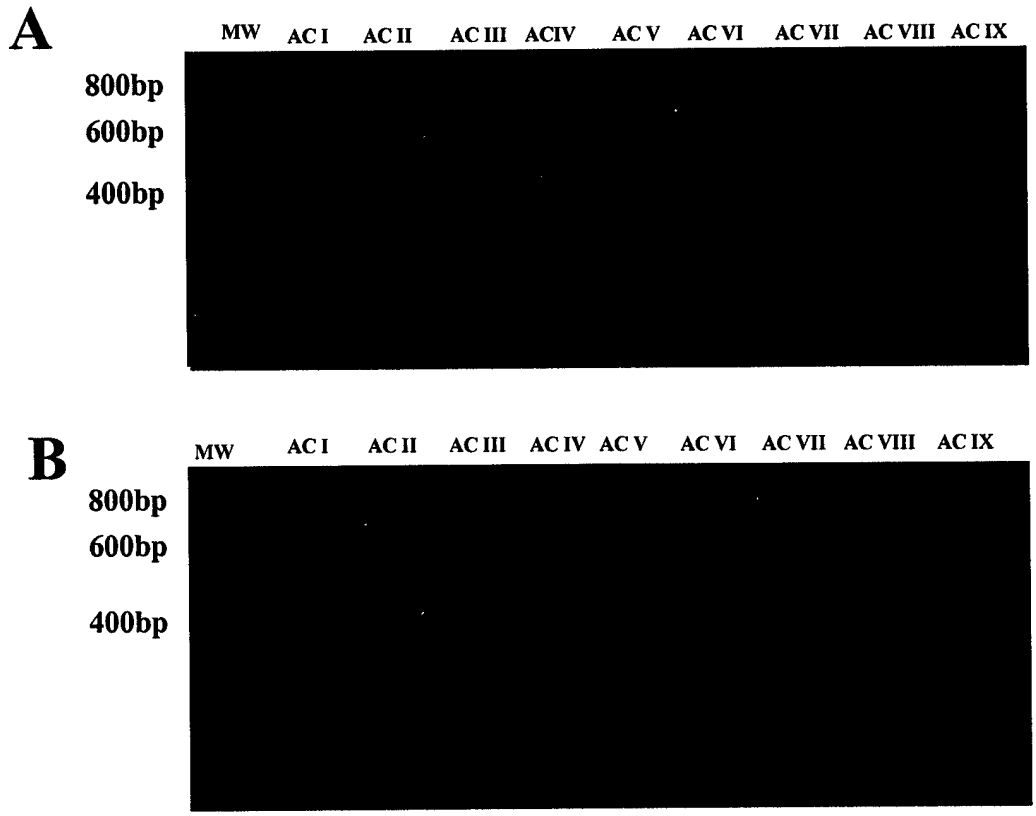

Figure 29. Types of adenylyl cyclases mRNA expression in Schwann cells. RT/PCR amplification products for AC I (1044 bp), ACII (581 bp), ACIII (772bp), AC IV(559bp) AC V(300bp), AC VI (774), AC VII (772 bp), AC VIII (695bp), and AC IX (469bp) in the T265 Schwann cell line (A) and in normal human adult Schwann cells (B). PCR products were separated on a 2% agarose gel stained with ethidium bromide. Molecular weight markers (MW) are derived from 100 base pairs ladder. These photographs are a representative experiment repeated twice.

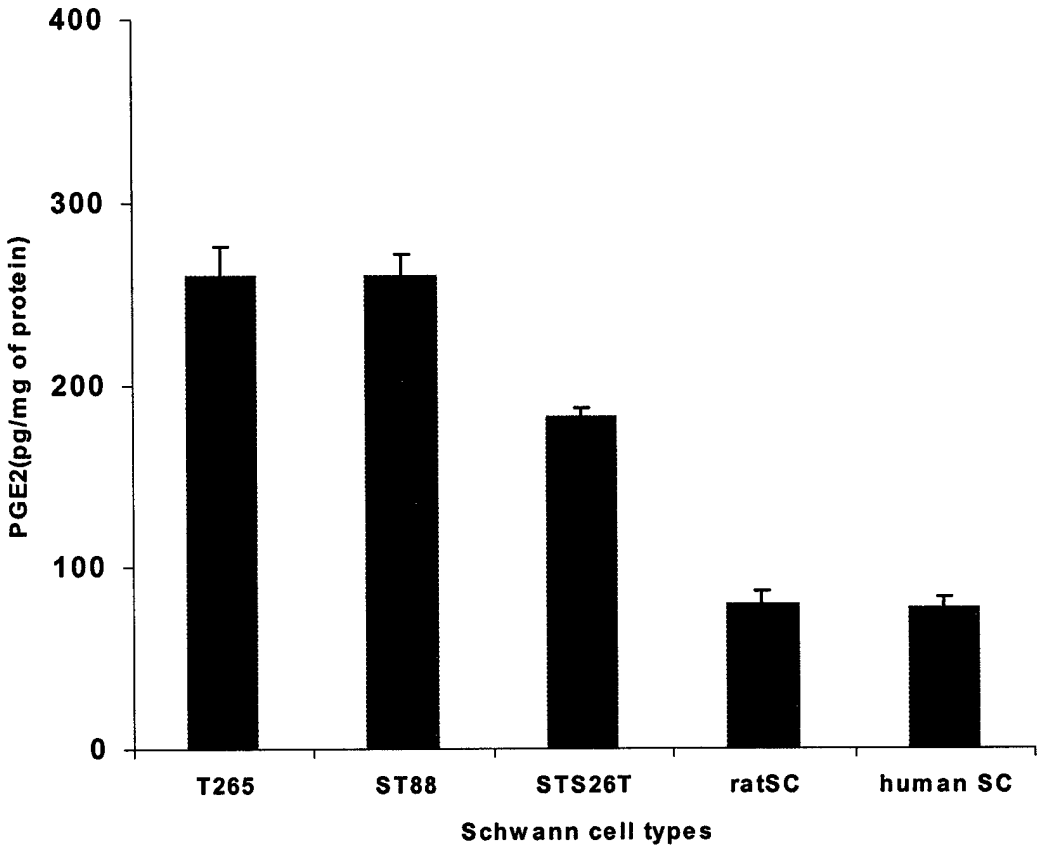

Figure 30. NF1 Schwann cells secrete higher levels of PGE2 than normal and non-NF1 Schwann cells. Cells were incubated for 3 hours in serum free medium. Conditioned media were collected and concentrations of PGE2 were measured by ELISA in triplicate. Values are expressed as mean 3 different experiments. Error bars represent +/-standard error of the mean.

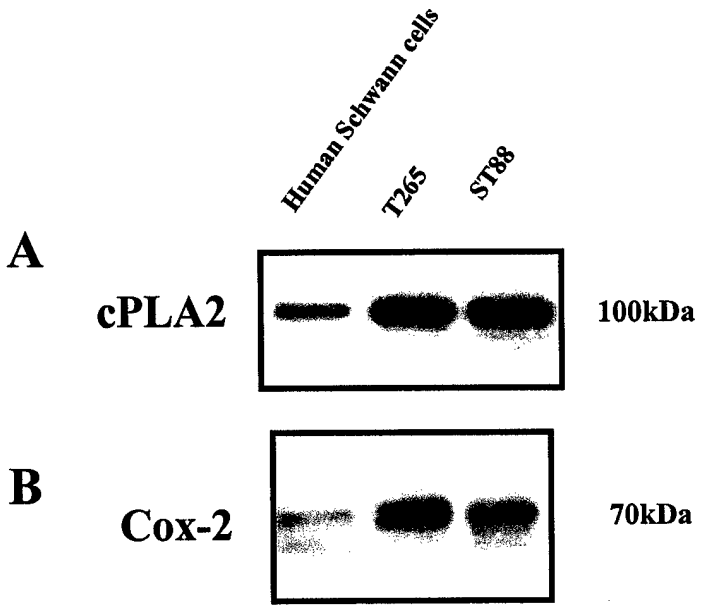

Figure 31. Expression of $cPLA_2$ and Cox-2 in Schwann cells. Schwann cells were lysed and 25ug of proteins were analyzed by immunoblotting with an antibody specific for $cPLA_2$ (A) or Cox-2 (B). These immunoblots are a representative experiment repeated 3 times with similar results.

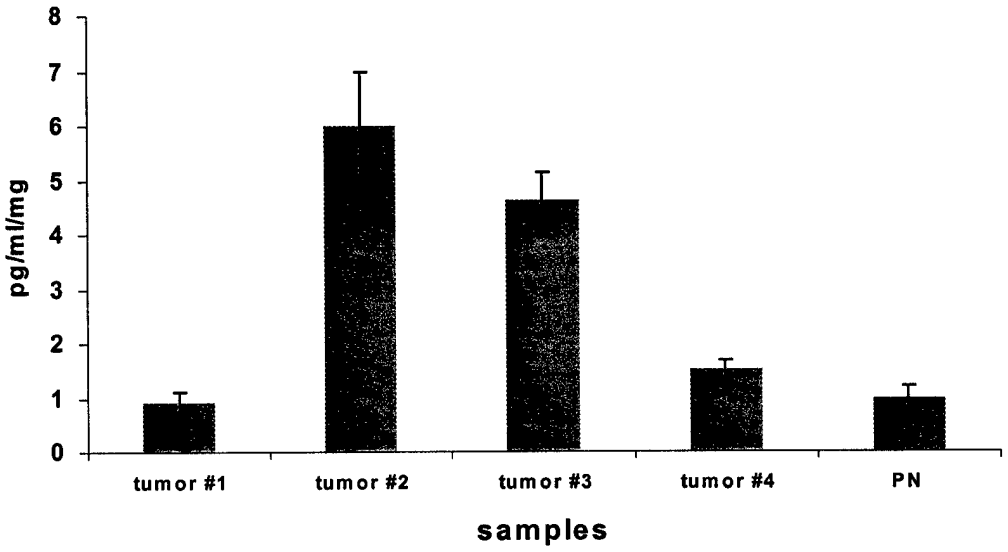

Figure 32. PGE_2 secretion by NF1 tumors. Tissue samples were incubated in serum free media overnight. Conditioned media were analyzed by ELISA in triplicate. Values are expressed as PGE_2 secretion levels that were normalized to protein levels. Error bars represent +/- standard deviation.

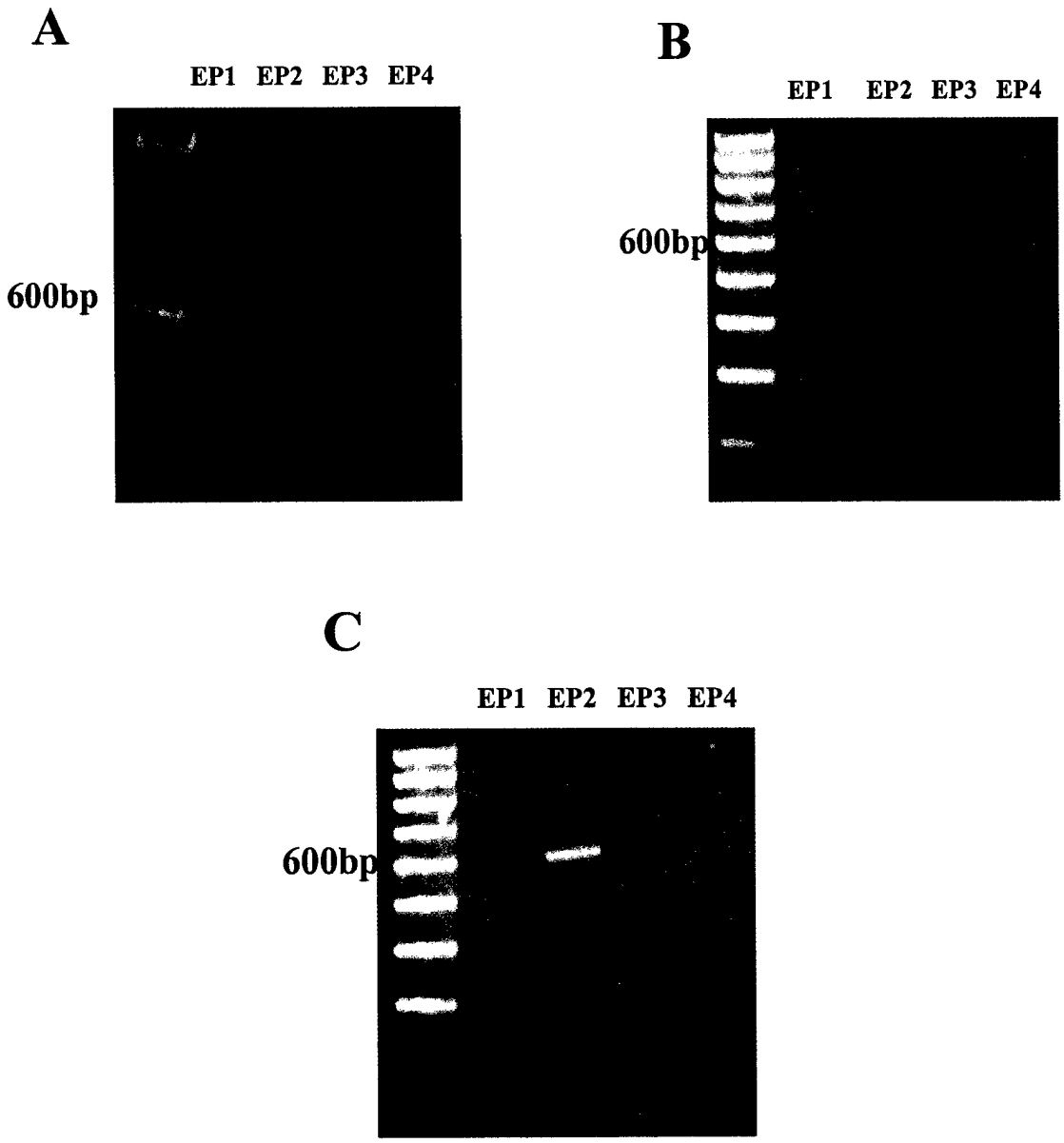

Figure 33. EP receptor mRNA in Schwan cells. RT/PCR amplification products for EP1, EP2, EP3, and EP4 receptors in NF1 Schwann cells (A), normal human adult Schwann cells (B), and non-NF1 Schwann cells (C). The PCR products were separated on a 2% agarose gel stained with ethidium bromide. Molecular weight markers are derived from a 100bp ladder. These PCR products are a representative experiment repeated 3 times with similar results.

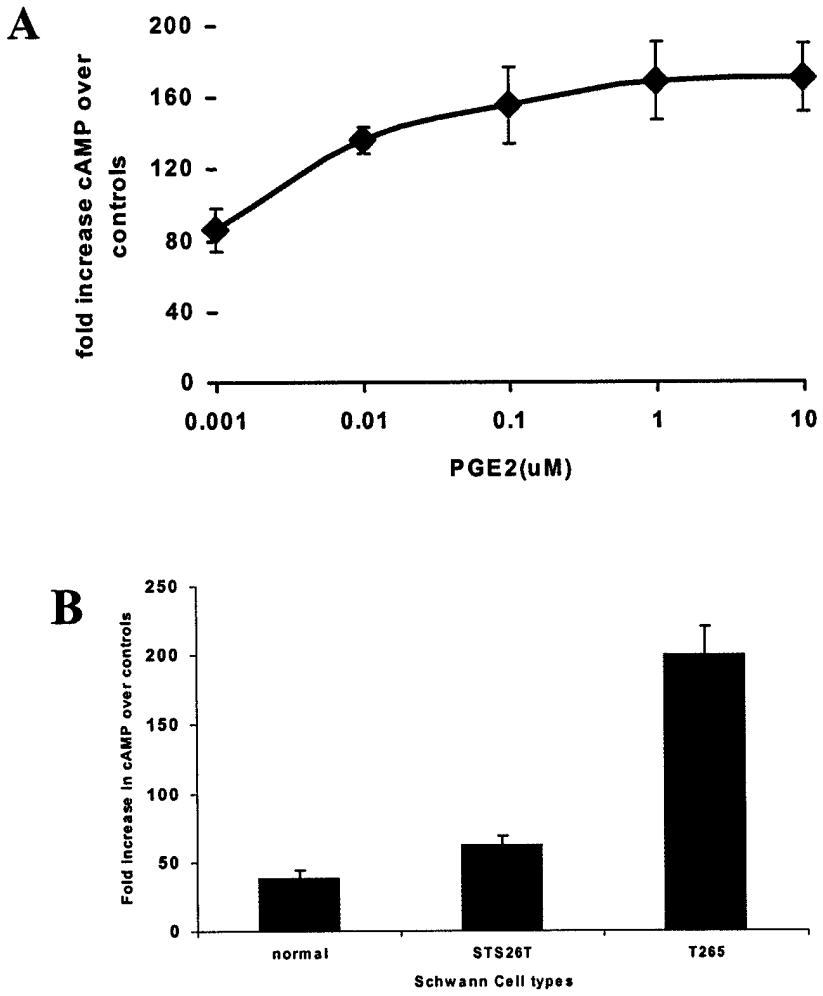

Figure 34. Effects of PGE2 on cAMP in Schwann cells. The NF1 Schwann cell line, T265, was incubated with increasing concentrations of PGE_2 (0.001 to 10uM) in the presence of 200uM of the phosphodiesterase inhibitor, IBMX, for 20 minutes. Cells were lysed and concentrations of cAMP were measured in triplicate by ELISA. Values are mean fold increases of cAMP in cells normalized to levels of unstimulated control cells of 3 replicates from 3 different experiments. Error bars represent +/- standard deviation of the mean (**A**). Normal human adult Schwann cells, non-NF1 Schwann cells, and NF1 Schwann cells were incubated with 1uM of PGE_2 and 200uM IBMX for 20 minutes. Cells were lysed and concentrations of cAMP from cell lysates were measured in triplicate by ELISA. Values are mean fold increases of cAMP in cells normalized to levels of unstimulated control cells of 3 replicates from 3 different experiments. Error bars represent +/- standard deviation of the mean (**B**).

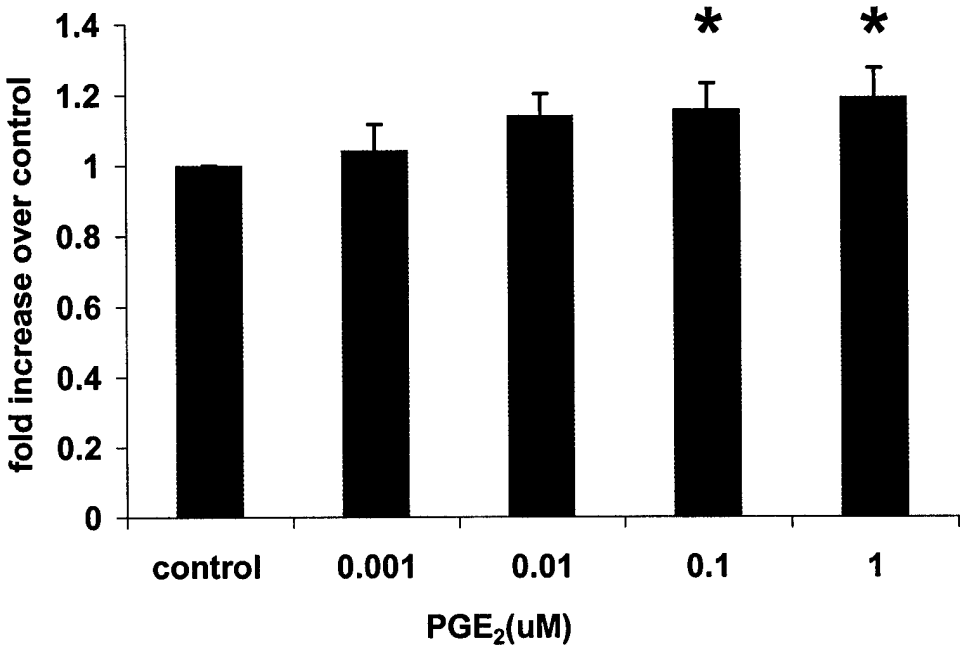

Figure 35. PGE_2 induces proliferation of NF1 cells. The T265 cells were cultured in serum free medium in the presence of increasing concentrations of PGE_2 alone for 72 hours. Cell number was evaluated by the colorimetric MTT assay after 72 hours in culture. Values are expressed as mean fold increase over controsl of 4 different experiments. Error bars represent +/- standard error deviation. The data were statistically significant using ANOVA ($F(4,15)=6.156$). Post-hoc comparisons were determined using Tukey's LSD (*, significantly different from control, $P<0.05$).

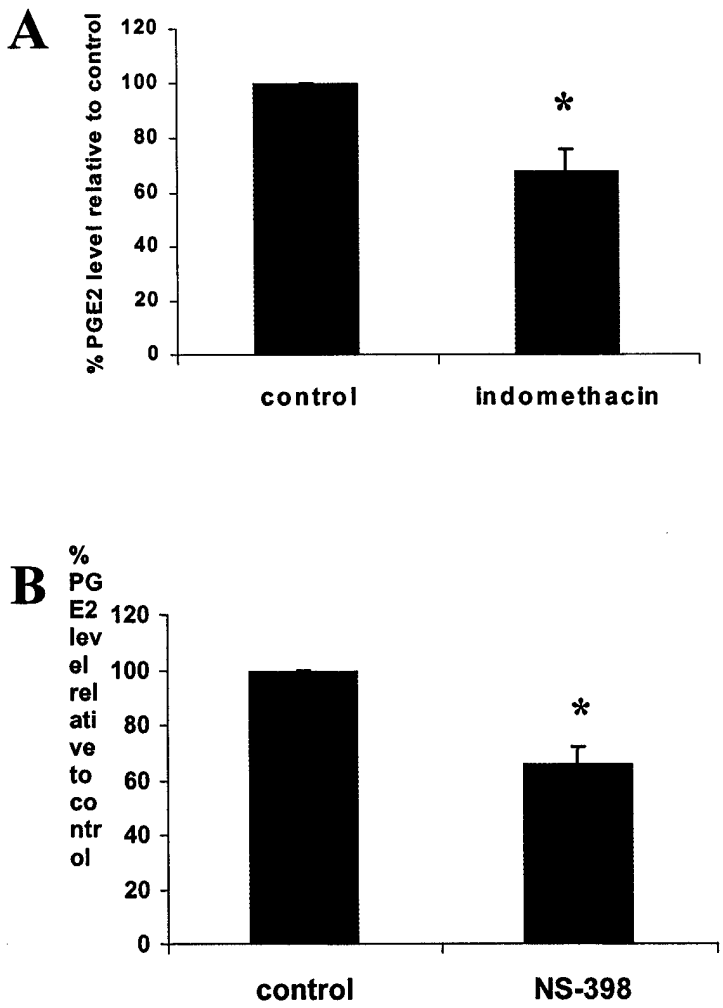

Figure 36. Cyclooxygenase 1 and 2 decrease the secretion of prostaglandin. Basal levels of PGE_2 secretion was inhibited by 50 uM of indomethacin (**A**). Basal levels of PGE_2 secretion was inhibited by 50 uM of NS-398 (**B**). Ratios are expressed as normalized levels of PGE_2 to protein levels over control levels. Values are expressed as mean of 3 different experiments. Error bars represent +/- standard deviation of the mean. The data were statistically significant using the t-test. *, significantly different from control, $P<0.001$.

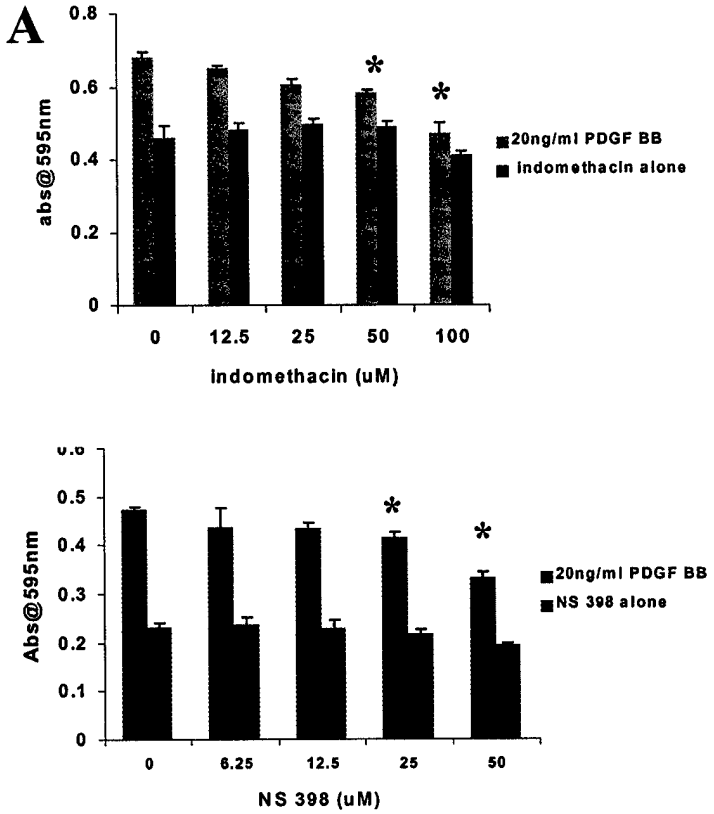

Figure 37. PDGF BB induced proliferation of NF1 cells is mediated by cyclooxygenase-1/2. The T265 Schwann cells were cultured in serum free medium in the presence of increasing concentrations of the Cox-1 and Cox-2 inhibitors, indomethacin, alone or in combination with 20ng/ml of PDGF BB for 72 hours (**A**). Schwann cells were cultured in serum free medium in the presence of increasing concentrations of the Cox-2 inhibitor, NS-398, alone or in combination with 20ng/ml of PDGF BB for 72 hours (**B**). Cell number was evaluated by the colorimetric MTT assay after 72 hours in culture. Values are expressed as mean of 4 replicates of an experiment repeated 3 times. Error bars represent +/- standard deviation of the mean. The data were statistically significant using ANOVA; for indomethacin $F(4,10)=12.416$ and for NS-398 $F(4,10)= 19.52$. The post-hoc comparisons were determined using the Newman-Keuls test in (A) (*, significantly different from control, $P<0.05$) and Tukey's LSD in (B)(*, significantly different from control, $P<0.05$).

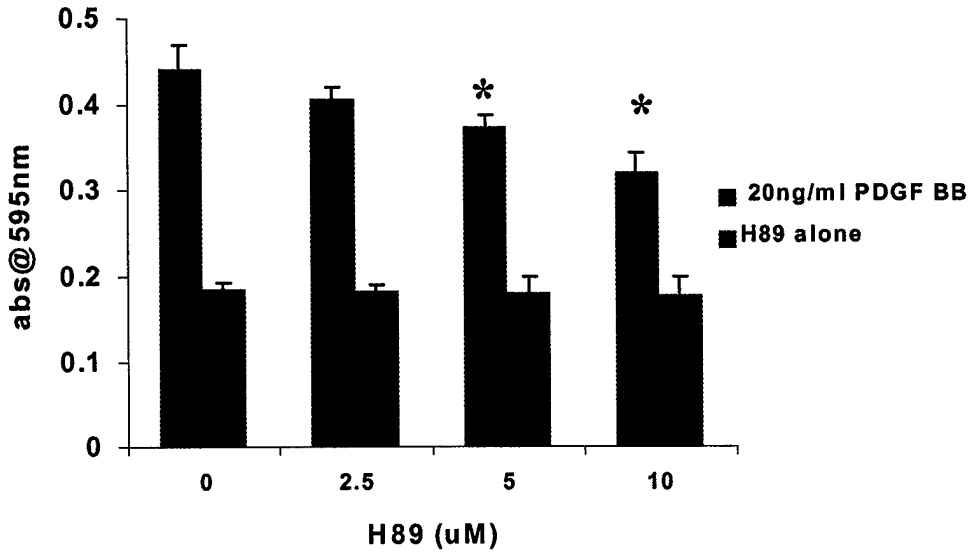

Figure 38. PDGF BB induced proliferation of NF1 cells is mediated by PKA. T265 Schwann cells were cultured in serum free medium in the presence of increasing concentrations of the PKA inhibitor, H89, alone or in combination with 20ng/ml of PDGF BB for 72 hours. Cell number was evaluated by the colorimetric MTT assay after 72 hours in culture. Values are expressed as mean of at least 3 replicates representative of an experiment repeated 3 times. Error bars represent +/- standard deviation of the mean. The data were statistically significant using ANOVA ($F(3,8)=17.19$). The pot-hoc comparisons were analyzed using Tukey LSD (*, significantly different from control, $P<0.05$).

Discussion

The second messenger cAMP regulates Schwann cell function. The proliferation of normal Schwann cells requires elevations of cAMP levels (Sobue et al., 1986). We report that Schwann cells derived from NF1 tumors have elevated levels of cAMP relative to levels of normal adult Schwann cells. Similar to our findings, a previous study reported that Schwann cells derived from Nf1 mutant mice also have increased basal cAMP levels compared to wild type (Kim et al., 2001). In both cases, the increased cAMP levels were in the same order of magnitude, a two to three fold increase compared with controls. These observations suggest that elevated cAMP levels may contribute to the aberrant proliferation of Schwann cells derived from NF1 tumors.

There are several factors that may contribute to the increased levels of cAMP in NF1 Schwann cells. First, the expression of several additional AC isoforms in NF1 Schwann cells may contribute to higher basal levels of cAMP (**figure 29**). However, we only investigated the mRNA, so that the protein expression and enzymatic activity of each AC isoform still need to be investigated to confirm the direct link between AC expression and cAMP levels in Schwann cells. This is the first study identifying the expression of the isoforms of AC mRNA in Schwann cells.

Another possibility for the increased cAMP levels in NF1 Schwann cells may be due decreased activities of phosphodiesterases (PDE) in degrading cAMP. Walikonis et al., (1998) reported that inhibition of phosphodiesterases resulted in increased cAMP levels in Schwann cells. However, we have not investigated for mRNA for PDE in this study. Our results suggest that conditions favoring cAMP synthesis over cAMP degradation may be responsible for the increased levels of cAMP in NF1 Schwann cells.

Elevated intracellular cAMP induce higher PKA activities leading to Schwann cell proliferation. PKA is directly activated by cAMP, and upon activation, the catalytic subunit of PKA enters the nucleus and phosphorylates numerous transcription factors, including cyclic response element binding protein (CREB). We report that H89, the inhibitor of PKA, decreased the proliferation of NF1 Schwann cells stimulated by PDGF BB (**figure 36**). These results suggest that the proliferation of NF1 Schwann cells in response to PDGF BB is mediated by PKA. PDGF BB is able to activate PKA by increasing cAMP levels through stimulating the secretion of PGE_2 in NF1 Schwann cells (Dang et al., unpublished observations). Similar to our studies, the elevation of cAMP by prostaglandins has been shown to contribute to the proliferation of smooth muscle cells (Graves et al., 1996) and colorectal cancer cells (Vadlamudi et al., 1999) in response to growth factors. Our findings in conjunction with other studies suggest that elevation of intracellular cAMP brought about by elevated PGE2 is able to mediate the proliferation of NF1 Schwann cells.

Similar to our findings, numerous reports have shown that the activation of PKA in Schwann cells results in cell proliferation. For example, Lee et al. (1999) reported that the axolemma enriched fraction (AEF) induces Schwann cell proliferation via the activation of PKA and CREB phosphorylation (Lee et al., 1999). Tabernero et al., showed that PDGF BB is able to stimulate the phosphorylation of CREB in normal Schwann cells (1998). It has also been repeated that neuregulin stimulates Schwann cell proliferation via PKA (Kim et al., 1997). Thus activation of the cAMP/PKA pathway is important for the proliferation of Schwann cells. However, the exact mechanism for activating PKA in normal Schwann cells is unknown. Given the elevation of cAMP in

NF1 Schwann cells, it is reasonable to believe that increased activation of PKA contributes to the aberrant proliferation characteristic of these cells.

The increased cAMP levels in NF1 Schwann cells may be due to abnormal prostaglandin metabolism. Prostaglandin PGE_2 induces the proliferation of NF1 Schwann cells (**figure 35**). We found that the addition of exogenous prostaglandin further stimulates the proliferation of NF1 Schwann cells (**figure 35**). As shown in **figure 34**, the elevated cAMP levels due to PGE_2 contribute to the proliferation of NF1 Schwann cells. Similar to our findings, elevating cAMP levels in Nf1-deficient mouse Schwann cells also result in Schwann cell hyperplasia (Kim et al., 1997). In contrast to our studies, Kim and co-workers used the pharmacological agent forskolin to elevated cAMP in Schwann cells, while in our studies the physiological stimulus prostaglandin was used to elevate cAMP.

Within the tumor, in addition to Schwann cells themselves there are several other sources of prostaglandin that may contribute to the proliferation of NF1 Schwann cells. A previous report has shown that mast cells are able to secrete prostaglandin (Marshall et al., 1999). Mast cells have been shown to be present in significant numbers in NF1 tumors (Isaacson et al., 1976; Ricardi et al., 1982). Thus secretion of prostaglandin by mast cells within the tumor could contribute to the elevated levels of cAMP levels in NF1 Schwann cells. However, the source of prostaglandin may also be the Schwann cells themselves. We report that NF1 Schwann cells secrete elevated levels of prostglandins compared to normal Schwann cells (**figure 28**). Similar to our findings, a previous report has shown that mice Schwann cells are able to secrete prostaglandin E_2 (Constable et al., 1994). Although cAMP levels and prostaglandin secretion do not directly correlate with

cAMP levels in NF1 Schwann cells, prostaglandin may still contribute to the formation of NF1 tumors.

The prostaglandin PGE_2 may contribute to the proliferation of NF1 Schwann cells induced by growth factors. We report that the proliferation of NF1 Schwann cells in response to PDGF BB is mediated by increased synthesis of PGE_2. Inhibitors to enzymes synthesizing PGE_2, (indomethacin and NS398) decreased the PDGF BB stimulated proliferation of NF1 Schwann cells (**figure 37**). Similar studies using Cox inhibitors have also shown decreased proliferation in colorectal tumor and glioma cells (Richter et al., 2001; Joki et al., 2000). In addition, we report that NF1 Schwann cells express higher levels of $cPLA_2$ and Cox-2 expression than normal human adult Schwann cells (**figure 31**), suggesting that these 2 enzymes may play a role in NF1 tumor formation. The $cPLA_2$ releases the substrate arachidonic acid from endogenous phospholipids, which is then converted to prostaglandin by Cox-2. The role Cox-2 in cell hyperplasia has well been documented in colorectal cancer cells. Several studies have reported that growth factor induced proliferation of colorectal cancer cells is mediated via the increased expression of Cox-2 and increased synthesis of prostaglandin (Coffey et al., 1997; Chinery et al., 1999). Thus the aberrant prostaglandin metabolism may contribute to the proliferation of NF1 Schwann cells leading to tumor formation.

The increased prostaglandin receptor expression in NF1 Schwann cells may contribute to the aberrant proliferation of NF1 Schwann cells in response to secreted prostaglandin. We report that normal human Schwann cells express only the EP4 receptor subtype, while NF1 Schwann cells express the EP2 and EP4 receptor subtypes (**figure 33**). These receptor subtypes are coupled with cAMP metabolism in numerous

cell types (Coleman et al., 1994). Activation of the additional EP2 receptor by secreted prostaglandins may contribute to elevated levels of cAMP leading to Schwann cell proliferation. However, we have only demonstrated the mRNA expression to all these receptors; protein expression by Western blotting still needs to be done to verify protein expression.

Conclusion

Our results suggest that the loss of neurofibromin in Schwann cells correlates with numerous intracellular signaling abnormalities leading to tumor formation as summarized in figure 39. We determined some of the metabolic changes, which can account for the increased cAMP levels in NF1 Schwann cells: increased expression of adenylyl cyclase subtypes, increased expression of the prostaglandin receptor isoform, and increased secretion of prostaglandin. In addition, the elevation of cAMP by exogenous PGE_2 stimulated the proliferation of NF1 Schwann cells. Finally, both Cox-2 and PKA contribute to the proliferation of NF1 Schwann cells induced by PDGF BB. Taken together, the aberrant prostaglandin metabolism and elevated cAMP metabolism contributes to the aberrant proliferation of NF1 Schwann cells.